RESPONSE OF RIVER COASTAL MARGINS TO HUMAN INDUCED VARIATIONS IN SEDIMENT SUPPLY AND ACCELERATED SEA-LEVEL RISE

Anna Marta Jalowska

A dissertation submitted to the faculty of the University of North Carolina at Chapel Hill in partial fulfillment of the requirements for the degree of Doctor of Philosophy in the Department of Marine Sciences.

Chapel Hill
2016

Approved by:

Brent A. McKee

Antonio B. Rodriguez

Jaye Cable

Richard Miller

Brian White

ABSTRACT

Anna M. Jalowska: Response of River Coastal Margins to Human Induced Variations in Sediment Supply and Accelerated Sea-Level Rise
(Under the direction of Brent A. McKee and Antonio B. Rodriguez)

My dissertation emphasizes that human-induced modifications to riverine sediment budget and changes in the rate of sea-level rise strongly influence bayhead-delta evolution. The response of bayhead deltas to these alterations is difficult to predict, but important to understand because they can lead to submergence and erosion of deltaic environments and loss of important habitat. Floodplains and the bayhead delta of the Lower Roanoke River, NC have the largest, most pristine bottomland hardwood forest ecosystem remaining in the mid-Atlantic region. The majority of this ecosystem is currently at 0 m above sea level (MASL) and is very vulnerable to sea-level rise and changes in sediment supply. The Lower Roanoke River has been impacted by human activities (land clearing followed by river damming), and climate change. Using multidisciplinary tools, I was able to reconstruct the geological history of the Roanoke Delta (core descriptions and radiocarbon and ^{210}Pb geochronologies), and define sources, fates and pathways of suspended sediments in the floodplains and delta environments on seasonal (radionuclide based sediment fingerprinting) and decadal to monthly (^{210}Pb geochronology) time scales.

My research reconstructed two episodes of retreat in the Roanoke delta during the past 6000 years. The first event occurred around 3700 BC when marine transgression flooded the Roanoke Paleovalley. The flooding formed an interdistributary bay that slowly filled with

sediments until the 17th century. During the 1600s, when the first European settlers began to clear forest and farm the drainage basin, the delta rapidly accreted and the interdistributary bay filled with legacy sediment from increased agricultural runoff. The regression was also facilitated by the low rates of sea-level rise until ca 1860AD. The second episode of bayhead-delta retreat started during the 19th century and continues today. Improved agricultural practices and dam construction decreased the amount of sediment delivered to the bayhead delta. Additionally, the rate of sea-level rise increased to 0.21 cm/yr at that time. Under these conditions, the delta entered an erosional phase and during 1954–2012, the rate of delta loss was 2469 m^2/yr. Decreases in sediment supply and more frequent inundations associated with the sea-level rise, led to a dramatic change in the function of delta plains. My research shows that at a 0 MASL elevation, the frequency and extent of flooding control erosion and deposition in the delta plain, and lead to loss of their ability to retain sediments. Hence, delta plains, regarded to be sediment sinks and sites of long-term sediment storage, become a source of sediment to the upper delta, as sea level rises and the delta retreats. This mechanism exposes a unique distribution of sediments in eroding deltas. In contrast to the previous paradigm emphasizing a unidirectional seaward dispersal of eroded deltaic sediments during transgression, my research illustrates that a landward-directed sediment migration pathway could occur, allowing nourishment and fortification of the upper bayhead delta to accelerated sea-level rise.

This dissertation is dedicated to Maja.

ACKNOWLEDGEMENTS

I would like to express my special appreciation and thanks to my advisors Dr. Brent McKee and Dr. Antonio Rodriguez, you have been tremendous mentors for me. I would like to thank you for encouraging my research and for allowing me to grow as a research scientist. Your advice on both research as well as on my career have been priceless. I would also like to thank my committee members: Dr. Jaye Cable, Dr. Richard Miller Dr. Brian White, and Dr. J. Patrick Laceby, for your time, brilliant comments and suggestions. I would especially like to thank my colleagues: John Biddle, Emily Elliot, Sherif Ghobrial, John Gunnell, Kristen Jarman, Robin Mattheus, Samuel Perkins, Ethan Theuerkauf, Patricia Rodriguez and the awesome undergraduate students I had a pleasure to mentor: Christiana Ade, Anna Atencio, Wayne Capps, Olivia Henley, Shelby Marshall, Katie McCabe, Gráinne O'Grady, Joseph Roberts, Lauren Speare, Alexander Stephan, and Danielle Wingler for your help with lab and field work.

A special thanks to people who supported me emotionally through last 7 years, Marine Sciences graduate students friends, especially Winnie Yu, John Paul Balmonte (and Hallie), Lisa Nigro and Tingting Yang, who supported me in the moments when there was no one to answer my queries. I really appreciate an amazing support from the Marine Sciences faculty and staff: Dr. Carol Arnosti, Dr. Harvey Seim, Dr. Larry Benninger, Dr. Barbara MacGregor and Howard Mendlovitz, and for the caring support form Dr. Leslie S. Lerea the Associate Dean of Student Affairs.

The biggest thanks go to Maja, who I hope will forgive me one day the hours spend with my dissertation instead with her (but I tried my best Kluseczko), and to my family who inspired and encouraged me all the time, for their love and support from cooking to hugging, and for standing by my side during my trials and triumphs. This work was supported by the North Carolina Sea Grant, grant number 10-HCE-B-10 and by the U.S. Department of Energy's Office of Science (BER) through the Coastal Center of the National Institute for Climatic Change Research at Tulane University grant number TUL-536-06/07, a one-year University of North Carolina Dissertation Completion fellowship and through the Department of Marine Sciences at UNC.

TABLE OF CONTENTS

LIST OF TABLES

LIST OF FIGURES

LIST OF ABBREVIATIONS

BHD- Bayhead Delta

LRR- Lower Roanoke River

TSM- Total Suspended Matter

INTRODUCTION

Bayhead deltas located at the interface between terrestrial and marine processes, are becoming more susceptible to sea-level rise and human activities. In response to natural and anthropogenic alterations, these dynamic sedimentary systems function through a series of feedback loops. Responses of the bayhead deltas vary over a range of spatial and temporal scales, controlled by a rate of sea-level rise and sediment supply, and may be observed as geomorphological changes preserved within the sedimentary record. Our understanding of the deltas modern and historical response to natural and anthropogenic changes is crucial to the future sustainability of valuable coastal ecosystems.

This dissertation broadly addresses sedimentation, and sediment dynamics in the Roanoke River bayhead delta with a focus on the linkages between sedimentary process in the River main trunk and bayhead delta floodplains. Lower Roanoke River, NC, extends 220 km from the fall line to the bayhead delta front in Albemarle Sound. This theses places the emphasis on how these vulnerable coastal systems respond to natural changes (e.g. climatic, sea level, episodic storms) and anthropogenic alterations to the system (e.g. land clearance, damming), and how these changes impact sediment dynamics, that eventually are preserved within the geologic record.

First chapter focuses on reconstructing the evolution of the bayhead delta in Holocene and Anthropocene. Stratigraphic records in the Roanoke River bayhead delta revealed two episodes of retreat during the past 6000 years. First retreat happened 3700 BC as sedimentation could not keep up with the rate of sea-level rise. During that time the prehistoric delta plain was

flooded and formed interdistributary bay. The interdistributary bay was slowly filling up with sediments, the rate of sea-level rise slowed down, the sedimentation rates were keeping up until the mid-1600s AD. Deforestation associated with the initiation of agriculture by settlers in the drainage basin and poor management of runoff introduced a large quantity of sediment into the river. Since 1643 AD, sediment deliveries greatly overwhelmed the low rate of sea-level rise at the time, resulting in rapid progradation of the bayhead delta. In mid 1800s AD rates of sea-level rise increased and at the same time agricultural practices improved reducing sediment loads. During that time a second retreat event in the bayhead delta started. Modern delta plain is at sea level and its low accretion rate cannot keep up with accelerating sea-level rise. The construction of impoundments, completed in 1963 AD, likely magnified erosion of the delta by retaining sediment behind the dams and causing a drastic decrease in sediment supply to the delta.

Second chapter presents the results of analyses of flooding frequency and depositional/erosional events in the floodplains of the Roanoke River bayhead delta. It confirms that delta in current state is not sustainable, and deltaic plains located in the lower and middle parts of the delta cannot keep up with sea-level rise. The processes governing the sediment dynamics show great variability and complexity. Upper parts of the delta have an optimal elevation, sediment concertation and inundation frequency and extend to outpace the sea-level rise. This chapter also reveals that during depositional and erosional events in the delta plain, sediments are being replaced with materials eroded from subaqueous, older parts of the delta.

Third chapter reveals modern sediment distribution in Lower Roanoke River with a focus on the bayhead delta. Placement of dams resulted in almost complete disconnection of the Lower Roanoke River from the upper watershed. The dams effectively restricted the suspended sediment delivery from the headwaters, making soils and sediments from the Lower Roanoke

River basin the primary source of suspended sediment. Fingerprinting modeling results shown that the Lower Roanoke River subsurface sediments contribute to the suspended load only in upper parts of the river, and its contribution decrease as the river approaches bayhead delta. Within the bayhead delta subsurface sediments are replaced by surface sediments from eroding delta plains to be again replaced by sediment originating from eroding prodelta at river's mouth. Without a substantial material to grow, the delta cannot outpace the sea-level rise and retreats. In the process of retreat, sediment-starved delta plains recycle sediment from eroding parts of the lower bayhead delta to fortify the upper bayhead delta. The landward sediment transport during the retreat process, results in BHD and its floodplains become source and sink for sediments at the same time.

CHAPTER 1: RESPONSES OF THE ROANOKE BAYHEAD DELTA TO VARIATIONS IN SEA LEVEL RISE AND SEDIMENT SUPPLY DURING THE HOLOCENE AND ANTHROPOCENE [1]

1.1 Abstract

The response of bayhead deltas to changes in the rate of sea-level rise and sediment supply is difficult to predict, but important to understand because these changes can lead to submergence and erosion of deltaic sediments and loss of important habitat. Here, we show that the Roanoke bayhead delta in North Carolina, USA experienced two episodes of retreat during the past 6000 years based on core descriptions and radiocarbon and ^{210}Pb geochronologies. The first event occurred around 3700 BC as sedimentation could not keep up with the rate of sea-level rise and a prominent flooding surface separating delta plain, below, from interdistributary bay, above, formed. Afterwards, sedimentation rates were keeping up with the low rates of sea-level rise until the mid-1600's AD, when the first European settlers began to clear forest and farm the drainage basin. During that time, the delta rapidly accreted and the interdistributary bay filled with legacy sediment from increased agricultural runoff. Regression was also facilitated by the low rates of sea-level rise at that time (-0.01 to 0.047 cm/yr). The second episode of bayhead-delta retreat initiated during the 19th century and continues today. Improved agricultural practices and dam construction decreased the amount of sediment delivered to the bayhead delta.

[1] This chapter was previously published as an article in *Anthropocene.* The original citation is as follow: Anna M. Jalowska, Antonio B. Rodriguez, Brent A. McKee. (2015), Responses of the Roanoke Bayhead Delta to variations in sea level rise and sediment supply during the Holocene and Anthropocene, Anthropocene, 9, 41–55, doi:10.1016/j.ancene.2015.05.002.

Additionally, the rate of sea-level rise increased to 0.21 cm/yr at that time. Under these conditions, the delta entered an erosional phase and during 1954-2012 the rate of delta loss was 2469m^2/yr and that loss is easily recognized by cypress trees stranded in adjacent Albemarle Sound. This study emphasizes that human-induced modifications to the sediment budget and changes in the rate of sea-level rise strongly influence bayhead-delta evolution.

1.2 Introduction

Bayhead deltas exist where rivers discharge into drowned-river-mouth estuaries, and are common features of wave-dominated estuaries (Dalrymple et al., 1992), (Figure 1a). Secluded from the ocean environment, bayhead deltas are natural harbors. Many major ports and port cities, including the Port of Houston, TX, San Jose, CA, Sydney, Australia, Rotterdam, Netherlands, Venice, Italy and Canton, China are located adjacent to, or on bayhead deltas. The protruding-open shelf deltas are affected (in both constructive and destructive manner) by waves, currents hurricanes and monsoons, while located in low-energy environments bay-head deltas respond more dramatically to anthropogenic modifications than to natural forces (Giosan and Goodbred, 2007; Pulich and White, 1991). Human activities within urban corridors have modified the geomorphology and ecological functions of bayhead deltas, mainly through channel dredging, spoil disposal, creation of levees, and water pollution (Phillips and Slattery, 2007; White et al., 2002). Bayhead deltas are also being impacted from watershed modifications including installation of dams and land-use changes that alter river hydrology and sediment load, (Gunnell et al., 2013; Hupp et al., 2015; Mattheus et al., 2009; Meade, 1982; White et al., 2002). In addition to these downstream and upstream watershed modifications, the position of bayhead deltas, relative to the river and estuary, is a product of sea-level rise, storminess, sediment supply and the morphology of the river valley. Bayhead deltas, along with their adjacent floodplains, serve as long-term storage sites for lithogenic and organic material (millennial time scales) and

are biogeochemically active sites on daily to decadal time scales contributing to global nutrient and carbon cycles (Hanson et al., 1993; Hupp et al., 2015; Noe and Hupp, 2009; White et al., 2002). Bayhead deltas host distinct, highly diverse ecosystems including swamp forest, hardwood bottomlands, and other wetlands (Hupp et al., 2009b; Pringle et al., 2000), and provide valuable ecosystem services related to water quality, stormwater catchment, and wildlife habitat. The global value of ecosystem services provided by natural bayhead-delta wetlands is $2.5 to 2.8 million/km^2/yr (in 2007 dollars) (Costanza et al., 2014; DeGravelles, 2010).

Bayhead deltas are very sensitive to changes in sedimentation and accommodation, thus, human alterations within watersheds greatly affect bayhead delta evolution (Nichols et al., 1986). Increased erosion in the watershed associated with deforestation, or land-use change, increases sediment supply (Hupp et al., 2009b; Mattheus et al., 2009; Ver et al., 1999), while construction of impoundments effectively restrict sediment delivery to the river mouth (Jaffe et al., 2007; Meade, 1982). Previous studies report bayhead deltas retreat rapidly (backstep) in response to a small increase in the rate of sea-level rise (Rodriguez et al., 2010), but the rate of retreat can also decrease as sediment supply increases or when transgression is confined by an abrupt increase of valley gradient at tributary junctions (Simms and Rodriguez, 2014). Current, conservative projections for a sea-level rise in this century range between 26 and 98 cm (IPCC, 2014), thus, it is crucial to understand the response of the bayhead-delta coastline to accelerating sea-level rise and to model impacts on coastal communities.

In this study, we examine bayhead delta evolution driven by natural processes during the late Holocene and anthropogenically-driven processes during the Anthropocene. We place the stratigraphy and geochemical data in context with a well-constrained high-resolution sea-level curve for the region to assess the effects of changes in the rate of sea-level rise on the bayhead

delta. In addition, we examine the impacts of the first European settlements in Virginia and North Carolina on bayhead delta evolution, followed by 20th century anthropogenic stressors, including the construction of impoundments.

1.3 Study Area

Albemarle Sound and the Roanoke Bayhead Delta at its head are located in Northeastern North Carolina (Figure 1a). The estuary is a part of a slowly subsiding - up to 0.1 cm/yr (Kemp et al., 2011), Albemarle Embayment sedimentary basin (Riggs, 2011). Albemarle Sound is 92 km long and its depth ranges between 0.45 to 14 m along its margin and axis, respectively. The Sound is isolated from the Atlantic Ocean by the Northern Outer Banks barrier-island chain. Exchange with the ocean and Pamlico Sound, to the south, is limited by a narrow passage located in the southeast at Croatan and Roanoke sounds (Figure 1a). This configuration results in astronomical tides being negligible in the western part of the Sound near the Roanoke Bayhead Delta (Figures 1b and c). In 1860, the United States Coast Survey published the first bathymetric survey of Albemarle Sound with a note "There are no regular lunar tides in Albemarle Sound, the rise and fall of the water is influenced altogether by the wind and the state of the rivers emptying into it. At the western end of the Sound, the water is depressed by northerly and westerly winds, and elevated by those in the south and east" (United States Coast Survey, 1860). Subsequent studies confirmed that wind is the most important force circulating water and changing its surface height within the estuarine system (Giese et al., 1979). At the mouth of the Roanoke River (Figure 1c), cyclical daily fluctuations in water levels, up to 0.6 m, have been associated with seiching (Luettich et al., 2002). During a typical year, Nor'easters, subtropical storms and hurricanes supply substantial wave energy to the system and alter water levels. Nor'easters can produce wind speeds of 25-50 mph and cause water-level fluctuations from 0.5

to1.5 m above MSL in the Sound (Riggs and Ames, 2003). The much higher winds associated with tropical depressions and hurricanes can elevate water level at the mouth of the Roanoke River up to 2 m (for example during Hurricane Irene, August 27, 2011 water level was 1.98 m (USGS station number 0208114150), above its mean elevation ~0.0 meters NAVD 88 . The salinity of the Albemarle Sound varies from the 5-15 ppt in the east to 0.5-5 ppt in the middle and < 0.5 ppt in its west end, at the mouth of the Roanoke River (NOAA SEA Division, 1998).

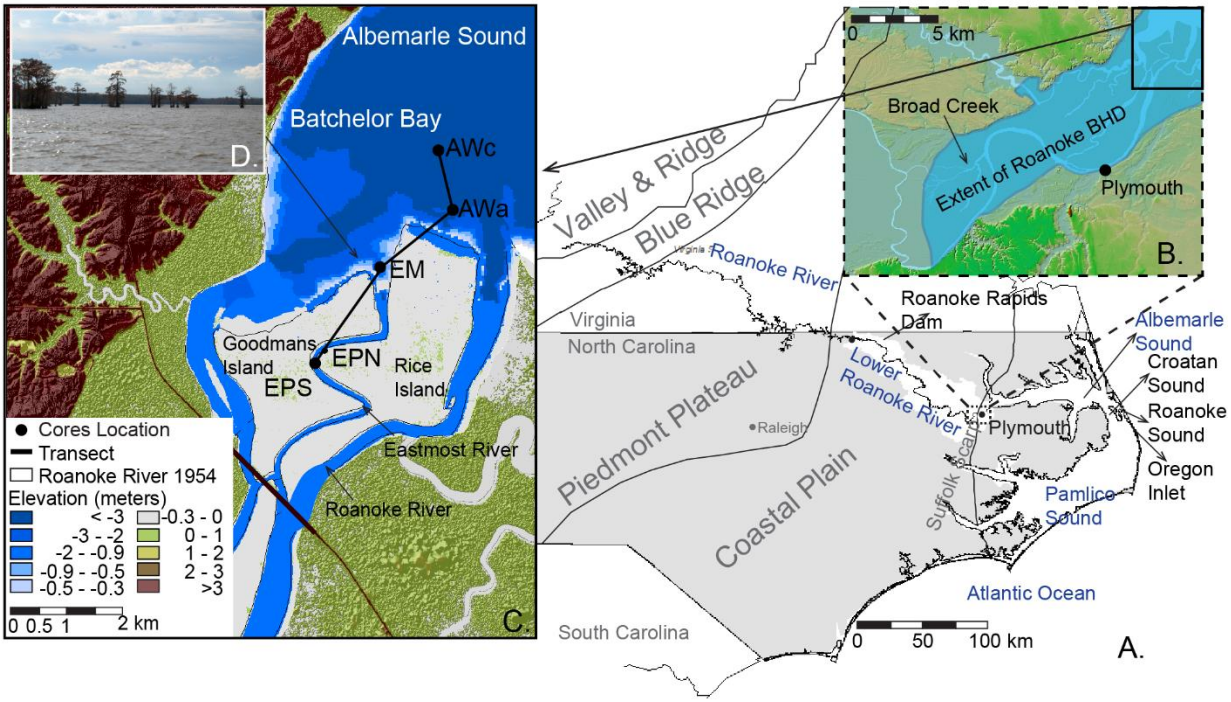

Figure 1. A. North Carolina geological provinces. B. Extent of the Roanoke Bayhead Delta (BHD) from Broad Creek - the first distributary channel- to the shoreline in Albemarle Sound. C. Elevation map of the study area and station locations. D. Bald cypress trees stranded in Albemarle Sound.

1.3.1. Geologic Settings.

During the Sangamon Interglacial (MIS 5), ca. 125,000- 75,000 years ago, sea-level in North Carolina reached a maximum level of about 7 meters above present MSL (Mallinson et al., 2008) and the highstand Suffolk Shoreline (Figure 1a), located 100 to 125 km landward of the

modern open-ocean shoreline (the Outer Banks), formed around that time (Lankford and Rogers, 1969; Riggs, 2011). During the Sangamon sea-level highstand, the Roanoke River Valley was inundated approximately 200 km inland from the current delta-front position (Parham et al., 2007; Riggs, 2011). During the subsequent fall in relative sea level that culminated in the last glacial maximum ca. 22,000-19,000 years ago (Yokoyama et al., 2000), the Roanoke River started to erode an 11-m deep, large valley, at the Sangamon Shoreline, as it adjusted to a new equilibrium profile (Riggs, 2011). During the last deglaciation, marine flooding caused transgression of the coastline and formation of modern Albemarle Sound as the Roanoke paleo-valley inundated. Previous studies showed that around 5,000 years BP, in the vicinity of the modern barrier islands, there was an open-marine embayment with estuarine conditions directly to the west in Albemarle Sound (Culver et al., 2008; Mallinson et al., 2005; Mattheus and Rodriguez, 2011) (Figure 2).

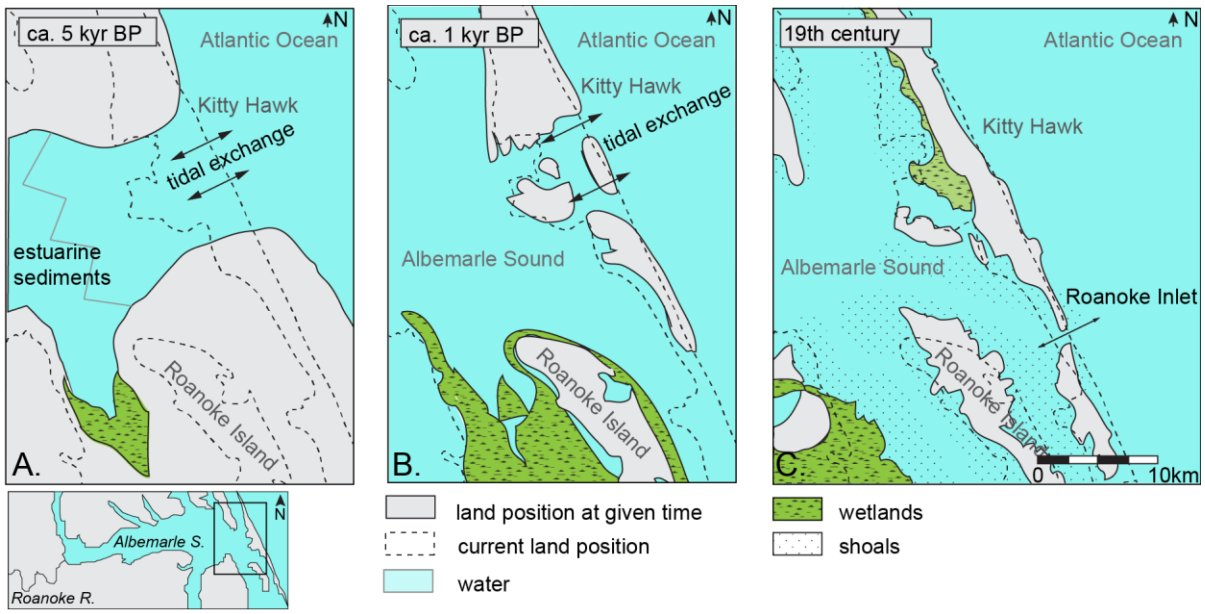

Figure 2. Paleogeographic reconstructions of Eastern Albemarle Sound based on Culver et al. (2008). A. Flooded paleo-Roanoke Valley became an open embayment 5,000 years ago. B. Closing of the embayment via tidal inlet constriction and shallowing initiated ca. 1,000 years. C. The Roanoke Inlet was 2 meters deep in 1775AD, continued to shallow in 1822AD and closed by 1833AD.

The Outer Banks (Kitty Hawk) formed around 3,000 years BP and a large tidal-inlet near Kitty Hawk, positioned over the valley axis, began to close ca. 1,000 years ago restricting ocean exchange to a few smaller inlets (Culver et al., 2008) (Figure 2). Exchange between Albemarle Sound and the open ocean ceased by 1833AD, when the Roanoke Inlet closed and the circulation of the estuary changed from astronomical-tide dominated to wind-tide dominated (Culver et al., 2008; Dunbar, 1958; Fisher, 1962) (Figure 2).

1.3.2. Roanoke River.

The Roanoke River originates in the Valley and Ridge province of the Appalachian Mountains in Virginia, has a total drainage area of 25,123 km^2 and empties into the west end of the Albemarle Sound at an average annual rate of 252 m^3/s (Giese et al., 1979; Molina, 2002) (Figure 1a). The Roanoke River flows through three geologic provinces of Virginia and North Carolina including, the Appalachian Mountains, Piedmont Plateau, and the Coastal Plain, before forming a bayhead delta near the Suffolk scarp (Brill, 1996; Oaks and DuBar, 1974) (Figure 1a). The provinces have distinct lithologies and weathering products. Most pronounced are the orange and red clay utisols produced by weathering of the igneous and metamorphic rocks of the Piedmont Plateau (Riggs and Ames, 2003).

The upstream boundary of the Lower Roanoke River is at the fall line, delineated by the transition between the Piedmont Plateau and the Coastal Plain. The Lower Roanoke River is 220-km long, drains an area of 3620 km^2 and meanders across Miocene sedimentary units overlain by Quaternary alluvium (Brown et al., 1972). The slope of the Lower Roanoke is steepest (ca 25%) 30 km below the fall line. The river's grade is very low below that, gradually losing 8 m of elevation from 30 km below the fall line to the bayhead delta. Due to the low

gradient, an extensive, up to 9-km wide, floodplain exists from 80 km below the fall line to the bayhead delta.

1.3.3. Roanoke Bayhead Delta.

The subaerial Roanoke bayhead delta is about 86 km^2, extending from Broad Creek- the first distributary channel- to the shoreline in Albemarle Sound (Figure1b). The delta is currently at ~0.0 m NAVD 88 (Figures 1b and c). The U.S. Army Corps of Engineers has been dredging the main-stem channel of the Roanoke River, modifying its morphology for navigational purposes, since 1871 and it was last dredged in 1964. Dredge spoils were deposited east of the River mouth in upper Albemarle Sound (Erlich, 1980).

The Eastmost River, a meandering distributary channel that separates Rice and Goodmans Islands (Figure 1c), was chosen as access for sampling the delta plain because it has not been impacted by dredging. The channel of the Eastmost River decreases in depth toward the Sound, from about 12 m to < 1 m at the mouth bar. Cross-channel morphology around meanders is asymmetrical, similar to meandering streams located on floodplains.

The delta contains several natural wetland communities, including approximately 20,000 acres of pristine cypress-gum swamp (Hupp et al., 2009b). Cypresses fringing the shoreline function as a natural bulkhead and groin system capable of dissipating erosive wave energy, supporting shoreline accretion (Bellis et al., 1975). However, the irregular distribution of trees allows some wave energy to pass between the trunks, causing slow erosion and sediment production from the bank (Riggs and Ames, 2003). Previous studies of bathymetric changes in upper Albemarle Sound, based on historical maps from 1860 and 1915, identified wave-induced erosion of the prodelta and shoreline retreat (Erlich, 1980; Giese et al., 1979; Pels, 1967; Riggs

and Ames, 2003). Evidence of this former delta-front shoreline remains as cypress trees stranded in the Sound (Bellis et al., 1975) (Figure 1c).

1.3.4. Anthropogenic Footprint.

The first European settlement in North America in the early 1600'sAD impacted the Roanoke River Watershed and Albemarle Sound. After the late 1600's, heavy deforestation and poor agricultural practices led to a large release of sediment to the river, which accumulated along the floodplains and banks (Jacobson and Coleman, 1986; Trimble, 1974; Wolman, 1967). This legacy-sediment layer is at least 5 m thick along upstream reaches of the Lower Roanoke floodplain, and decreases downstream (Hupp et al., 2015).

Industrial development, placement of impoundments and better agricultural practices in the Roanoke watershed during the nineteenth century decreased the sediment loads entering Albemarle Sound. After a major hurricane made landfall in August 1940, causing excessive flooding to farmlands and property along the river, the US Army Corps of Engineers (USACE), constructed the John H. Kerr Dam (1947-1953). Following the completion of that dam, Virginia Railway and Power Company (currently Dominion), constructed two other dams further downstream: Roanoke Rapids Dam at the fall line in 1955 (Figure 1a) and in 1963-Lake Gaston Dam above the fall line. Prior to construction of the dams, the water level and flow of the Lower Roanoke River was characterized by extreme variability in response to seasonal variations and individual storms (Richter et al., 1996). Dam-controlled releases of water for flood prevention and electric power production changed the hydrologic regime of the river. Before damming, high-magnitude discharge events exceeding 1000 cubic meters per second (m^3/s) occurred, on average, 12 times per year; since damming, discharge has exceeded 1000 m^3/s, on average, once a year. Low flows <100 m^3/s were eliminated and the frequency of medium flows ca 600 m^3/s,

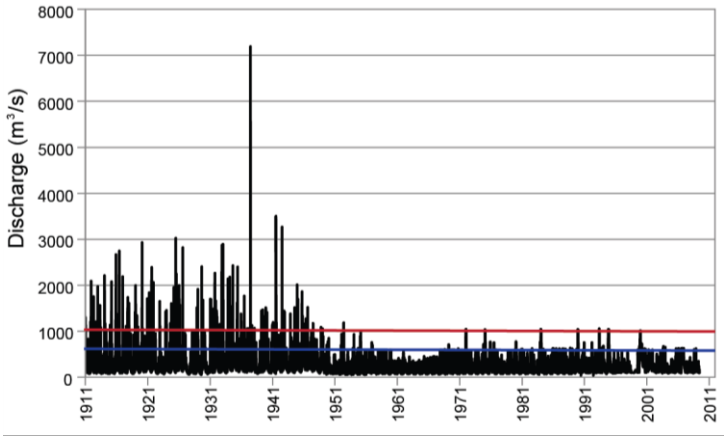

Figure 3. Roanoke River discharge measured at Roanoke Rapids, NC (USGS 02080500). Since construction of the first dam (1947-1953), discharge has not exceeded 1000 m^3/s (marked with a red line). The frequency of the 600 m^3/s flow (blue line) increased six times since dam construction.

increased over 6 times after the dam was installed (Richter et al., 1996) (Figure 3). Eliminating high-magnitude flows decreased the hydrological capacity of the river and connectivity between the upper and lower parts of the river. Consequently, sediment discharge to the Lower Roanoke was reduced by 86 to 99% (Meade et al., 1990; Simmons, 1988). The remaining sources of sediment to the delta and Albemarle Sound include the Lower Roanoke watershed and reworking of the river banks, channels and floodplains, which are filled with legacy sediment. Despite increasing turbidity downstream (Hupp et al., 2009a) and sediment accumulation in floodplain backswamps (up to 0.59 cm/y) (EPA et al., 2008; Hupp et al., 2015; Schenk et al., 2010) a loss of the delta shoreline has been observed (Riggs et al., 2008) indicating that sediments are not being dispersed to the proximal portion of Albemarle Sound.

1.4 Methods

1.4.1 Cores.

A 3.3 km long transect of five cores was collected across the lower part of the Roanoke Bayhead delta from the delta plain to the prodelta (Figure 1c). Each core location was occupied twice. Initially, we collected 7.6 cm diameter vibracores at the sites, but always encountered tree logs and roots that limited penetration depths to between 132 cm and 634 cm. To increase sampling depths, we reoccupied the sites using a different coring method, and collected 5.4 cm

diameter, 122 cm long cores at discreet depths using the Geoprobe Macro-Core™ tool. The core barrel was plugged while it was driven to the sampling depth with a gas-powered jackhammer. At the sampling depth, which ranged from 730 cm to 1100 cm, the plug was removed and the barrel was driven an additional 122 cm to collect the core. Cores EPS and EPN were taken along the Eastmost River at a meander on the border of Rice Island. Core EPS was located south of the meander on the subaqueous point bar and core EPN was located inland on the delta plain. Core EM was taken at the channel-mouth bar of the Eastmost River (delta front). From upper Albemarle Sound the proximal and distal prodelta was sampled in core AWa and AWc, respectively. The cores were transported to the lab then split, photographed, described and subsampled for grain-size analyses and radiocarbon dating. Interpretation of the depositional environments was based on lithologic data (Figure 4, 5).

1.4.2. Grain Size.

402 subsamples of cores EM (6), EPN (314), EPS (23), AWa (9) and AWc (50) were analyzed for grain size using a CILAS 1180 to measure particle sizes from 0.04 μm to 2500 μm in 100 size classes by laser diffraction. The sub-samples are representative of the different stratigraphic units sampled in the cores (Figs. 5, 6a and 6b).

1.4.3. Radiocarbon dating.

Eleven organic samples and six bulk sediment samples were recovered from the cores and sent for analyses to The National Ocean Sciences Accelerator Mass Spectrometry Facility (NOSAMS) at Woods Hole Oceanographic Institution (Table 1). Organic samples were either individual pieces of wood or multiple pieces of wood, seeds, seedpod, or charcoal. Samples were chosen to measure accretion rates of the various depositional environments and the timing of flooding surfaces. NOSAMS measured carbon isotope ratios, $\delta^{13}C$, of the samples to normalize

radiocarbon results for isotopic fractionation. The conventional radiocarbon dates were calibrated with Oxcal 4.1 (Ramsey, 2009) using the IntCal 13 and Marine 13 calibration curves (Reimer et al., 2013) and reported as BC (Before Christ) and AD (Anno Domini). The calibrated (95.4% probability) age intervals were averaged with an error reflecting the standard deviation, which is similar to the methodology presented in (Horton et al., 2009) and (Kemp et al., 2011), and has been used to place radiocarbon dates from cores in context of sea-level rise. Averaged radiocarbon dates were rounded to the nearest decade, and used to determine the timing of the events and to calculate sedimentation rates. In core EPN, historical records support using the maximum date from the age interval instead of the average date. Data interpretations were performed with the assumption that the radiocarbon dates of the sampled organic material reflect the time of deposition.

Table 1. Radiocarbon dates**.**

Core Name Depositional Environment	**AWc** Prodelta	**EM** Delta Front	**EPN** Delta Plain	**EPS** Delta Plain
LAT/ LON	35.95365/-76.7021	35.94141/-77	35.93253/-76.7183	35.93096/-77
Sample Depth (cm)	699	625	101	845
^{14}C age	3570 ± 30	280 ± 30*	340 ± 20	190 ± 30 *
Calibrated age range (95.4%)	2022 – 1781 BC	1498 – 1795 AD	1470 – 1643 AD	1648 – 1950 AD
Date for sedimentation rates	**1900±120 BC** (Mean at 95.4%)	**1650±150 AD** (Mean at 95.4%)	**1643 AD**** (Highest at 95.4%)	**1648 AD***** (Lowest at 95.4%)
Sample Depth (cm)	802	715	123	962
^{14}C age	3700 ± 40	2210 ± 35	575 ± 20	4530 ± 40
Calibrated age range (95.4%)	2203 – 1972 BC	382 – 184 BC	1310 – 1415 AD	3365 – 3097 BC

Date for sedimentation rates	**2090±120 BC** (Mean at 95.4%)	**280 ± 100 BC** (Mean at 95.4%)	**1360±50 AD** (Mean at 95.4%)	**3230 ± 130 BC** (Mean at 95.4%)
Sample Depth (cm)	882	777	211	
^{14}C age	4930 ± 40	4110 ± 40	1350 ± 20	
Calibrated age range (95.4%)	3786 – 3645 BC	2871 – 2505 BC	646 – 686 AD	
Date for sedimentation rates	**3720±70 BC** (Mean at 95.4%)	**2690±180 BC** (Mean at 95.4%)	**670 ±20 AD** (Mean at 95.4%)	
Sample Depth (cm)	1096	835	435	
^{14}C age	6030 ± 40	5120 ± 35	2800 ±20	
Calibrated age range (95.4%)	5034 – 4806 BC	3991 – 3797 BC	1006 – 904 BC	
Date for sedimentation rates	**4920±110 BC** (Mean at 95.4%)	**3890±100 BC** (Mean at 95.4%)	**950±50 BC** (Mean at 95.4%)	
Sample Depth (cm)		933	467	
^{14}C age		5420 ± 35	2880 ±20	
Calibrated age range (95.4%)		4357 – 4071 BC	1124 – 996 BC	
Date for sedimentation rates		**4210±140 BC** (Mean at 95.4%)	**1060±60 BC** (Mean at 95.4%)	
Sample Depth (cm)			581	
^{14}C age			3180 ± 20	
Calibrated age range (95.4%)			1499 - 1421BC	
Date for sedimentation rates			**1460±40 BC** (Mean at 95.4%)	

* Radiocarbon date beyond range of calibration curve (Reimer et al., 2013)
** Historical records support using the maximum date from the age interval instead of the average date.
*** If put in context with the timing of initial deposition of legacy sediment in a nearby core – EPN (1643 AD), the date 1648 AD is more probable.

1.4.4. ^{210}Pb geochronology.

Cores AWc, AWa, EM, EPN and EPS were subsampled in 1 or 2 cm intervals. The bulk sediment was freeze dried and dry mass recorded. ^{210}Pb activities were determined via isotope-dilution alpha spectrometry for ^{210}Po, granddaughter isotope of ^{210}Pb, acknowledging that ^{210}Po and ^{210}Pb are in secular equilibrium with each other (Flynn, 1968; El-Daoushy et al., 1991; Matthews et al., 2007; de Vleeschouwer et al., 2010). To calculate excess ^{210}Pb, the supported (^{226}Ra) activity was subtracted from the total ^{210}Pb value (Appleby and Oldfield, 1992). Supported (^{226}Ra) activity was measured via gamma spectrometry. Freeze-dried and homogenized samples were packed into plastic petri dishes and sealed for over 19 days to allow sample equilibration with ^{222}Rn. Gamma counting was conducted on well and planer germanium detectors, calibrated with certified natural reference standard IAEA-300. ^{226}Ra was measured indirectly, by calculating emission of it daughters ^{214}Pb (at 295 and 351 keV) and ^{214}Bi (at 609.3 keV) (Benninger and Wells, 1993).

1.4.5. Side scan sonar.

To reconnoiter the subaqueous geomorphology, side-scan sonar data were collected, from the prodelta using an Edgetech 4200 dual-frequency (120/410 kHz) system. Data were collected using 410 kHz, at a 50-m range and in a discontinuous grid pattern. Data were processed by applying a time-varying gain and mosaicked using Chesapeake Technology Inc. SonarWiz software. Interpretations were verified in the field with diver observations.

1.4.6. Maps and aerial photography.

To assess changes in the morphology of the delta over centennial and decadal time scales, digital historical maps were obtained from the University of North Carolina Map collection. Maps from 1738 (Wimble, 1738), 1775 (Mouzon, 1775), 1808 (Price and Strother, 1808), 1818

(Lewis and Carey, 1818), 1822 (Fielding and Kneass, 1822) and 1833 (Brazier et al., 1833) were examined to reconstruct morphologic changes associated with the closing of the Roanoke Inlet. To reconstruct the maximum extent of the bayhead delta and its shoreline movements, we used historical bathymetric charts from 1860 (United States Coast Survey, 1860) and 1864 (United States Coast Survey et al., 1864). All map images were georeferenced using a spline transformation method and 15-27 referencing points per map in ArcMap software (ESRI (Environmental Systems Resource Institute), 2015). Georeferencing of the historical map images caused significant distortion that prevented quantitative analyses, however the maps provided sufficient information for qualitative assessment of morphologic change in the study area. Modern aerial photographs from 1954 (U.S. Geological Survey (USGS), 1954) and 2012 (U.S. Department of Agriculture (USDA), 2012) were used to calculate modern land loss and rate of shoreline retreat using ArcGIS software (ESRI (Environmental Systems Resource Institute), 2015).

1.5 Results and Interpretation.

1.5.1 Depositional Environments.

The depositional environments sampled in the cores include: delta plain, fluvial channel, interdistributary bay, delta front, prodelta and subaqueous point bar (Figure 4). Lithologic descriptions of the cores were used to differentiate the environments and develop a stratigraphy. The characteristics used in describing the sediments were color, grain-size, sedimentary structures, and the presence of plant remains. The top of all cores are composed of orange-stained poorly sorted sediments that contain a bimodal grain-size distribution of clayey coarse silt (Figures 4, 5 and 6b). The origin of these sediments are likely ultisols of the piedmont and the sediments were previously interpreted as legacy sediments (Hupp et al., 2009b, 2015; James,

2013). A radiocarbon date from the bottom of the orange-stained units in cores EPN and EPS (Table 1) correspond with the time of the first settlements in the 17th century, when intensive deforestation and agriculture accelerated erosion within the Roanoke watershed.

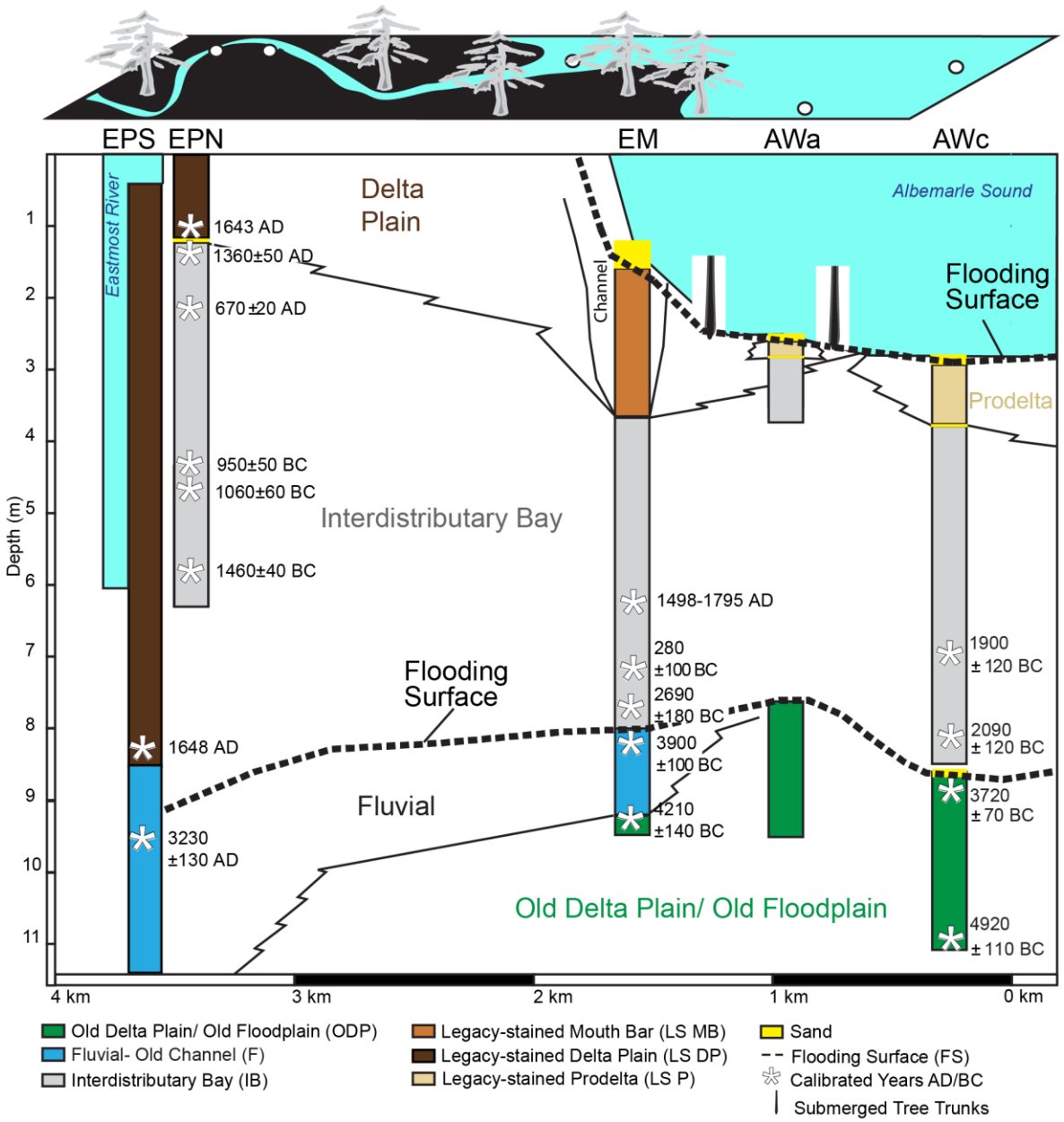

Figure 4. Crossection of the study area in the Eastmost River, presenting stratigraphy, depositional environments and flooding surfaces. Asterisks mark depths of radiocarbon-dated material expressed as averaged calibrated dates (95.4% probability) radiocarbon dates in parenthesis.

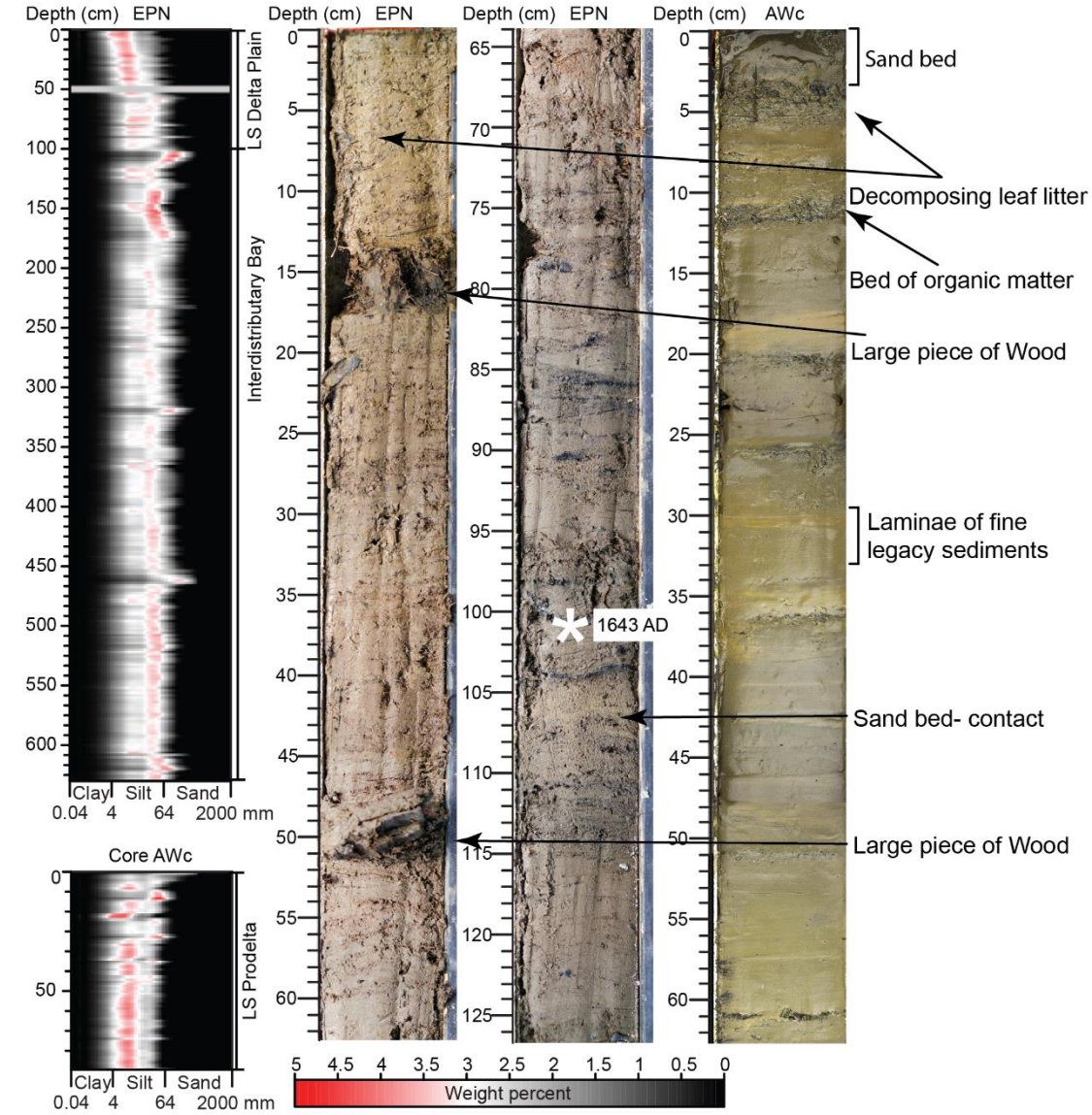

Contacts

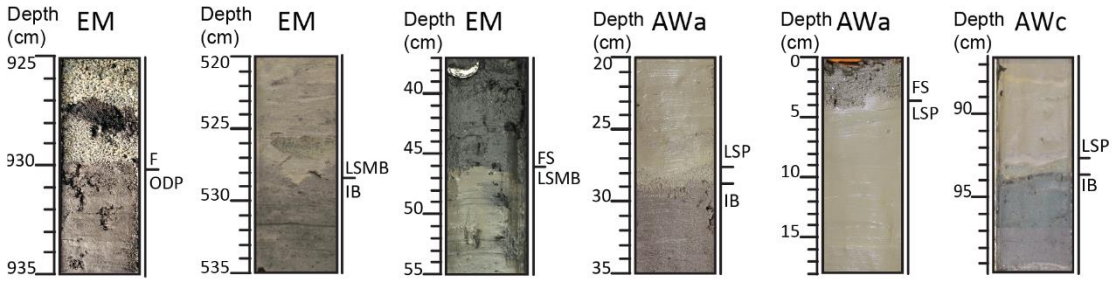

Figure 5.

Figure 5. Grain-size distribution with depth in core EPN shows a sharp transition between finer delta plain and coarser interdistributary bay units. Photos show the distribution of legacy sediments and contact between delta plain and interdistributary bay in core EPN. Grain-size distribution with depth in core AWc shows the upper sand bed and silty prodelta unit. Photos of core AWc show beds and laminae of red legacy sediment delivered to the prodelta during high-discharge events. Lower core photos show contacts between different sedimentary units (abbreviations explained in Figure 4).

Delta plain The top 112 cm of core EPN , collected from the delta plain, sampled orange-stained grading to dark brown at depth, carbonaceous sediment, with large pieces of woody material including roots and tree branches, and smaller pieces of decomposing leaves (Figures 4, 5). The sediment is moderately sorted and has a bimodal grain-size distribution with peaks at φ 4.7 (coarse silt) and φ 6.2 (fine silt), with a small percentage of clay (mean grain size of φ 4.6-6.7) (Figure 6a). Organic material dated at the base of the unit is from 1643AD (Table 1). A nearly identical unit, the only difference being its dark brown color, was sampled at depth in cores EM, AWa and AWc and was interpreted as an older delta plain unit (Figures 4, 6a). Organic material from the older delta plain unit was radiocarbon dated at 1096 cm depth in core AWc as 4920±110BC, at 933 cm depth in core EM as 4210±140BC, and at 882 cm in core AWc as 3720±70BC (Table 1).

Subaqueous point bar Core EPS, collected adjacent to the Eastmost River Channel, sampled an 845 cm thick, orange clayey silt unit with laminae of medium-grained sand, and organic material. The unit has a bimodal grain-size distribution with a primary mode of coarse silt and a secondary mode of fine silt (Figure 6b). Organic material sampled from the base of the unit was dated at 190 ± 30 BP, which is too recent to assign a single calibrated date to it. Radiocarbon calibration curves (Reimer et al., 2013) suggest that the layer started forming between 1648AD and 1950 AD; however, if put in context with the timing of initial deposition of legacy sediment in a nearby core – EPN (1643 AD), the date 1648 AD is more probable.

Fluvial Channel Cores EPS and EM, collected adjacent to the Eastmost River Channel, sampled a poorly sorted fine to coarse sand (mean 1.0 to 2.4 phi) at their base from 875-1150 cm and 800-920 cm, respectively (Figure 6a). Core EPS was collected 1 m from the channel thalweg and core EM was collected from the mouth. Erich (1980) also sampled fluvial channel deposits as moderately to poorly sorted sand in 16 cores in our study area at depths 2.7- 11.9 m and the unit is likely continuous below the entire bayhead delta. Organic material sampled from the fluvial unit at 962 cm in core EPS and 835 cm in core EM was dated as 3230±130BC and 3890±100BC, respectively (Table 1).

Interdistributary Bay Cores EPN, EM, AWa and AWc sampled gray bioturbated mud with beds and laminae of organic material (0.2-5 cm thick) and coarse-grained sand (0.3-5 cm thick). Sand-filled *Chondrites* and *Thalassinoides* burrows were also found in the unit (Figure 4, 5, 6a). The unit shows an overall fining upward sequence and whole pieces of wood were encountered at its base. Overall, the unit contains less organic material than the delta plain sediment. The mean grain size of the unit in cores EPN and AWa are between 4.3, 5.5 phi, and 5.5 to 5.8 phi, respectively (Figure 6a). The unit is thick and cores EM and AWc sampled it in its entirety as 325 and 515 cm, respectively. Currently, there is no interdistributary bay present to sample and compare to this unit, but the unit is similar to interdistributary bays sampled at the Mobile Bayhead Delta (Rodriguez et al., 2008) and the Trinity Bayhead Delta (McEwen, 1969) along the northern Gulf of Mexico strand. Multiple radiocarbon dates were obtained from the interdistributary bay unit indicating deposition between 2690±180BC and 1650±150AD (Table 1).

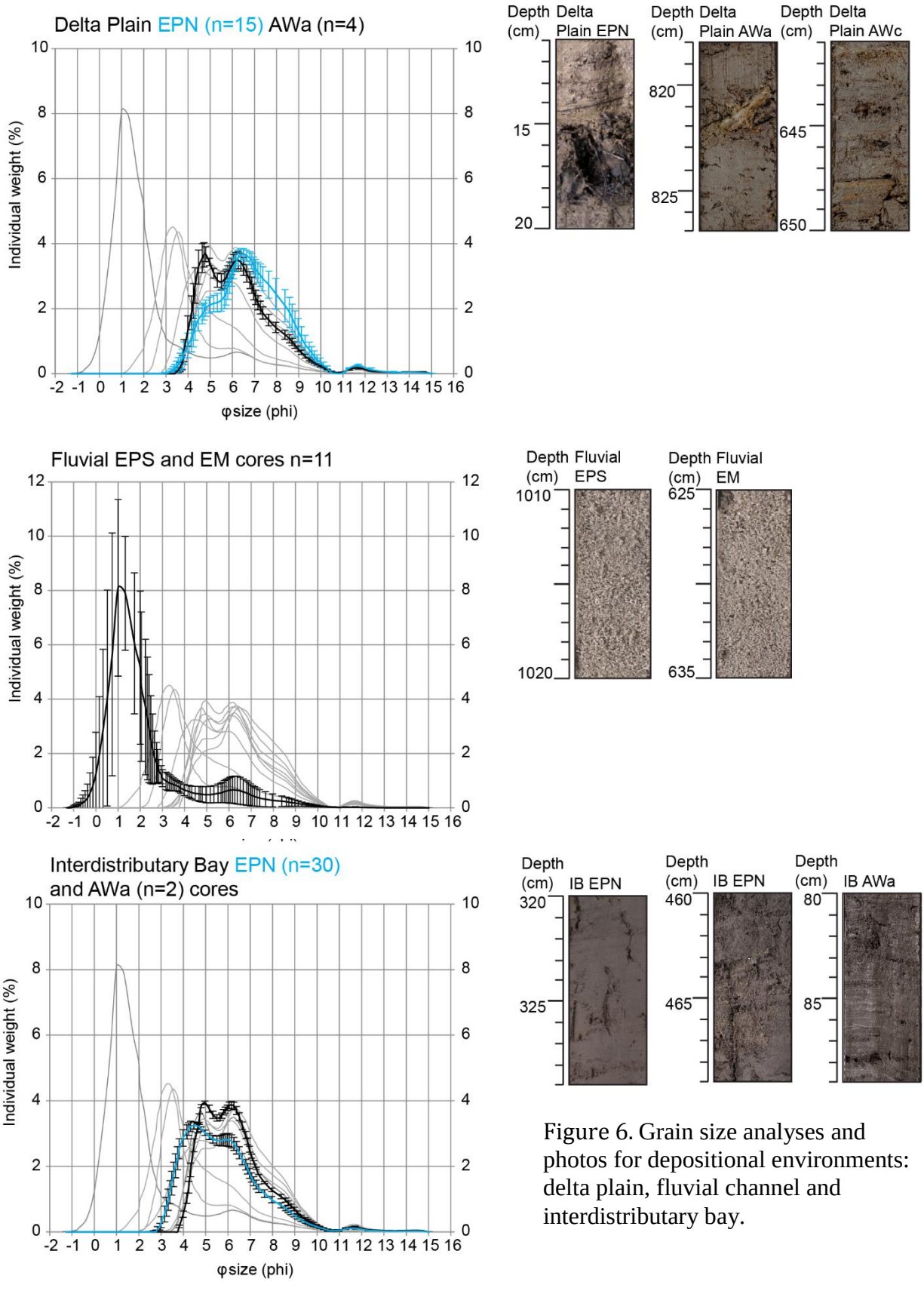

Figure 6. Grain size analyses and photos for depositional environments: delta plain, fluvial channel and interdistributary bay.

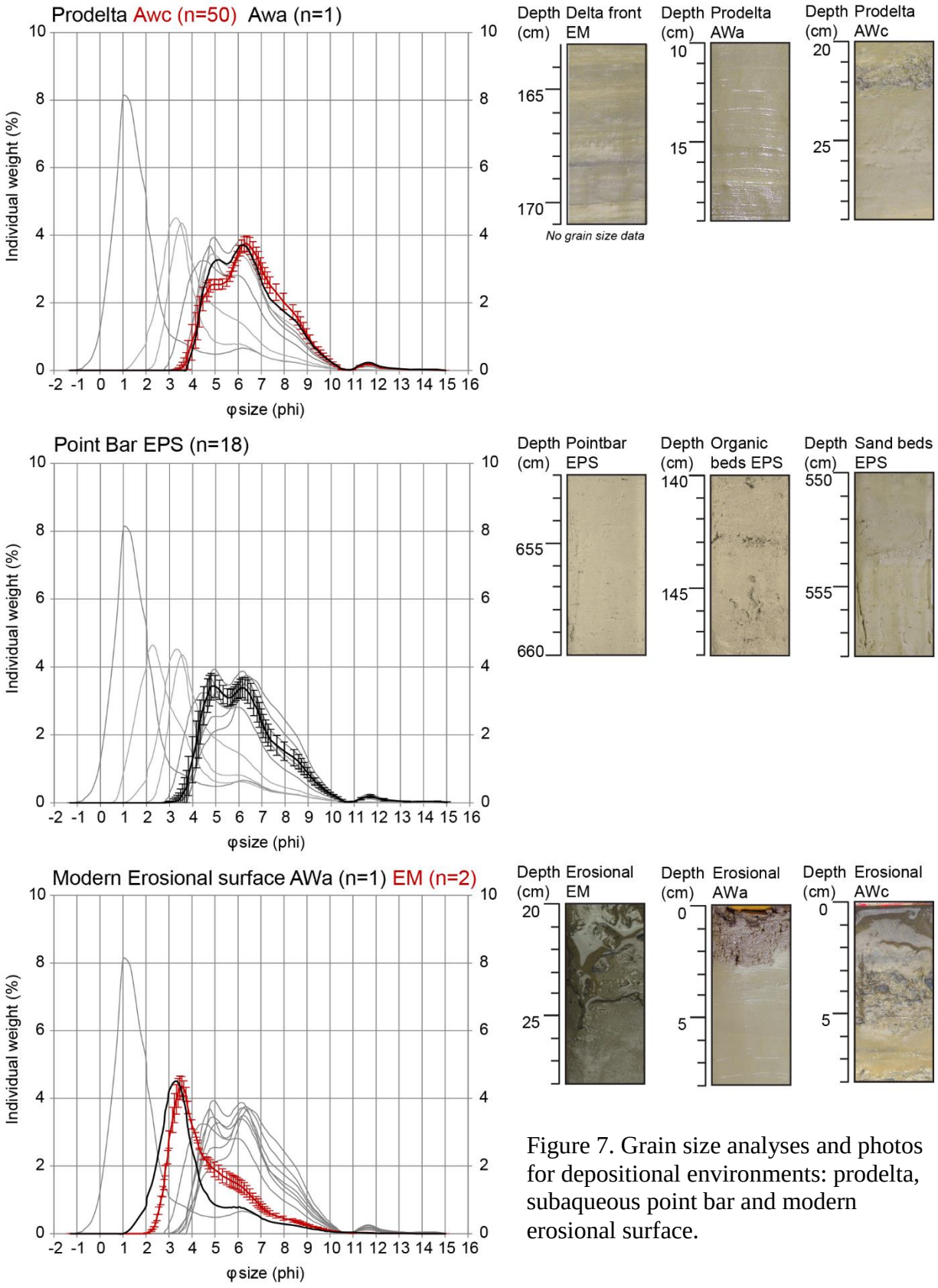

Figure 7. Grain size analyses and photos for depositional environments: prodelta, subaqueous point bar and modern erosional surface.

Delta front Core EM, taken from the mouth-bar of the Eastmost River, sampled orange and gray fining upward clayey silt from 212 to 36 cm. The unit shows beds of orange-stained legacy mud (5 cm -12 cm thick), beds and laminae of organic matter (0.3 cm- 1.5 cm thick) and sand laminae (0.2- 0.4 cm thick) (Figures 4, 5). At the bottom of the unit are burrows filled with fine sand. The modern mouth bar at the top of the core has sampled fine sand 0-36 cm.

Prodelta Cores AWa and AWc, collected from upper Albemarle Sound, sampled orange and gray fining upward poorly sorted clayey silt (Figures 4, 5). The grain-size distribution is bimodal with a primary mode of coarse silt and a secondary mode of fine silt. The mean grain size ranges from 4.8-6.9 phi, which are the smallest particle sizes sampled from the delta (Figure 6b). The unit contains discrete beds and laminae of gray clayey silt and laminae of organics and fine-grained sand. The unit thickens seaward to 110 cm sampled in core AWc (Figures 4, 5).

1.5.2. Stratigraphy

The oldest and the deepest unit sampled in the cores was the delta plain. This basal unit is overlain by interdistributary bay sediment seaward, and fluvial-channel sand landward (Figure 4). The most seaward core, AWc, sampled a 2 cm-thick sand layer at the contact (860 cm) between delta plain and interdistributary bay, interpreted as an erosional flooding surface. Organic material sampled below and above the sand layer in core AWc constrains the timing of the environmental transition to between 3720±70 BC and 2090±120 BC, respectively (Table 1). Farther landward, core EM sampled fluvial channel sand in sharp contact at 800-cm depth, with the interdistributary bay mud, above (Figure 4). Dates below and above the contact constrain the timing of the environmental change to between 3890± 100BC and 2690±180BC, respectively (Table 1). The contact is interpreted as the landward extension of the flooding surface sampled in core AWc, based on its similar age. Orange-stained legacy sediment, in sharp contact with the

underlying interdistributary bay unit, was sampled in all of the cores. In core EPN, a 1-cm thick sand bed marks the contact with delta plain sediment that extends to the surface and forms the modern delta plain landscape (Figure 4). That environmental change occurred between 1360±50AD and 1643AD (Table 1) based on dates below and above the sand bed, respectively. The regressive stratigraphic succession of interdistributary bay below delta plain (EPN) and mouth bar (core EM) environments, and presence of fluvial channel below the point bar deposits (EPS), indicates a change in depositional regime to rapid sedimentation. The time of increased sedimentation coincides with falling relative sea level (Figure 7) (Kemp et al., 2011), which likely contributed to the regression. Farther into Albemarle Sound, prodelta clayey silt was deposited above the interdistributary bay mud in cores AWa and AWc (Figure 4).

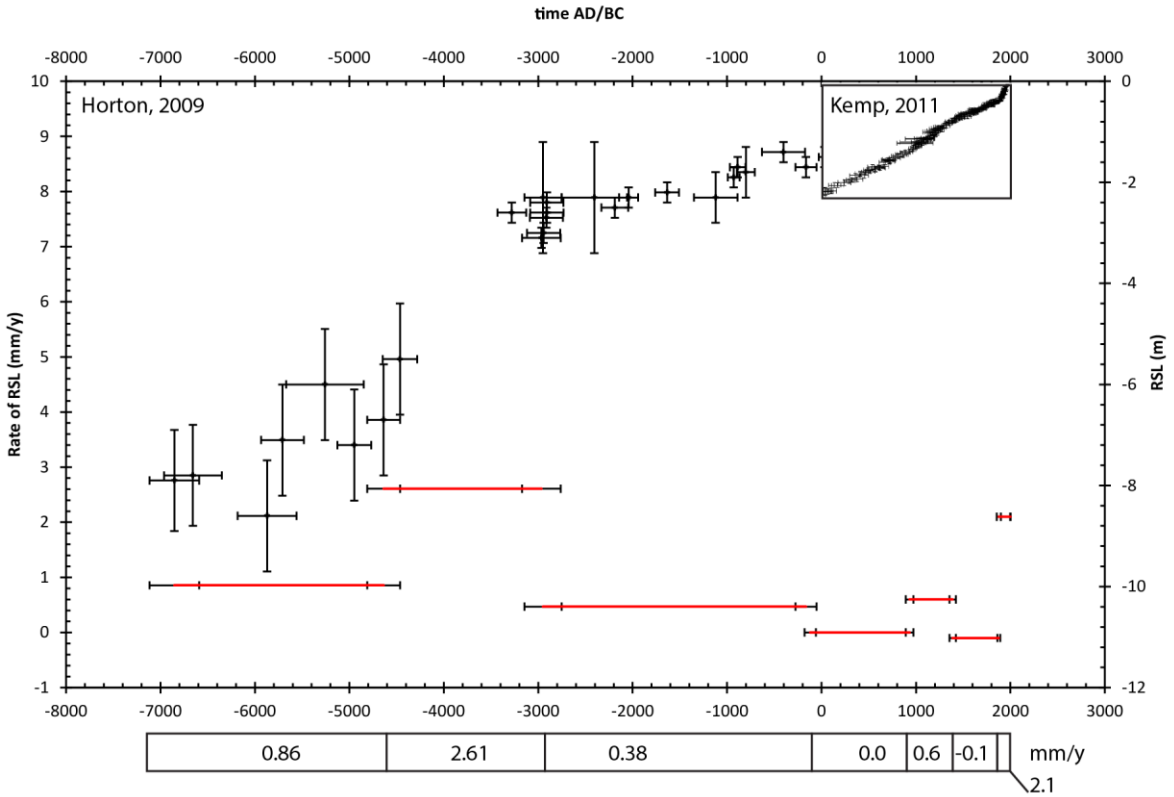

Figure 8. Holocene sea level points for North Carolina. Rates of sea-level rise and fall are marked in red and black, respectively (Horton et al., 2009; Kemp et al., 2011).

The interbedded orange and gray color changes of the prodelta unit likely indicate variations in river discharge with the orange legacy sediment delivered to the prodelta during high discharge events. In core AWc, a 1-2 cm thick sand bed was sampled at the contact between the interdistributary bay and prodelta, but no radiocarbon dates were collected above or below this transgressive surface. Based on the presence of legacy sediment, the environmental change must have occurred after the first European settlements in the Roanoke watershed. A dark gray fine-grained sand bed (2-40 cm in thickness) was sampled at the top of cores EM, AWa, and AWc, and interpreted as a lag deposit associated with modern erosion of the delta front.

1.5.3 ^{210}Pb geochronology

Inventories of excess ^{210}Pb (total quantity per cm^2 of sediment surface) elucidate recent depositional and erosional episodes in the delta. Inventories of excess ^{210}Pb ($t_{1/2}$= 22.23 yr (Be et al., 2008)) were calculated by summing decay-corrected excess ^{210}Pb activities (dpm/g) and aerial section dry mass (g/cm^2) for all core sections. Based on soil and salt-marsh cores collected from Eastern North Carolina, inventories of excess ^{210}Pb that are supported by atmospheric deposition in our study area, are expected to average 26.52 dpm/cm^2 (Benninger and Wells, 1993). Inventories for each core are presented in table 2 as a relative inventory (RI), the ratio of measured inventory (MI) and expected inventory, 26.52 dpm/cm^2 (Benninger and Wells, 1993). RI below 1 indicates a net removal of sediments due to erosion. Cores AWa (prodelta) and EM (delta front) show no excess ^{210}Pb activity, MI of 0 dpm/cm^2, RI of 0 and was interpreted as an erosional site. Seaward, core AWc (prodelta) has a very low RI of 0.01 (MI 0.22 dpm/cm^2) and is interpreted as a non-depositional/erosional site. Two cores with higher inventories are a delta plain core EPN with 0.21 RI (MI 5.5 dpm/cm^2) and subaqueous point bar core EPS with RI 0.09

(MI 2.5 dpm/cm^2). The inventories for these two sites also suggest that both sites are net erosional.

Table 2. Excess ^{210}Pb inventories and sedimentation rates.

Core	AWc Prodelta	AWa Prodelta	EM Delta front	EPN Delta plain	EPS Point-bar
Depth of the LS layer (cm)	75	25	240	101	850
Active ex^{210}Pb depth 1875-2009 AD (cm)	4	0	0	37	80
Measured Inventory (dpm/cm^2)	0.22	0	0	5.5	3.0
Relative Inventory	0.01	0	0	0.21	0.11
Highest ex^{210}Pb activity (dpm/g) and date (CIC)	0.91 (1941 AD)	0 (<1875AD)	0 (<1875AD)	7.41 (2009AD)	2.05 (1966AD)
Sedimentation rates (cm/yr) in **early Anthropocene 1643AD- 1875AD**	0.31	>0.11	>1.0	0.28	3.32
Sedimentation rates (cm/yr) in **recent Anthropocene 1875AD-present**	Non-depositional/ erosional	Non-depositional/ erosional	Non-depositional/ erosional	0.28 Net erosional	0.88 Net erosional

The net sedimentation rates (cm/yr) of the legacy sediment were derived for two periods and are expressed as a change in depth through time (cm/yr). The first period (early Anthropocene), from 1643AD to 1875AD, and the second period (recent Anthropocene) from 1875AD until present. For the purpose of this study, we use AD 1500 as the beginning of the Anthropocene following a timeline proposed by Braje and Erlandson, (2014), as this was "the beginning of the Columbian Exchange, which created vast faunal, floral, ecological, and cultural changes globally". The date of 1643AD, in the early Anthropocene period, is a maximum calibrated (95.4%) radiocarbon date from the base of the legacy-sediment unit in core EPN (Table 1) and represents the beginning of legacy-sediment deposition in the Roanoke Delta. The end of the early Anthropocene period, 1875AD, is derived from the highest excess ^{210}Pb

concentration measured in the Roanoke Delta (7.41 dpm/g), decay corrected 6 half-lives (133.4 years), down to the supported level (excess activity of 0.1 dpm/g), and marks the bottom of the excess ^{210}Pb active layer. Sedimentation rates derived for the early Anthropocene are the highest at EPS (3.32 cm/yr), 0.28 cm/yr at EPN and 0.31 cm/yr at AWc. Since cores EM and AWa have no active excess ^{210}Pb layer, age of the top of the cores could not be derived, and thus the sedimentation rates for both cores presented in table 2 are underestimated.

The sedimentation rate for the recent Anthropocene was derived from the base of the excess ^{210}Pb active layer (1875AD) to the top of the core. Cores with an excess ^{210}Pb active layer had significantly different maximum excess ^{210}Pb activities in the top layer. The highest activity was 7.41 dpm/g, measured in core EPN, with cores EPS and AWc yielding lower activities of 2 dpm/g and 0.91 dpm/g, respectively (Table 2). In core EPN, sedimentation rates were the same for both early and recent Anthropocene (0.28 cm/yr). Lower activities in the top layer of cores EPS and AWc are consistent with the low MI and RI values and non-depositional/erosional nature of these two sites. In order to calculate the age of the top layers in cores EPS and AWc, a constant initial concentration dating model (CIC) (Goldberg, 1963; Krishnaswamy et al., 1971; Sanchez-Cabeza and Ruiz-Fernández, 2012) was implemented, assuming an initial concentration of 7.41 dpm/g (the highest recorded concentration in top layer of the EPN core). For cores EPS and AWc, the top layers were deposited in 1966AD and 1941AD, respectively (Table 2), and both sites are currently non-depositional. At core EPS during the recent Anthropocene, the sedimentation rate was almost four times smaller (3.32 cm/yr) than during the early Anthropocene (0.88 cm/year). At core AWc, the active excess ^{210}Pb layer is only 4-cm thick, a depth that can be easily disturbed by currents and waves, therefore, we interpret AWc as non-depositional or erosional during the recent Anthropocene.

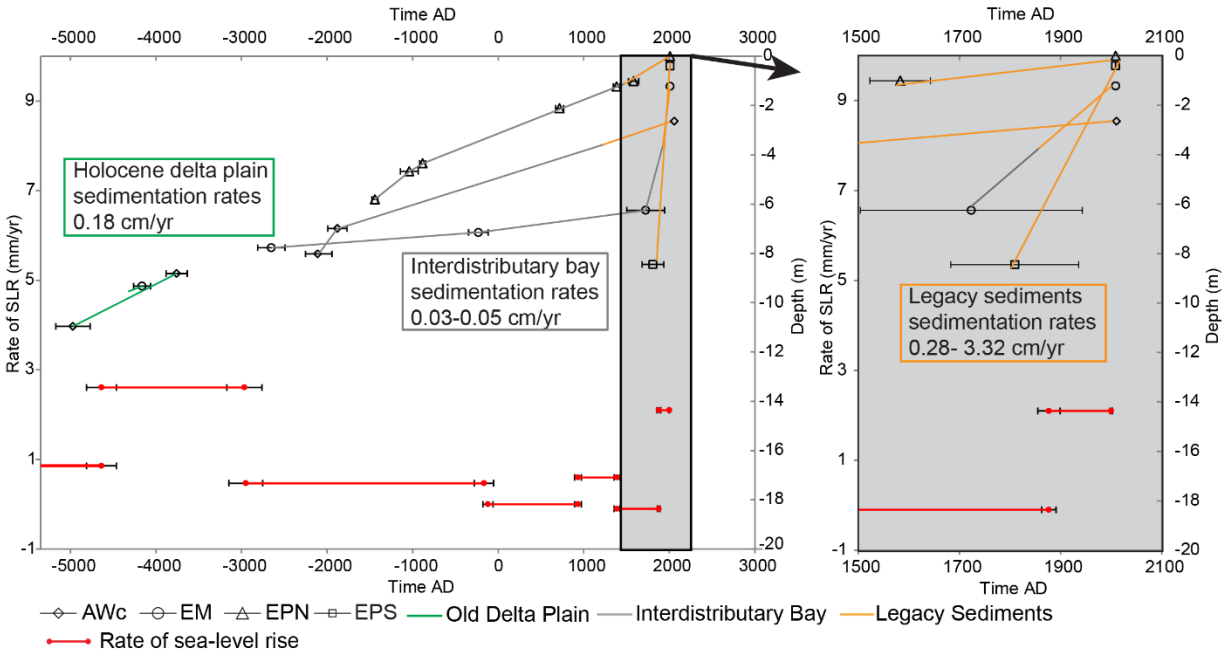

Figure 9. Accumulation Rates in the Roanoke Bay-head Delta. Accumulations expressed in colors: green for an early Holocene delta plain (0.18 cm/yr), grey for the interdistributary bay (0.03-0.05 cm/yr), and yellow for legacy sediments (0.28-10.03 cm/yr).

1.5.4 Historical Shoreline Changes.

Changes in the morphology of the delta front were constrained from historical maps (1860, 1864, 1954, and 2012) and the side-scan sonar data (Figure 9). The side-scan sonar imaged multiple targets that cast shadows from circular and linear objects that ranged from 0.5 m to 2 m in height (Figure 9). Diver observations confirmed that the targets were submerged tree stumps and logs. The seaward limit of tree stumps and logs were mapped from the discontinuous grid of mosaicked side-scan sonar data. The georeferenced maps of the Roanoke Delta from 1860 and 1864 (United States Coast Survey, 1860; United States Coast Survey et al., 1864) show that the current tree stumps position is in line with features marked on those nineteenth century maps as the seaward edge of "shoals" at less than 90-cm water depth, with "tree stumps" and "submerged trees". The delta-front shoreline must have been at the location of the submerged tree stumps and the shoal, sometime before the 1860 map was made, suggesting a long history of

delta front retreat (Figure 9). Based on analyses of aerial photographs, between 1954 and 2012, the modern shoreline retreat rate was ~2469 m^2/yr.

1.6. Discussion

1.6.1. Holocene Delta Evolution.

Between 4920±110BC and 3720±70 BC, the paleo-Roanoke delta extended into modern Albemarle Sound and an extensive vegetated delta plain existed in the study area (Figure 10a). This delta plain unit, sampled in cores EM, AWa, and AWc, accreted at a rate of 0.18 cm/yr (Figure 8). Sea-level during that time was rising at rate of 0.261 cm/yr (Horton et al., 2009) (Figures 7, 8), which caused an increase in accommodation and landward movement of the paleo-Roanoke River mouth (Figure 10b). The study area started transitioning to an interdistributary bay environment sometime after 3700 BC, marked by the erosional surface overlaying the delta plain in core AWc (Figure 4). Sand and organic material was likely supplied to the interdistributary bay episodically during flood events that overtopped channel levees and sediment mixing occurred during intervening times by benthic organisms. In core EM the delta plain is overlain by fluvial deposits (Figure 4, 5). This sequence suggests that the river channel changed its position and eroded the top of the paleo delta plain unit at the core location. Sedimentation rates within the interdistributary bay unit were similar to the rate of sea-level rise, 0.03-0.05 cm/yr. The interdistributary bay unit is crowned with a 1-cm thick sand layer that marks a change in depositional regime to higher sedimentation associated with the deposition of legacy sediment during the early Anthropocene (Figure 4, 5).

1.6.2. Early Anthropocene Delta Evolution (1643AD to 1875AD).

All modern deltaic depositional environments sampled (delta plain, delta front and prodelta) have a distinct orange color indicative of legacy sediment. Legacy sediment was

introduced to the lower Roanoke delta in the late 17th century after the first Europeans settled in the watershed and cleared forest for agriculture. During that time until the 19th century, sea-level was stable or falling (Kemp et al., 2011) (Figure 7). With a high sediment supply and a stable sea level, an extensive bayhead delta plain formed and extended into upper Albemarle Sound. Between 1643AD and 1875AD, the orange-stained legacy sediment prodelta in core AWc was accreting at a rate of 0.31 cm/yr (Table 2). The legacy prodelta sediment unit sampled in core AWa is located between tree stumps, suggesting a patchy distribution of prodelta clays at this proximal prodelta location. The entire prodelta unit at AWa was deposited prior 1875AD at the rate of 0.11 cm/yr or higher (Table 2). In core EM, collected from the channel mouth bar, there is no excess ^{210}Pb present in the legacy sediment unit, thus the entire layer was deposited prior 1875AD at rate of 1.03 cm/yr or higher (Table 2). In the Early Anthropocene, sediments in the delta plain at the EPN core location accumulated at a rate of 0.28 cm/yr (Table 2) and are higher compared to the sedimentation rates in the Holocene delta plain unit that accreted at rate of 0.18 cm/yr (Figure 8). The highest sedimentation rates of 3.32 cm/yr were found in the subaqueous point bar core EPS (Figure 8, Table 2) and are similar to the rates reported for the same time period by Hupp et al., (2015) for the levees up river from the study area (2.3-4 cm/yr). Sedimentation rates are higher in core EPS than in core EPN due to the more continuous supply of sediment to the subaqueous point bar as opposed to the subaerial delta plain. A line of submerged tree stumps (Figure 9, 10c) marks the eastward extent of the bayhead delta during the early Anthropocene.

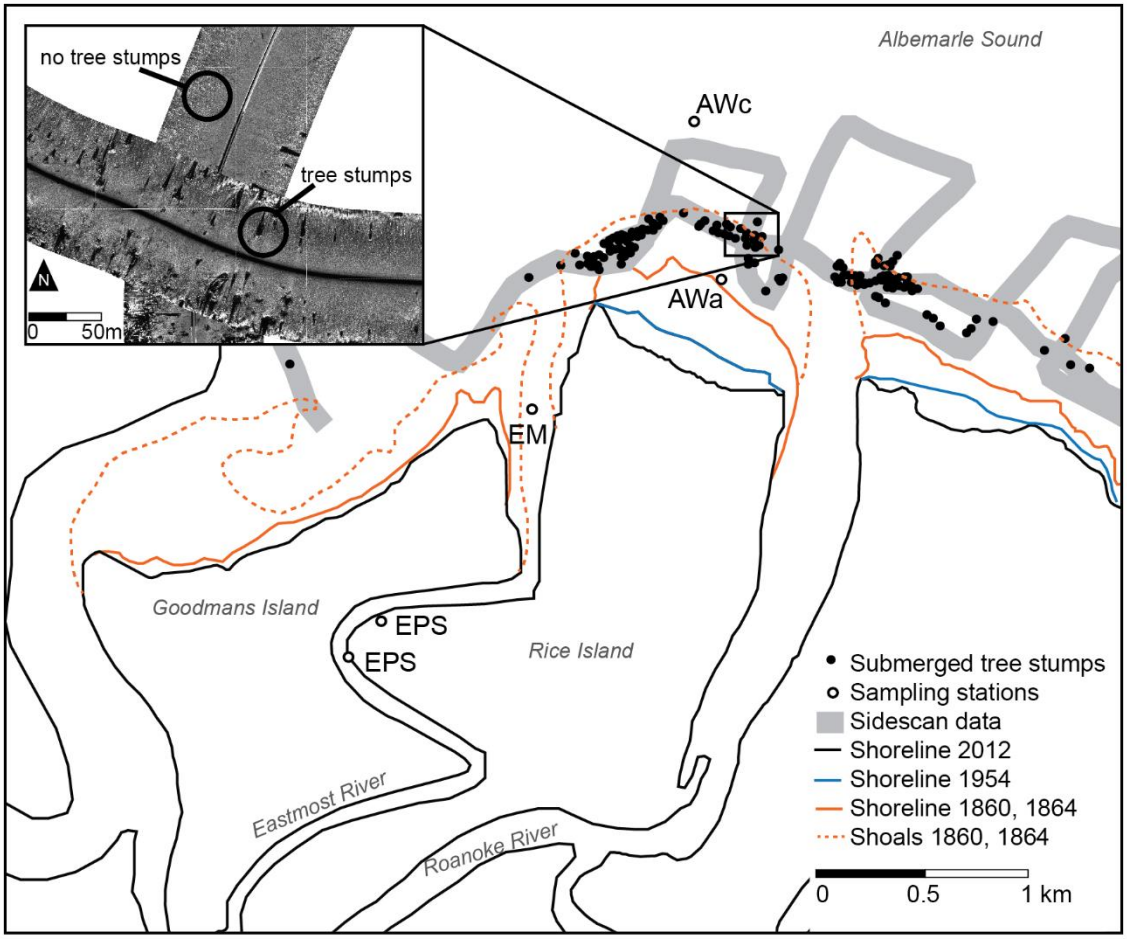

Figure 10. Reconstruction of the Roanoke bayhead delta shoreline during the early and recent Anthropocene based on historical maps from 1860 and 1864 in orange (United States Coast Survey, 1860; United States Coast Survey et al., 1864), from 1954 and 2012 aerial photography in blue (U.S. Geological Survey (USGS), 1954) and in black (U.S. Department of Agriculture (USDA), 2012), respectively. Position of submerged tree stumps imaged with the side-scan sonar (inset) are marked with black dots on the map.

1.6.2. Recent Anthropocene Delta Evolution.

Sometime before 1860AD, the delta changed its sedimentation regime from depositional to non-depositional and/or erosional. This change, recorded in stratigraphic and geochemical data, coincided with the recent rapid increase in the rate of relative sea-level rise (40 cm rise since 1860) (Kemp et al., 2011) (Figure 7), a decrease in sediment supply associated with better agricultural management in the 19th century, and dam construction in the 20th century (Hupp et al., 2015; Meade, 1982; Trimble, 1974). The sand bed at the top of cores AWc, AWa and EM are

indicative of the erosional state of the prodelta and delta front. The ^{210}Pb data confirm that those sites have been non-depositional/erosional since before 1875AD. Sedimentation rates in the delta plain during the recent Anthropocene, based on the depth of the excess ^{210}Pb active layer and the top of the core, were 0.28 cm/yr, similar to sedimentation rates measured for the early Anthropocene. However, even though the measured excess ^{210}Pb inventories in the delta plain (EPN) are the highest recorded in the study area (MI=5.5 dpm/cm^2), the RI value is very low (0.21), suggesting that today the delta plain at this site is net non-depositional/erosional. Geochemical data also show a shift towards lower sedimentation rates during the recent Anthropocene at the subaqueous point bar site EPS (Table 2). Excess ^{210}Pb inventories are half of that measured in core EPN, but the active layer is much thicker at the point bar (80 cm thick) with sedimentation 0.88 cm/yr for period 1875-1966AD almost four times lower than during the early Anthropocene. Low inventories in that core as well as lack of sediments deposited after 1966 suggests that the point bar became a non-depositional and/or erosional site at that time. Map analyses confirm findings from geological and geochemical data (Figure 9). The bayhead delta retreat started some time before 1860 (Figure 9), and between 1954 and 2013 the mean horizontal shoreline retreat rate is 120 cm/yr to 410 cm/yr and accounted of 2469 m^2/yr of delta loss. Improved farming practices, dams and an increase in the rate of sea-level rise, all likely contributed to reducing sediment supply to the delta front and the erosion documented here (Figure 10). Shoreline erosion in Western Albemarle Sound was previously measured by (Bellis et al., 1975; Riggs et al., 1978) at 60 cm/yr due to wave erosion. Results from our study show rates of shoreline loss more than double those reported in previous studies because stratigraphic data and the position of submerged tree stumps in the subaqueous delta were included.

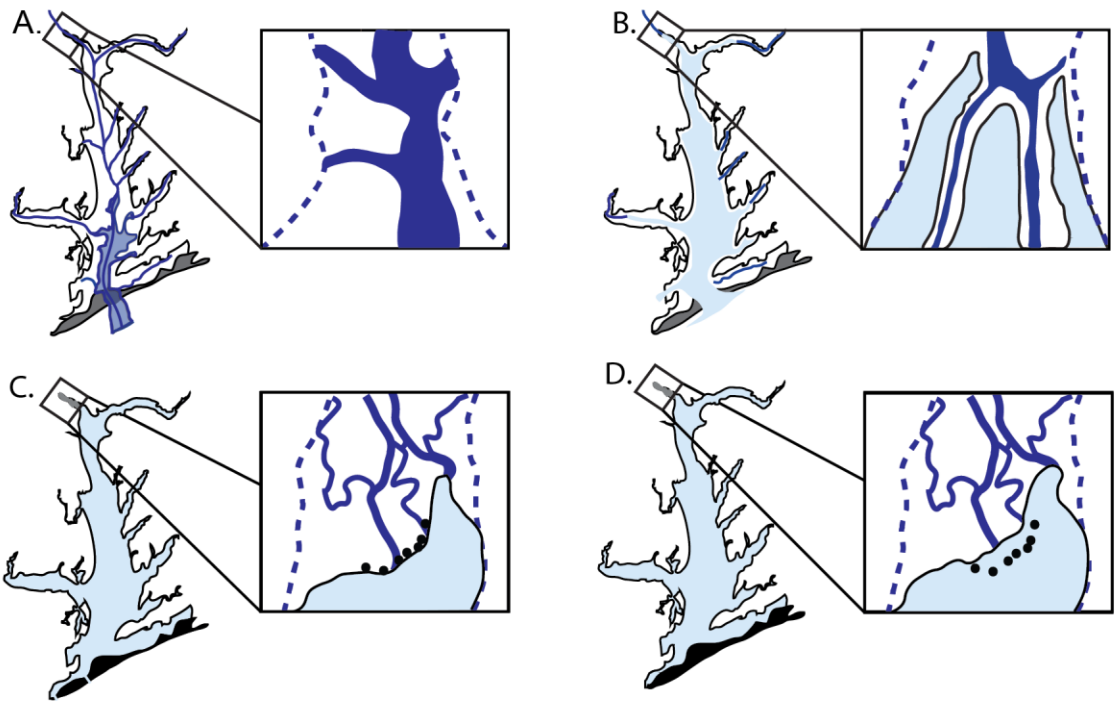

Figure 11. Conceptual model illustrating evolution of the bayhead delta in context with Albemarle Sound. A. Late Pleistocene, Early Holocene Paleo-Roanoke Valley during the Last Glacial Maximum ca. 18 kyr BP (in dark blue). In the study area, floodplain inundation only occurred during overbanking events. B. Holocene ca 4 kyr BC flooding of the study area and formation of the interdistributary bay. C. Early Anthropocene increase in sediment supply associated with land-use change, islands trapped sediment facilitating accretion. The delta reached its maximum extent ~1860AD. D. Recent Anthropocene Improved agriculture practices and installation of a series of impoundments in the watershed resulted in decreased sediment supply followed by erosion and bayhead delta back-stepping since late 1800'AD. The evolution of Albemarle Sound based on Culver et al., (2008), paleo-Roanoke channel in A based on Erlich, (1980)).

1.7. Conclusions

During the last deglaciation, marine flooding caused transgression of the coastline and formation of modern Albemarle Sound as the Roanoke paleo-valley inundated. At least by 4770 BC an extensive Roanoke delta plain existed in upper Albemarle Sound. Inundation continued and the delta plain turned into an interdistributary bay around 3700BC, and continued to slowly accrete and fill sediment accommodation until the 17th century. Sedimentation rates were

keeping up with the low rates of sea-level rise until 1600-1700AD. With the arrival of the first colonists in the Roanoke watershed the natural sediment load of the river was disrupted. Deforestation associated with the initiation of agriculture by settlers in the drainage basin and poor management of runoff introduced a large quantity of sediment into the river. Since 1643AD, sediment deliveries greatly overwhelmed the low rate of sea-level rise at the time, resulting in rapid accretion of the bayhead delta. At that time, the interdistributary bay filled with over two meters of delta plain sediment. 200 years later, rates of sea-level rise increased and agricultural practices improved, increasing sediment accommodation and decreasing the amount of sediment delivered to the mouth of the Roanoke River. These two changes led to the initiation of bayhead delta retreat and land-loss. The construction of impoundments, completed in 1963AD, likely magnified erosion of the delta by retaining sediment behind the dams and causing a drastic decrease in sediment supply to the delta. At present, the delta plain is at sea level and its low accretion rate cannot keep up with accelerating sea-level rise. This study stresses that bayhead deltas are highly sensitive to changes in sediment supply, the rate of sea-level rise and human-induced modifications to the sediment budget. Findings presented here should be taken under consideration in management efforts to conserve bayhead deltas, globally. With current predictions of accelerated sea-level rise, bayhead deltas are subject to back-stepping; however, changes in management of runoff in the watershed and/or river flow could increase the supply of lithogenic material to the shore and improve sustainability of the bayhead delta wetlands.

CHAPTER 2: CONTROLS ON DEPOSITIONAL AND EROSIONAL EVENTS IN THE MODERN DELTA PLAIN OF RETREATING BAYHEAD DELTA

2.1 Abstract

River deltas form at river-ocean interfaces, where riverine sediments accumulate faster than rivers can disperse into the ocean. Proximity to rich alluvial soils and access to fresh-water and marine resources make deltas among the most populated areas in the world. Raising sea-level threatens all coastal environments, but deltas due to the complex processes governing their existence, may have a different sensitivity and time scale of response. Aggradation of deltaic plains is well documented on geological- millennial time scales in well-preserved delta plain stratigraphic records. Situated at the nexus of anthropogenic changes and rising sea level, information about deltaic processes is need on more detailed time scales to address restoration and protection efforts of deltaic environments. This study presents outcome of 4.5 years of measurements of sediment deposition/erosion, and inundation time series in the retreating bayhead delta (BHD) of the Roanoke River in North Carolina, USA. The results show that on centennial time scales, the entire bayhead delta is erosional, but on annual time scales, the upper BHD is depositional and the lower BHD plains are erosional. The study shows that delta plain floodplains are governed by different processes than alluvial floodplains and that on much shorter time scales, the depositional/erosional processes happen much faster than sampling frequency of the study period (approximately monthly). Sedimentation rates can equal or exceed

rates of sea-level rise only where key factors to deltaic sustainability (elevation, suspended sediment concentrations and inundation frequency) are optimal.

2.2 Introduction

Delta plains and lowland floodplains are vegetated, subaerial parts of the deltaic systems and are the location of valuable wetland habitats. Depending on local geomorphology, hydrology, and dominant marine forcing, deltaic plains are occupied with wetlands of different characteristics: fresh and salt-water marshes, mangroves or swamps.

The role of river deltas, floodplains and lowlands has clearly been identified as an important component of global biogeochemical cycles (Kremer et al., 2005; Mckee, 2003). Previous studies showed that particulate materials and associated carbon may spend a significant part of their time stored within the deltas, channel bed, floodplains, gullies and ditches (Lecce et al., 2006; McKee, 1998). When in transport, particulate material undergoes a variety of physical, chemical and biological transformations before reaching the ocean (Dagg, 2004). These processes maybe altered by anthropogenic changes (Bianchi and Mead, 2009; Jalowska et al., 2015; Kondolf et al., 2014; Mattheus et al., 2009; Syvitski, 2008).

Aggradation and sedimentation processes are well documented on geological time scales in well-preserved delta plain stratigraphic records. Over centennial to millennial time scales overbank aggradation is episodic and driven by autogenic processes (Shen et al., 2015) while aggradation rates change through time as a function of fluctuating fluvial sediment discharge and relative sea-level change (Stanley et al., 2000). Studies performed in bay-head deltas suggest that on modern time scales deltas prograde or retreat in a response to land use change (Jalowska et al., 2015; Mattheus et al., 2009). Placement of impoundments, urbanization or channel regulations isolate large parts of the delta plain from riverine input (Blum and Roberts, 2009;

Day et al., 1995; Giosan, 2014; Snedden et al., 2007) causing delta's degradation. Deltas are also vulnerable to sea-level rise. The sea level on the coast of North Carolina has been rising, and since 1900 it has risen ca. 0.4 m (Kemp et al., 2011). With rising sea level, coastal environments are expected to experience more flooding of lowlands and a greater lateral extent of storm impacts (Kopp et al., 2016). Current rate of sea-level rise in North Carolina is 0.3-0.4 cm/year.

Deltaic environments are considered net depositional; many previous studies have documented both loss of sediment from erosion, transport and rapid episodic deposition (Aller et al., 2008; Gomez et al., 1999, 1998; Phillips, 1992; Trimble, 1983; Walsh and Nittrouer, 2004). However the role of river delta environments is changing dramatically from burial to erosional settings and may act as sources of particulate material in response to accelerating sea level rise and sediment cutoff, caused by the placement of dams (Jalowska et al., 2015).

Previous studies looked into the physical drivers governing aggradation and erosion in modern deltaic plains. Bellucci (2007) found a strong relationship between inundation frequency and sediment aggregation in the marshes of Po river delta plain. Another study in North Carolina marshes found insignificant correlations between inundation frequency and deposition (Lagomasino et al., 2013). This study stressed that the dynamics of marsh deposition in wind-dominated environments are complex, involving relationships between wind patterns, water levels, and marsh geomorphology. In both cases, delta plain inundations were governed by water fluctuations in adjacent lagoon/estuary.

To describe sediment dynamic in delta plains, an understanding of many processes are derived from floodplain research. For example Lecce (2004) showed that sedimentation on floodplains are affected by large floods only as long as there is sediments available, similar conclusions were derived for marsh environments habitats (Chmura, 2013), and deltaic

environments (Battin et al., 2009; Bianchi and Mead, 2009; Zehetner et al., 2009). However, deltaic plains experience more frequent inundations, and may respond to changes within the watershed on different time scales than alluvial floodplains.

Purpose of this study is to investigate sediment dynamics in the transgressive delta plains, and time scales of depositional and erosional events. This project, an extensive 5 year study using geochemical and hydrological tools, addressed the question of what governs sediment dynamic during delta retreat, with a special focus to sea-level rise, sediment supply and flooding events.

2.3 Background

2.3.1 Study Area.

Roanoke River bayhead delta is located in the western part of Albemarle Sound. The Roanoke River originates in the Valley and Ridge province of the Appalachian Mountains in Virginia, has a total drainage area of 25,123 km^2 and empties into the west end of the Albemarle Sound at an average annual rate of 252m^3/s (Giese et al., 1979; Molina, 2002)(Figure 12). Before entering the Sound, the Roanoke River forms a bayhead delta. The subaerial Roanoke Bayhead Delta is about 86 km^2, extending from Broad Creek – the first distributary channel – to the shoreline in Albemarle Sound (Figure 12). The delta hosts a Cypress Gum Swamp habitat of national significance (Hupp et al., 2008).

The Roanoke River Valley and Albemarle Sound were impacted by the first European settlement in North America in the late 1600's AD. Heavy deforestation and poor agriculture practices led to the release of a significant amount of sediment to the river (Jacobson and Coleman, 1986; Jalowska et al., 2015; Wolman, 1967), that resulted in a rapid delta progradation between 1600-1800 (Jalowska et al., 2015). In following decades between 1871 and 1964, the

main trunk of the river was dredged by the U.S. Army Corps of Engineers for navigational purposes, and dredge spoils were deposited east of the River mouth in upper Albemarle Sound (Erlich, 1980).

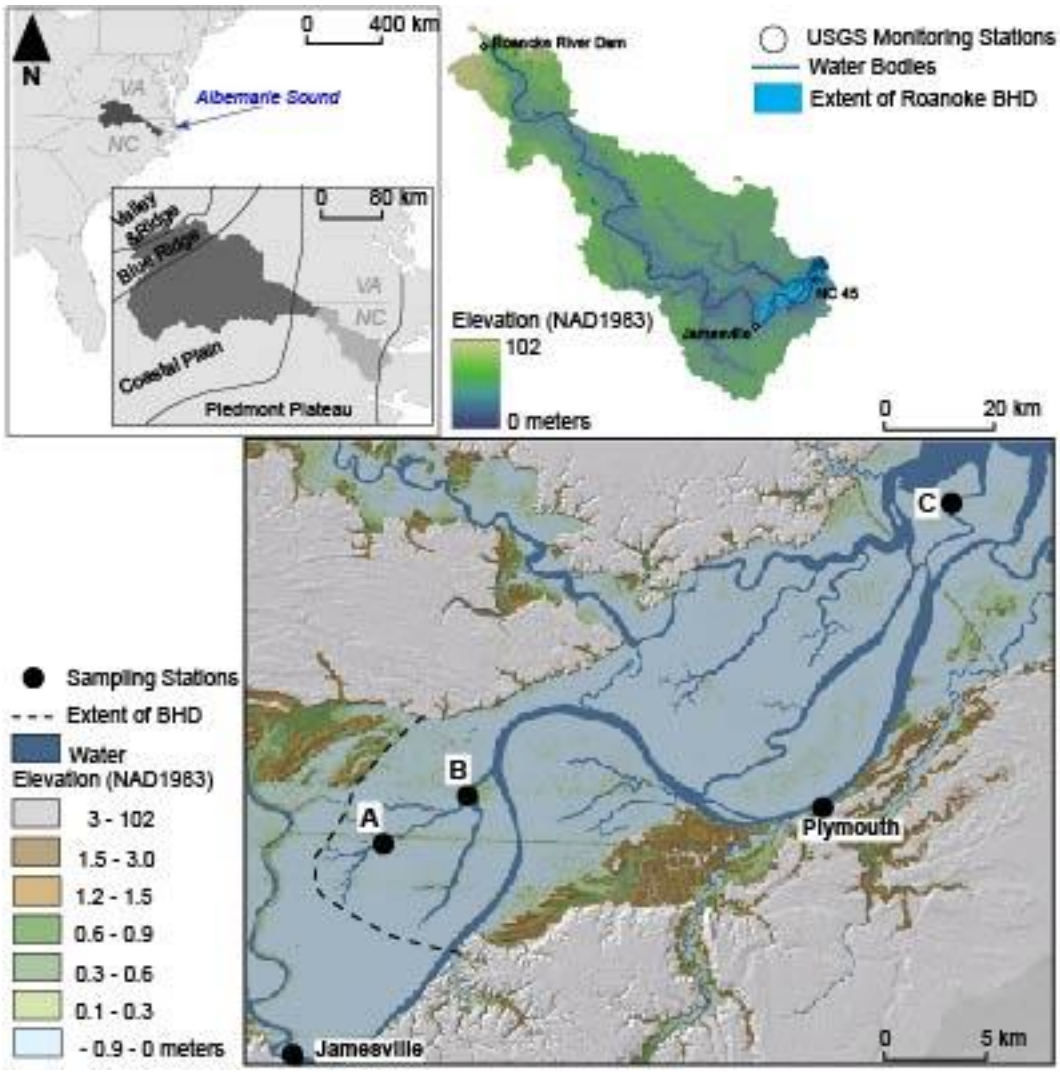

Figure 12. Roanoke Bayhead Delta and Sampling Stations.

In the middle of 20th century, three major dams were constructed on the Roanoke River. The first dam was placed at the fall line in Roanoke Rapids, NC and was finished in 1955. Completion of the Roanoke Rapids dam was followed by a construction of two other dams further upstream, by 1965. Placement of impoundments caused sediment delivery to the Lower Roanoke and consequently to the delta was reduced by 99% (Meade et al., 1990) leaving banks,

channels and floodplains seaward from the dam as the only source of sediments to the BHD (Jalowska et al., submitted.; Schenk and Hupp, 2008). Furthermore the dam placement resulted in eliminating maximum and minimum flows, leaving a medium flow a dominant one (Jalowska et al., 2012; Richter et al., 1996). Depending on the magnitude and duration of water releases from the dam, the counteracting energy generated by the seiche can be carried as up to Williamston, 70 km up the river (Jalowska et al., 2015; Luettich et al., 2002). The water level within the bayhead delta is controlled by the water movement in Albemarle Sound, and the connectivity with dam releases is negligible (Jalowska et al., submitted). The delta is currently at 0.0m NAVD 88 (Figure 12). National Elevation Data show lack of banks downstream which enables connectivity with the floodplains and anabranch channels. Depending on river flow dynamics this may result in particulate accumulation onto or removal from the floodplain. As a consequence, delta plain may also become a source of particles previously stored for a long time (Jalowska et al., submitted). Previous studies reported sedimentation in distal parts of the bayhead delta at the rate of 0.2-0.8 cm/year (EPA, 2010; Schenk and Hupp, 2008) while front of the delta is retreating and shifts from depositional to non-depositional or erosional state. The process is associated with sea-level rise and a decrease in sediment supply associated with improved agricultural practices and damming (Jalowska et al., 2015).

2.3.2 Site description.

Three sampling sites were chosen to represent a gradient in the deltaic plain environment and to accommodate accessibility (Figure 12).

Sampling site A (Figure 13) is located in Broad Creek, a distributary channel and anabranch channel to the Roanoke River. The channel connects the Roanoke River meander with a narrow, deep channel and distributes water along complex system of smaller distributary

channels and backswamps. Site A is located in the floodplain at the junction of the anabranch channel with the distributary channel, approximately 10 meters from the river channel. Subaqueous parts of the river bank were composed of the unconsolidated mud. Subaerial sections were fortified with knees of the cypress roots and covered with perennial vegetation, mostly grasses and aquatic plants.

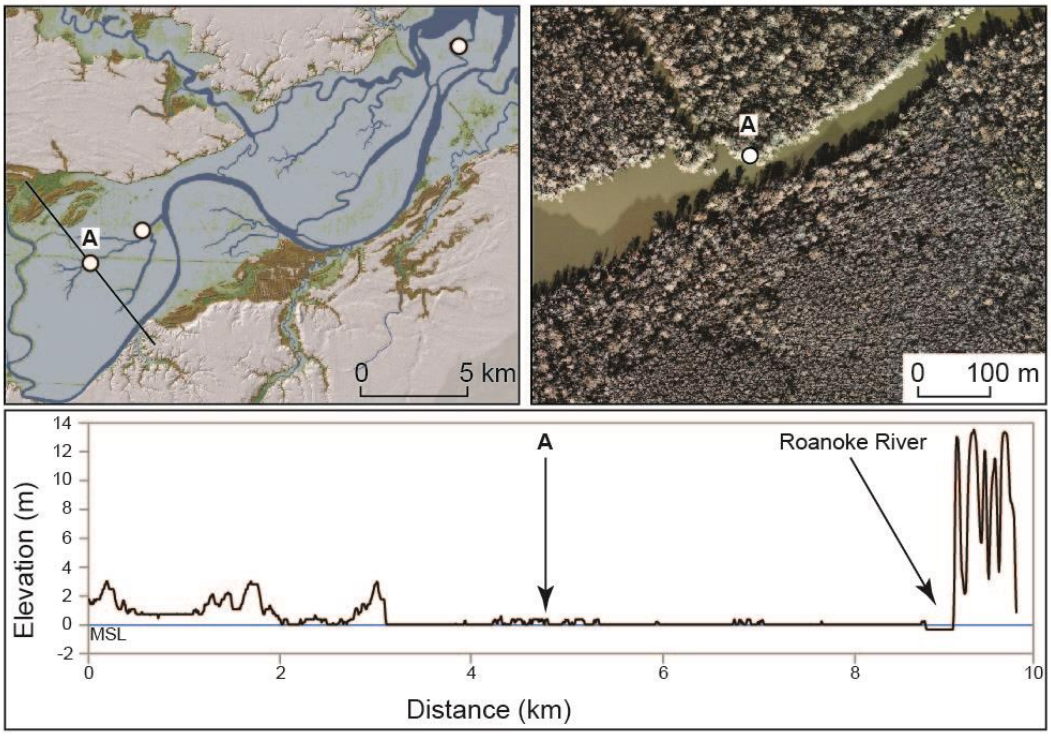

Figure 13. Location of sampling station A.

Sampling site B (Figure 14) was located in the floodplain of the Broad Creek at the junction of distributary channels, closer to the Roanoke River main trunk. The sampling site was located behind a natural, vegetated levee, approximately 5 meters from the river bank, in a hollow filled with unconsolidated mud. The sampling site was surrounded by vegetation consisting of trees, bushes and shrubs, with only some grasses, but there was minimal vegetation growing at the sampling site.

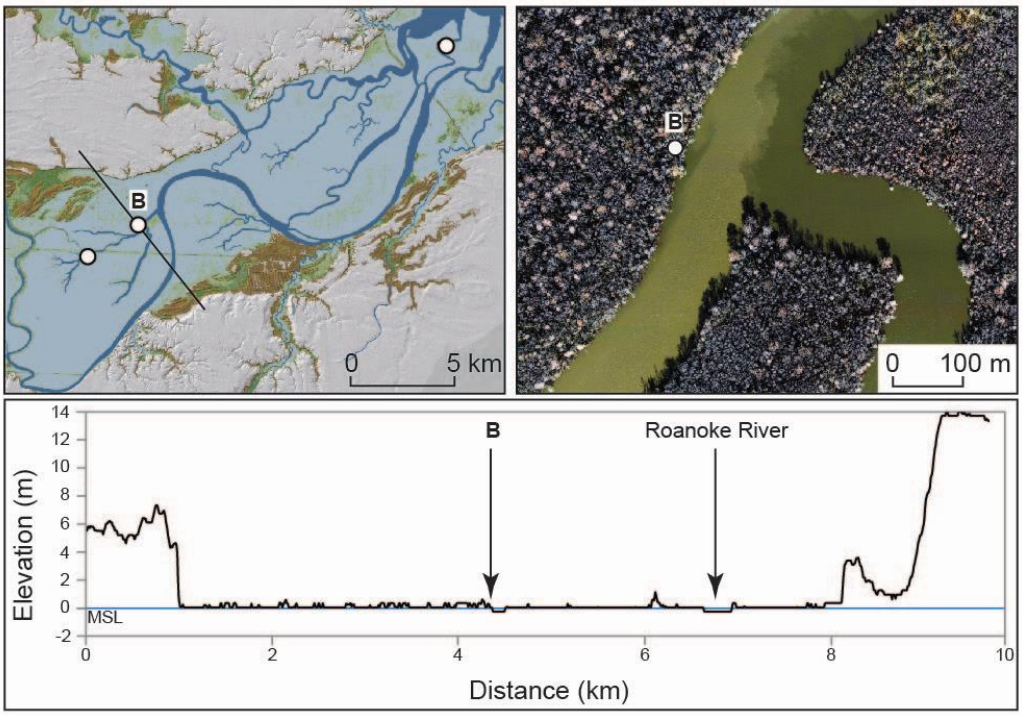

Figure 14. Location of sampling station B.

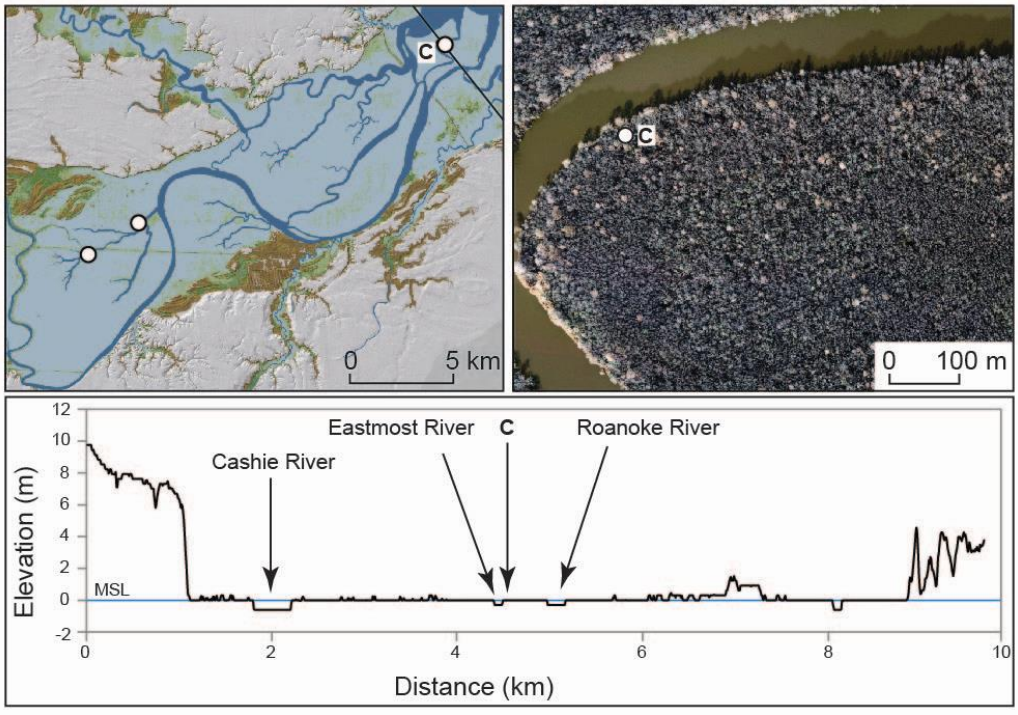

Figure 15. Location of sampling station C.

Sampling site C was located in the floodplain of the Roanoke distributary channel-Eastmost River on the Rice Island (Figure 15). The Eastmost River is a meandering distributary channel that separates Rice and Goodmans Islands (Figure 12). The sampling site was located proximately 10 m from the riverbank on the seaward site of the meander. There was no visible levees at this site. The sampling site was characterized by mixed vegetation of trees, grasses and aquatic plants.

2.4 Methodology

2.4.1 Elevation.

Three attempts to measure the elevation of each site, relative to the North Atlantic Vertical Datum of 1988, using GPS and the North Carolina Virtual Reference System failed due to the dense tree canopy, which prevented the Trimble 5800 to receive satellite signals. The relative elevation was calculated based on the differences between water levels recorded at each site, and water level recorded at the USGS station in Plymouth (Figure 12), and assumption of 0 MASL elevation at site C.

2.4.2 Sample collection and radionuclide analyses.

Total of 27 short cores were collected at three sampling sites (A, B and C; Figure 12) from October 2010 to April 2015 (4.5 years) and represent 13 sampling periods. The push cores were 10 cm in diameter, and were subsampled in 1 cm intervals. The bulk sediment samples were weighted, freeze-dried, homogenized, and then re-weighed to calculate sediment density. Samples then were analyzed for ^{7}Be and $^{210}Pb_{xs,}$ commonly used geochronometers in aquatic environments (Appleby and Oldfield, 1992; Golosov and Walling, 2015; Sanchez-Cabeza and Ruiz-Fernández, 2012; Walling, 2013).

^{7}Be is produced in the upper atmosphere by cosmic ray spallation of nitrogen and oxygen and is transported to the lower atmosphere mostly by wet fallout. ^{7}Be has a half-life of 53.3 days and is useful to determine sedimentation rates on monthly time-scales(Bhandari et al., 1970; Kaste et al., 2003; Lal et al., 1960)..

^{210}Pb (Curie et al., 1898; Rutherford, 1904) has half-life $t_{1/2}$ = 22.23 yr (Bé et al., 2008) and is a naturally produced radionuclide; a decay product of ^{238}U present in the Earth's crust. It has two pathways of becoming part of the lithogenic particle. A direct contribution through a ^{238}U decay chain in the particle's matrix referred to as a supported ^{210}Pb. The indirect path is through wet and dry fallout, associated with the escape of ^{222}Rn (part of ^{238}U decay chain) from soils to the atmosphere and its decay to ^{210}Pb, referred to as the 'unsupported' or 'excess' ^{210}Pb (^{210} Pb_{xs}) (Goldberg, 1963).

2.4.2.1 Gamma spectrometry.

Top 10 cm of each core were subsampled, packed into standardized petrie dishes, and sealed for three weeks to allow ^{222}Rn equilibration. $^{210}Pb_{xs}$ and ^{7}Be activities were measured by direct gamma spectrometry. Gamma counting was conducted on one of four low-background, high-efficiency, high-purity Germanium detectors (Coaxial- and BEGe-types) coupled with a multi-channel analyzer. Detectors were calibrated using a natural matrix standard (IAEA-300) at each region of interest in the standard counting geometry for the associated detector. Activities were corrected for self-adsorption using a direct transmission method (Cutshall et al., 1983). Total ^{210}Pb and ^{7}Be activity was directly determined by measuring the 46.5-KeV and 477.6-KeV gamma photo-peaks respectively. Supported levels of ^{210}Pb (^{226}Ra activity) was determined by measuring the gamma activity of ^{226}Ra granddaughter- ^{214}Bi (609 KeV).

2.4.2.2 Alpha spectrometry

Additionally, depending on the core depth 10-40 cm of each core was analyzed for ^{210}Pb activities alpha spectrometry (Appendix).

2.4.3 Inventories and Sediment Accumulation.

$^{210}Pb_{xs}$ and ^{7}Be can be supplied to floodplains by two pathways a direct deposition from the atmosphere (atmospheric flux) or supply of inorganic particulate material from sediment in transport. Inventories of excess ^{7}Be and $^{210}Pb_{xs}$ were calculated by summing the quotients of activities (dpm/g) and aerial section dry masses (g/cm^2) for all core sections. The total inventory was divided into two components: residual inventory (inventory of previous sampling period decay-corrected to the date in the middle between previous and present sampling), and new inventory (total inventory (present sampling) - residual inventory). Next, the atmospheric flux was subtracted from the new inventory (as a background). The new inventory was divided by the mean activity in the surface region, to yield mass accumulation or removal (mass balance) over the time between samplings (Canuel et al., 1990). Additionally, based on total inventories, the radionuclide flux (total inventories multiplied by a decay coefficient of given radionuclide) at given site at given time was calculated, and compared to the atmospheric flux and presented as a ratio. Ratio below 1 indicates a net removal of sediments due to erosion and ratio above would indicate focusing accumulation (Benninger and Wells, 1993).

^{210}Pb fluxes vary with latitude and show insignificant monthly variations (Baskaran, 2011). $^{210}Pb_{xs}$ atmospheric flux were based on the review work by Baskaran, 2011, providing assumption for $^{210}Pb_{xs}$ atmospheric flux in North Carolina to be 0.08 dpm/cm^2/month or 0.96 dpm/cm^2/yr.

^{210}Pb fluxes vary with latitude and show insignificant monthly variations (Baskaran, 2011). $^{210}Pb_{xs}$ atmospheric flux were based on the review work by Baskaran, 2011, providing assumption for $^{210}Pb_{xs}$ atmospheric flux in North Carolina to be 0.08 dpm/cm^2/month or 0.96 dpm/cm^2/yr.

The production of ^{7}Be is controlled by the cosmic ray flux which varies with altitude, latitude and solar activity (Kaste et al., 2003; Lal et al., 1960). ^{7}Be deposition occurs as wet deposition (Dibb, 1989; Olsen et al., 1985; Wallbrink and Murray, 1994) thus the magnitude of annual fallout fluxes varies primarily in response to annual precipitation amount and latitude (Walling, 2013) and is not affected by canopy through-fall (Karwan et al., 2014). Taking these variabilities into consideration, the atmospheric flux of ^{7}Be at the study site was calculated based on 137 measurements from sites proximate to North Carolina. For coastal North Carolina (Canuel et al., 1990), northeastern Maryland (Karwan et al., 2014), Chesapeake Bay area (Kim et al., 2000), Oak Ridge, Tennessee (Olsen et al., 1985) and Norfolk, Virginia (Olsen et al., 1985; Todd et al., 1989) and Stillpond, MD (Kim et al., 2000). Based on the assumption by Karwan (2014) about relationship between ^{7}Be flux and type of rain events, and presented in Olsen (1985), Dibb (1989), and Wallbrink and Murray (1994) about relationship between ^{7}Be flux and amount of precipitation, the measurements were modeled with rain events using linear regression (Figure 16). Coefficients of determinations (R^2) varied between 0.5 and 0.8 for each study, and combined, all the observations fit the model with R^2=0.4. The linear regression based on 137 samples was used to model ^{7}Be fluxes for each sampling period in the sampling area, using local precipitation record for Plymouth, NC. Additionally, flux associated with tropical storm Irene, recorded in Christina River Basin, MD (Karwan et al., 2014) was used directly to validate the linear regression model fit.

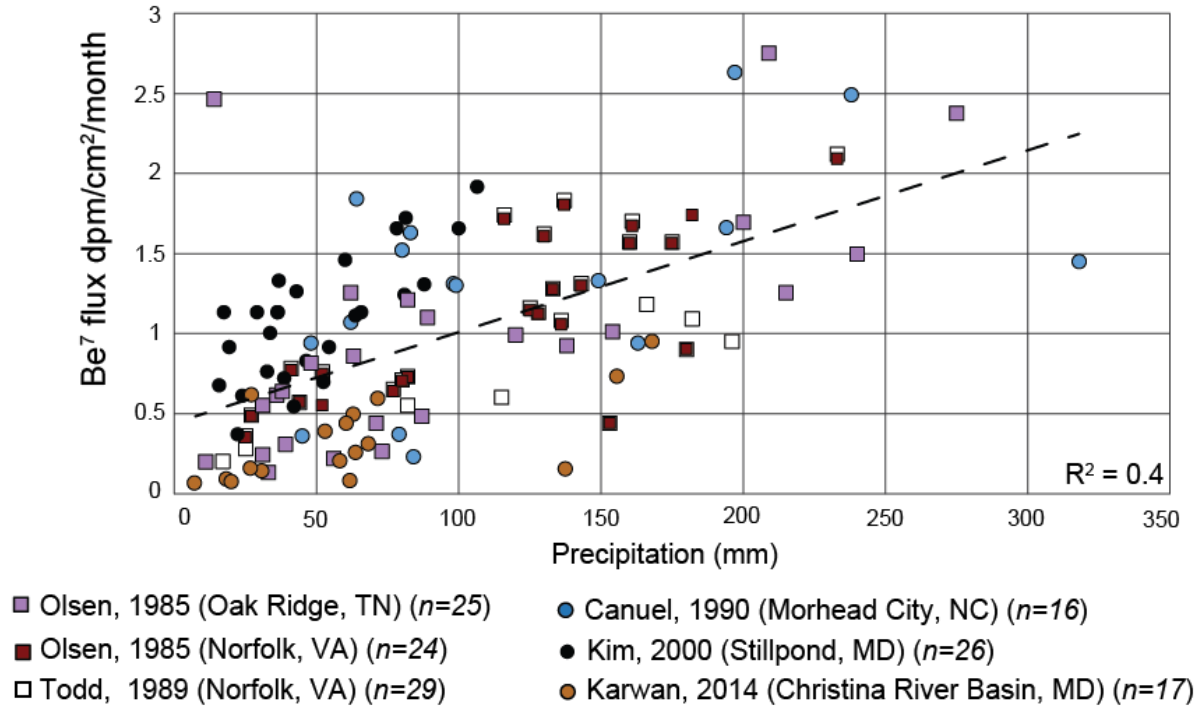

Figure 16. ^{7}Be fluxes by storm total precipitation from studies reporting event-based collections in the proximity to study area: coastal North Carolina (Canuel et al., 1990), northeastern Maryland (Karwan et al., 2014), Chesapeake Bay area (Kim et al., 2000), Oak Ridge, Tennessee (Olsen et al., 1985) and Norfolk, Virginia (Olsen et al., 1985; Todd et al., 1989) and from a Stillpond, MD (Kim et al., 2000).

The $^{210}Pb_{xs}$ chronologies were first modeled using a ‘‘Constant Rate of Supply’’ (CRS) model (Appleby and Oldfield, 1978; Sanchez-Cabeza and Ruiz-Fernández, 2012). The ultimate assumption of this model is that the $^{210}Pb_{xs}$ flux to the sediment surface is constant with time regardless potential accretion at the site or different sources. For comparison Constant Initial Concentration (CIC) model was applied (Appleby and Oldfield, 1992, 1978; Crozaz and Picciotto, 1964; Goldberg, 1963) that assumes that the $^{210}Pb_{ex}$ initial concentration is constant and requires using linear regressions in model calculations, regardless variation in core activities associated with sediment sourcing. Assumptions for both models are not valid in the erosional environments. Additionally, deposition in delta plain environments is directly connected to

episodic overbanking (Shen et al., 2015; Wolman and Leopold, 1957), what causes discontinuity in sediment supply and negation of CRS model. Furthermore, sediments deposited in floodplains come from different sources that may include sediments eroded from channel or banks depleted in $^{210}Pb_{xs}$, violating the assumption of the CIC model.

2.4.4 Feldspar Clay Marker Horizons.

Feldspar clay horizon is an artificial marker layer and is a common method for measuring a short-term net sedimentation. In March 2012 at each of the sampling sites, an artificial marker horizon was set down by placing a 2-3 cm thick, 1 m^2 layer of powdered white feldspar (16-17 kg) on the surface, which was previously cleared of vegetation and debris. White feldspar horizons have been used previously for reconstructing short-term accretion (Cahoon and Turner, 1989; DeLaune et al., 1983; Noe and Hupp, 2009). The corners of the feldspar horizon were marked with vertical PVC pipes for future localization (DeLaune et al., 1983; Schenk and Hupp, 2010). Feldspar horizons were cored 5 times during five consecutive trips, at each sampling site.

2.4.5 Weather and Water Level Data.

Weather data including wind speed and direction, was obtained for weather station in Plymouth, NC from Weather Underground website (weatherunderground.com) measured at the Edenton Bay Plantation weather station (KNCEDENT7).

For better understanding of the connectivity between the main channel and the floodplain along with inundation patterns and sediment pathways in the Roanoke Delta, the Water Level Data Loggers (HOBO U20-001-04) were deployed at all there sampling locations (A, B and C). Water level loggers recorded a continuous measurements of the water level at the site every 10 minutes. To compensate for changes in barometric pressure, and additional logger was installed

2 meters above ground at site C. The maximum error of loggers is ±0.1% FS (full scale) or 3 cm of water depth.

Data from the loggers were verified against the gage height data for the Roanoke River USGS stations at NC45 NR Westover, NC (station number 0208114150, located downstream from Plymouth), obtained from the USGS Water Data for the Nation website (United States Geological Survey, 2012).

In this study the site was considered to be flooded every time when water logger data was >0 cm because the pressure sensor was positioned at the elevation of the floodplain. One-day flood was defined if the maximum water level for a day was >0 cm and minimum water level for a day was 0cm. The beginning of two- day or longer flood was defined when maximum and minimum water levels for consecutive days were >0 cm, and the flood ended when the minimum water was 0 cm.

To determine if flooding affects floodplain accretion/erosion, averages of flooding frequency and duration over the same time intervals corresponding to the temporal resolution of sampling dates, and calculated correlations between time-averaged flooding frequency/duration and accretion/erosion at the sampling sites were calculated (Bellucci et al., 2007).

2.4.6 Total Suspended Matter and water level data.

Total Suspended Matter (TSM) is a measurement of the concentration of particulates in the water column. Concentration of total suspended matter was determined ate each sampling date for each sampling site. The one-liter bottle, surface-water samples were collected at each site and vacuum-filtered through a pre-weighed 0.22 µ, nitrocellulose filters. After filtering, samples were flushed with 1L of deionized water to remove salts. The filters were then dried in a 40^{o}C oven for 48 h and weighed again to determine the TSM concentration river water samples

were collected in one litter, acid cleaned bottles. Water was then filtered through a pre-weighed 0.2µm filters. Concentration of total suspended matter was recorded as mg/L.

2.4.7 Cartographic information.

Crossection profiles of the river valley at each site were based on a 6 meter digital elevation model (DEM) for North Carolina and calculated in ArcGIS software (ESRI (Environmental Systems Resource Institute), 2015). Data used to create the DEM was derived from LIDAR collected by NC Floodplain Mapping Program and processed by NC DOT- GIS Unit (North Carolina Department of Transportation, 2003).

2.5 Results

2.5.1 Elevation.

The relative elevation of sites A and B in regard to site C was presented in figure 17. Site A is 8.5 cm higher than site C, and site B is 22.1 cm below site C.

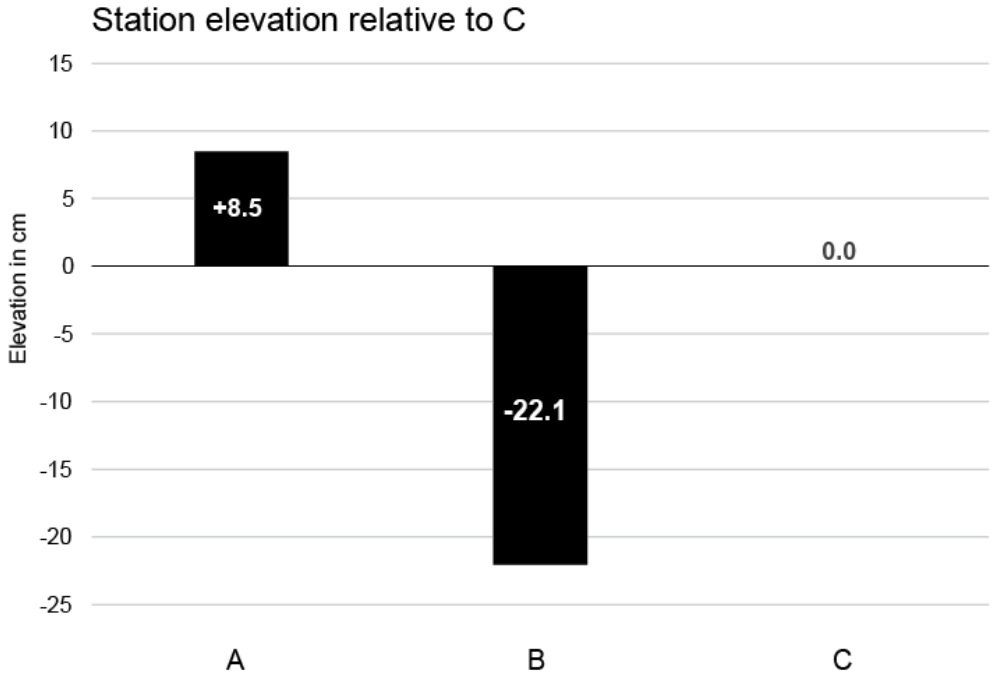

Figure 17. Elevation of sampling stations.

2.5.2 Inundations and wind data.

Verified water level data was analyzed for frequency and extent of flooding events. Inundation time series for the sampling period for each site are presented in figure 18 and distribution of inundation magnitude at each site is presented in figure 19.

Site A was flooded only 23% of the sampling period. Total number of floods was 194, and most of them (168) were one-day floods. Maximum flood height at A was 1.2 m, and at the same time the longest one (15 days), was associated with tropical storm Irene in August 2011. Average flood height during the sampling period at site A was 0.06 m (Figures 18 and 19).

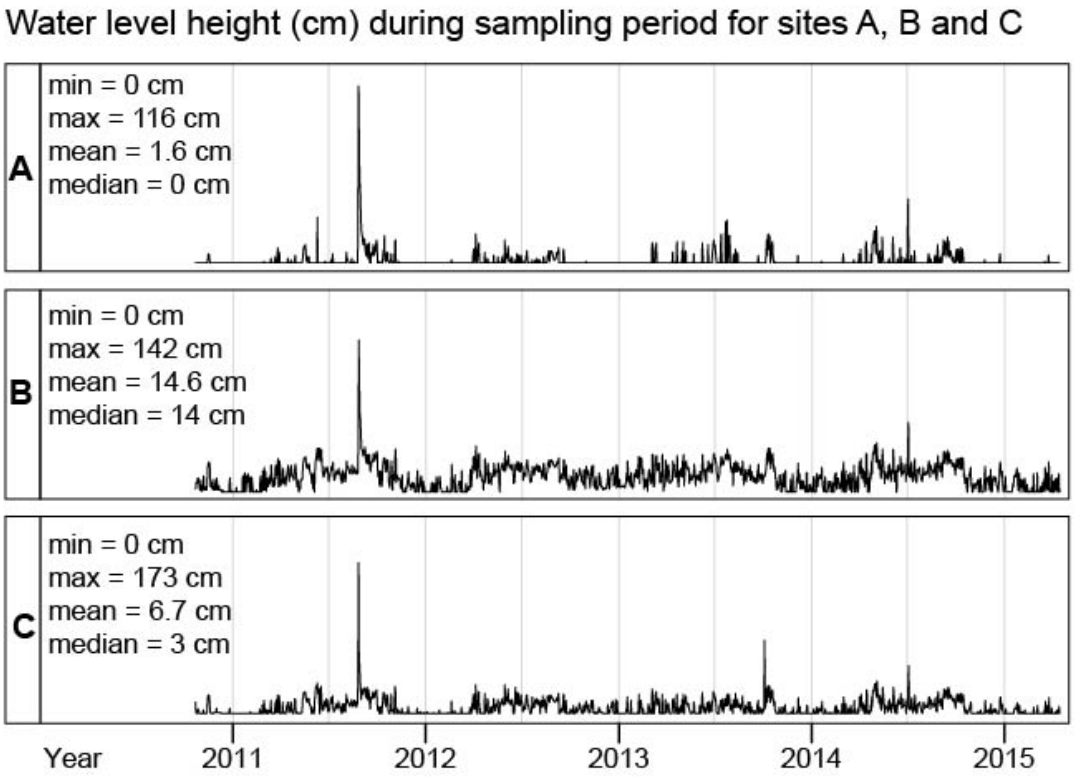

Figure 18. Plots present inundation time series at each station with water level above 0 cm.

Site C was flooded for 65% of the time, and 87% of the inundation events were one-day floods. Maximum water associated with Irene level at the site was 1.73 m, and the flood caused

by the storm lasted 22 days. Average flood height 0.1 meter. The site is dominated by short floods and it was inundated for longer than 10 days only 7 times (figures 18 and 19).

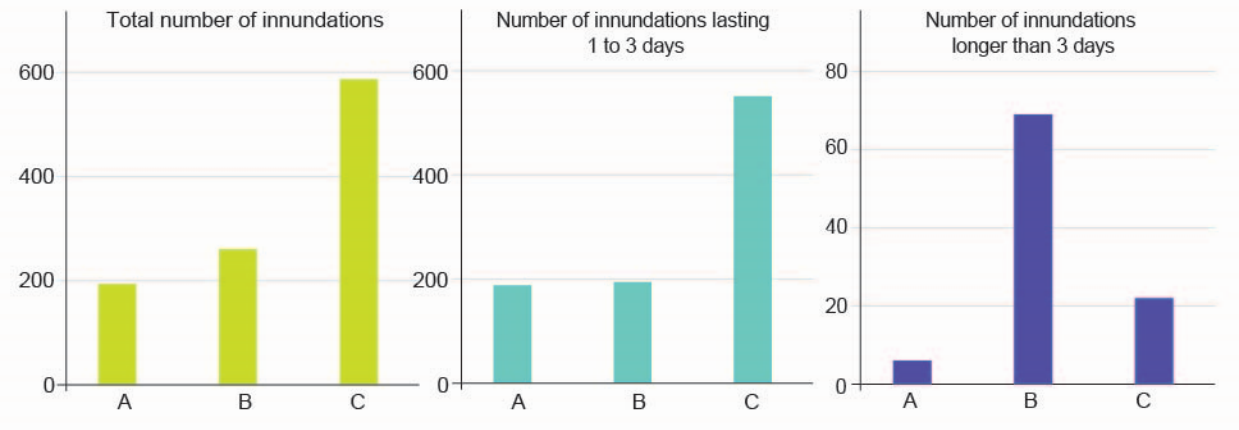

Figure 19. Total number of inundations per sampling site, and number of floods shorter and longer than 3 days.

A seasonal pattern of the inundation magnitude was examined and presented in figure 20. Sampling site A shows the largest seasonal variability in inundation magnitude between summer, spring fall and winter. At site A the highest inundations happen during the summer and fall. During winter and spring recorded water levels were very low. At site B most of summer floods were higher than during other seasons, yet the range of flooding magnitude was smaller. Sampling site B has the highest frequency of floods higher than 10 cm and even in winter months, the floods were exciding 10 cm. At site C summer inundation exceed water levels from spring and fall floods. Winter floods at site C, correspondingly to site A, recorded the lowest magnitude of inundations, and were dominated by water levels lower than 5cm.

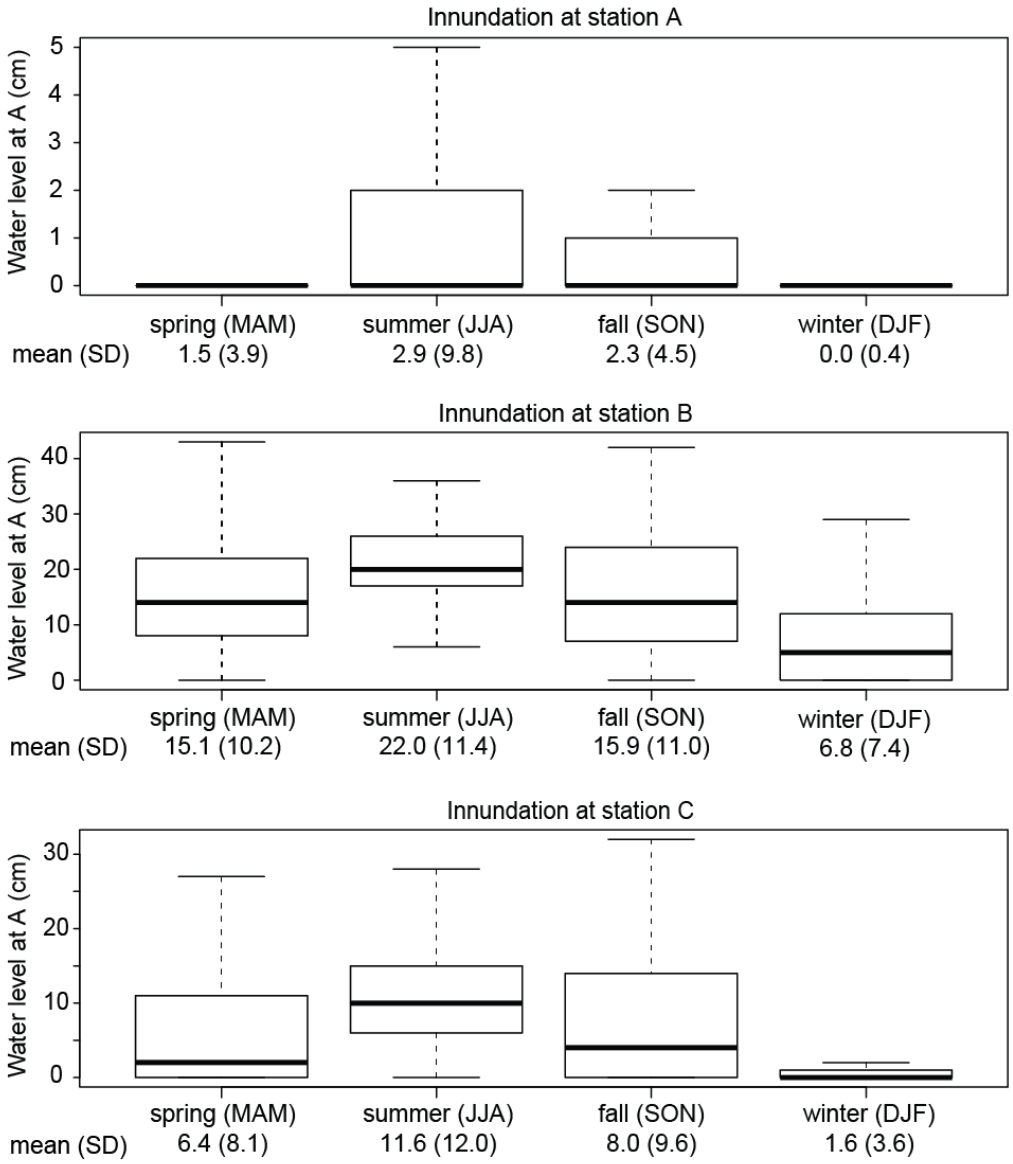

Figure 20. Seasonal variations of inundation magnitudes (cm) at each station, with derived means and standard deviations (SD) provided under each plot. Spring: March, April, May (MAM), summer: June, July, August (JJA), fall: September, October, November (SON) and winter (DJF).

To establish a connection between wind speed direction and inundation, wind patterns were analyzed, and presented in figure 21. The wind roses show the wind fields in the study area were dominated by southwesterly (13-15% of the time) and northeasterly winds (12% of the time) during the entire study period. Wind direction varies with seasons. Strong south and southwesterly winds are characteristic to spring and summer, while north and northeasterly wind

are more common in the fall and winter. The winter winds show most variability in wind direction. During the study period the strongest winds recorded were associated with a tropical storm Irene on August 27th, 2011 (17 m/s) and during a tornado outbreak on April 25th, 2014 (17.4 m/s).

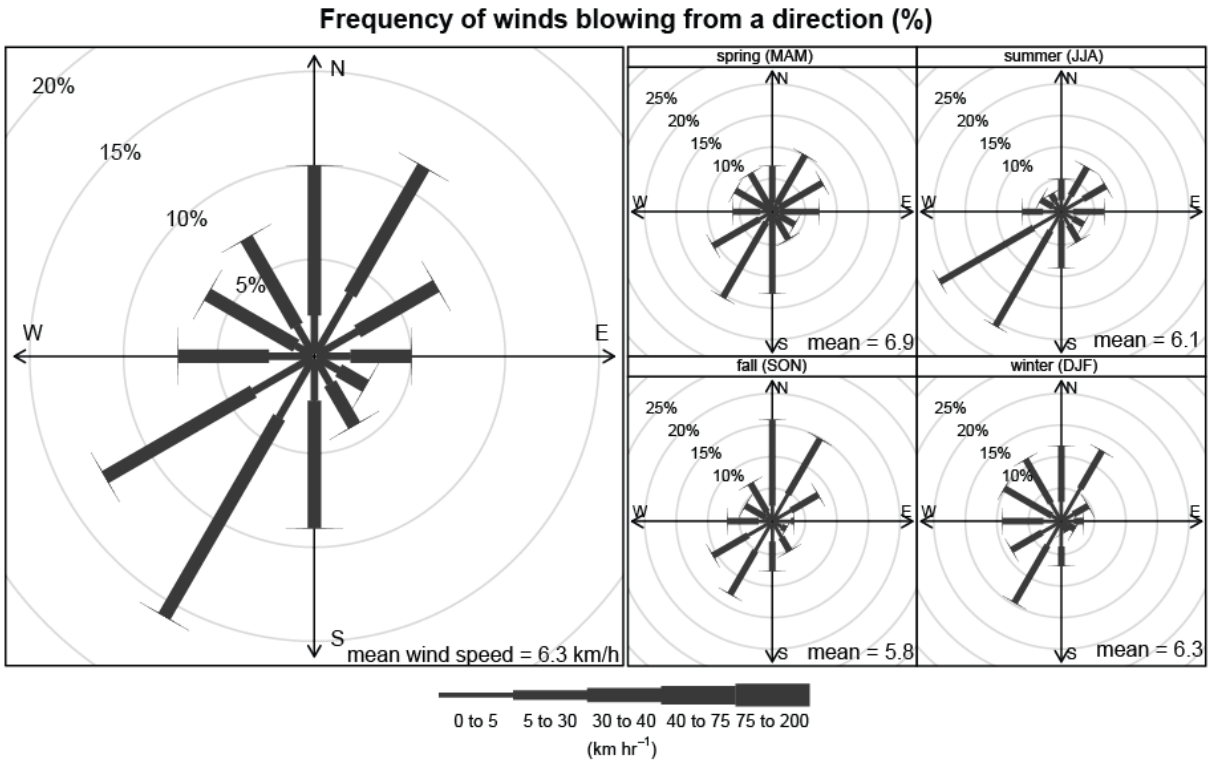

Figure 21. Left panel: meteorological wind direction and speed (km/s) for a whole sampling period. Right panel: meteorological wind direction and speed (m/s) for the sampling period divided into seasons.

Additionally correlation analyses between recorded inundations and releases from the dam and precipitation showed that these two factors are negligible in control of flooding at the study sites. Jalowska et al., (submitted) showed small (0.12) correlation with dam releases for the time period between February 2009 and March 2012. During the time discussed in this study (October 2010 and April 2015) correlations with dam releases are very small and negative: -0.01

at site A and -0.06 for sites B and C. Precipitation has small, positive correlation at site A off 0.11, and 0.17 and 0.22 at sites B and C correspondingly.

2.5.3 Total Suspended Matter (TSM).

Suspended sediment concentrations (TSM) during the study period are presented in mg/L in figures 22 and 24. TSM values in the main River trunk at Jamesville are the highest, and decrease in Plymouth, indicating loss of suspended sediments in the water column as river enters bayhead delta. Within the bayhead delta, highest suspended sediment concentrations were recorded at site A with the average of 10.4 mg/L that drops down to 8.8 mg/L at site B. That may indicate loss of suspended sediments to channel or floodplain deposition between these two sites. The rest of the suspended sediment enriches the suspended sediment load in the main channel, at site C sediment concentration in the water column drops and is the lowest in the bayhead delta.

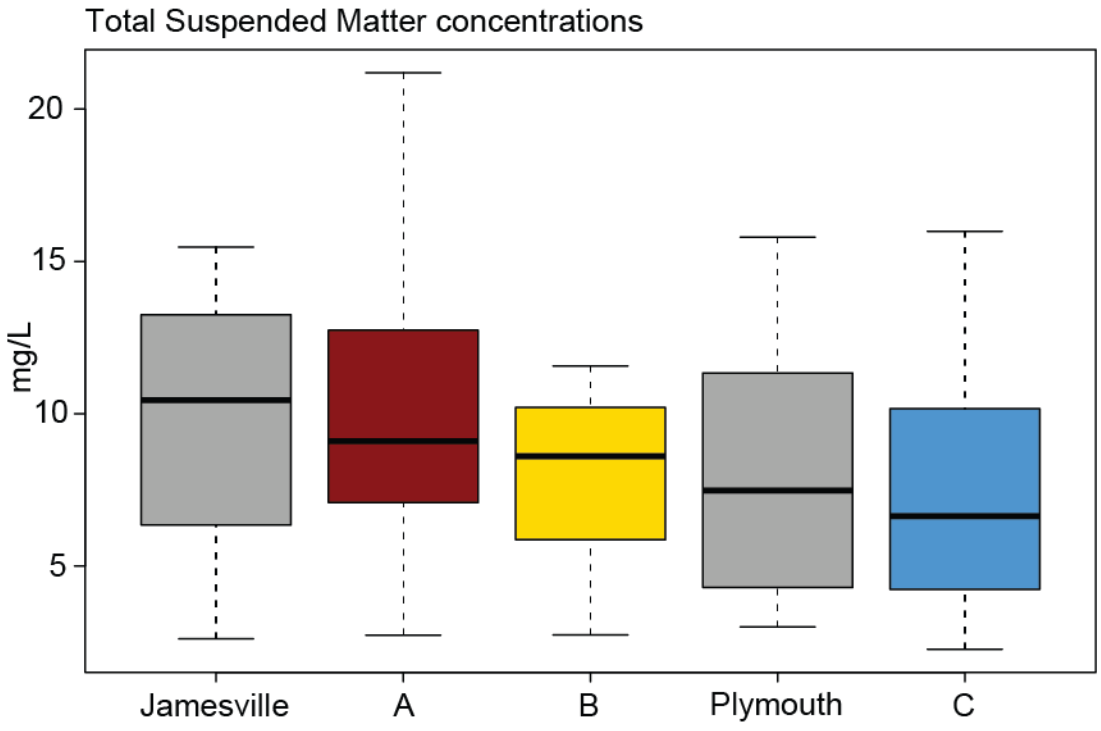

Figure 22. Total suspended matter concentrations at each station during the sampling period (mg/L).

Figure 23 shows the relationships between the suspended sediment concentrations and water level at the day of TSM measurement, for each site during the sampling period.

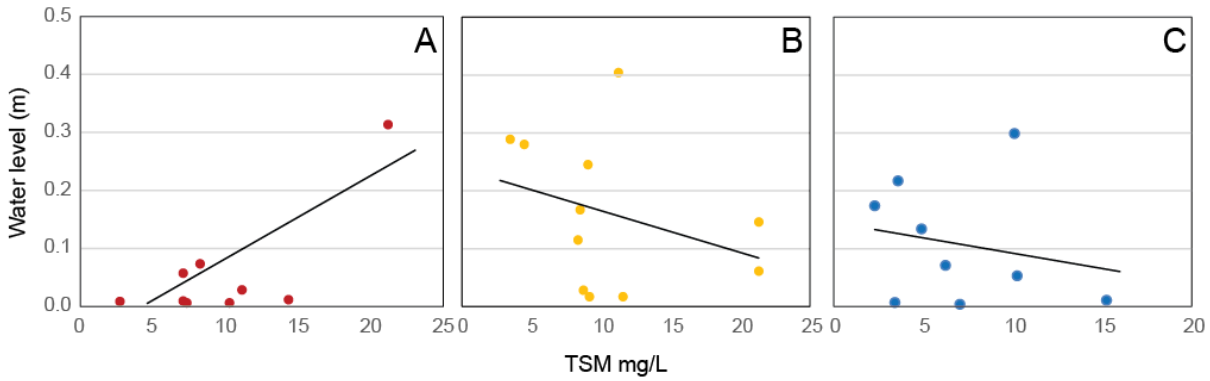

Figure 23. Relationship between water level and concentration of the suspended sediment in the water column.

Site A shows significant positive correlation of 0.6 between TSM and water level. Sites B, Plymouth and C show insignificant negative correlations (-0.2, -0.1, -0.3 respectively).

Additionally, the study recorded seasonal variation in suspended sediment concentration (Figure 24). Highest sediment concentration at all three sites was recorded in spring and lowest in the fall.

2.5.4 Mass Accumulation.

All the radionuclide activities were corrected to the last day of sampling (8/15/12) to compare the mass accumulation in cores with each other.

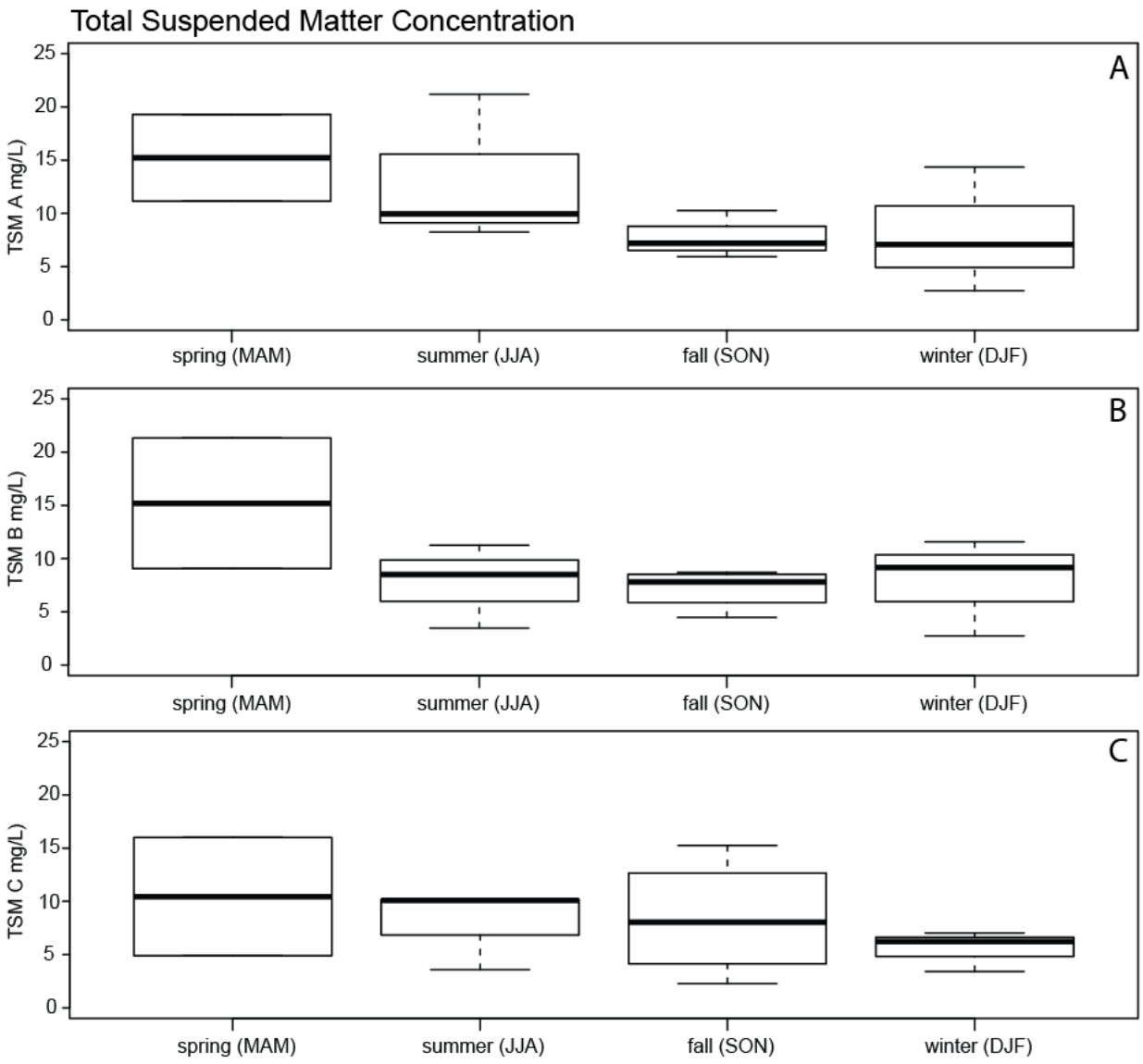

Figure 24. Seasonal mean suspended sediment concentrations at each site.

2.5.4.1 Mass accumulation and inundations at sampling station A.

The distribution of mass accumulation based on ^{7}Be activity in the upper 6 cm of each core is presented in the upper panel of figure 25. Total ^{7}Be inventories ranged from -0.8 to 5.8 dpm/cm^2, with the highest seasonal inventory occurring on September 22nd, 2011, that was a sampling date following tropical storm Irene. Mass accumulation at site A ranged between -2.6 and 1.5 g/cm^2, and is net depositional showing net sediment accumulation of 1.1g/cm^2.

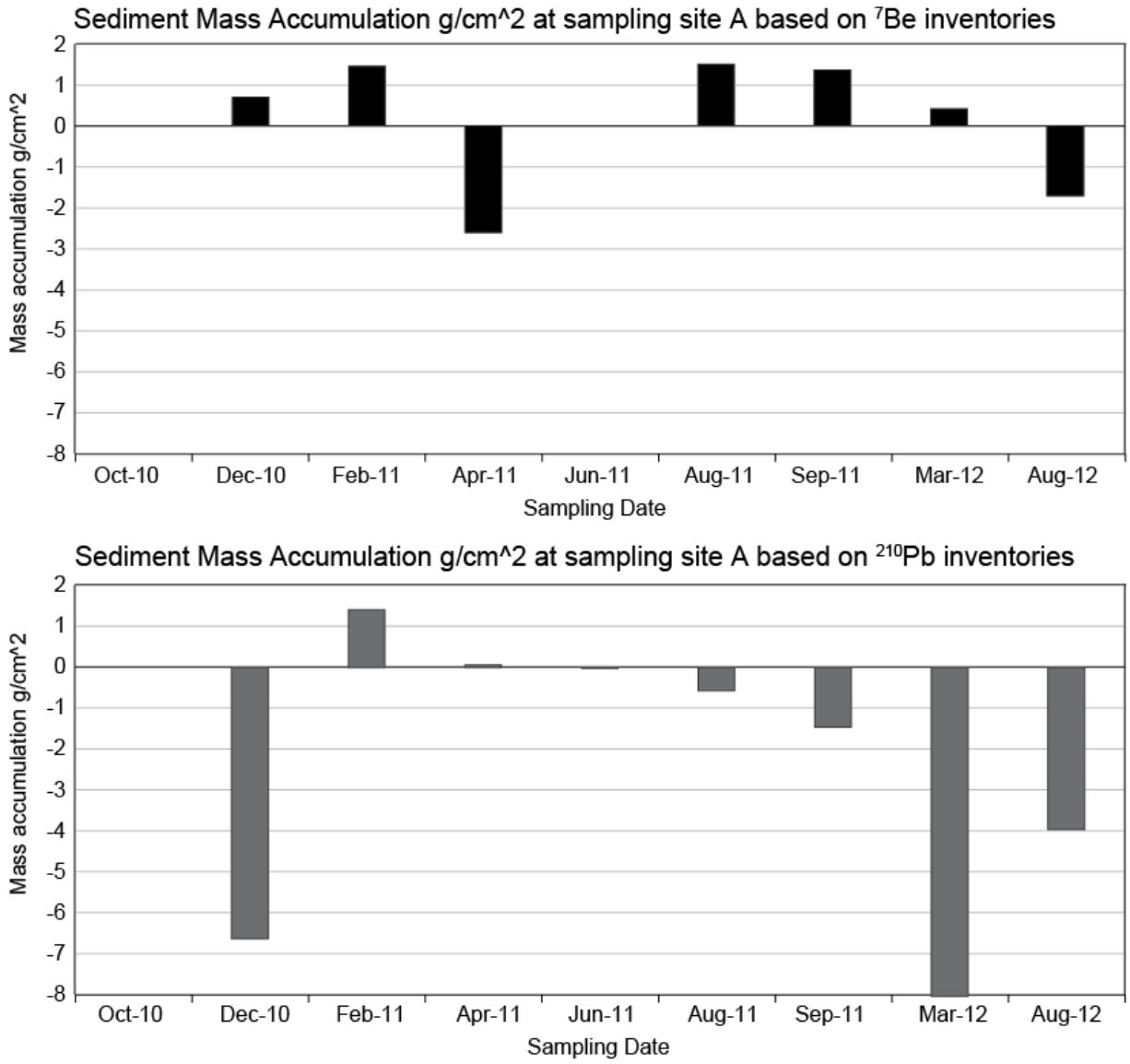

Figure 25. Mass accumulation in g/cm^2 at sampling site A based on ^{7}Be and ^{210}Pb inventories.

The distribution of ^{210}Pb activity in the upper 10 cm at site A is illustrated in the lower panel of figure 25. Total ^{210}Pb inventories ranged from -7.2 to 1.3 dpm/cm^2. Mass accumulation at site A ranged between -7.2 and 1.3g/cm^2, and is net erosional showing net sediment erosion of -15.3 g/cm^2.

2.5.4.2 Mass accumulation and inundations at sampling station B.

The distribution of mass accumulation calculated based on ^{7}Be activity in the upper 6 cm of each core at sampling site B is presented in the upper panel of figure 26. Total ^{7}Be inventories ranged from -0.1 to 3.8 dpm/cm^{2}. Mass accumulation at site B varied between -0.5 and 1.3 g/cm^{2}, and is net depositional showing net sediment accumulation of 2.9 g/cm^{2}.

The distribution of ^{210}Pb activity in the upper 10 cm at site B is illustrated in the lower panel of figure 26. Total ^{210}Pb inventories ranged from -6.5 to 7.1 dpm/cm^{2}. Mass accumulation at site B ranged between -4.2 and 1.0 g/cm^{2}, and is net erosional showing net sediment erosion of -6.1 g/cm^{2}.

2.5.4.3 Mass accumulation and inundations at Eastmost Pointbar North (C).

The distribution of mass accumulation calculated based on ^{7}Be activity in the upper 6 cm of each core at sampling site C is presented in the upper panel of figure 27. Total ^{7}Be inventories ranged from -0.2 to 5.9dpm/cm^{2}, with the highest seasonal inventory occurring on September 22nd, 2011, that was a sampling date following tropical storm Irene. Mass accumulation at site C varied between -0.3 to1.3 g/cm^{2}, and is net depositional showing net sediment accumulation of 4.5 g/cm^{2}. The distribution of ^{210}Pb activity in the upper 10 cm at site C is illustrated in the lower panel of figure 27. Total ^{210}Pb inventories ranged from -5.5 to 28.4 dpm/cm^{2}. Mass accumulation at site C ranged between -4.8 and 6.5 g/cm^{2}, and is net depositional showing net sediment accumulation of 0.1 g/cm^{2}.

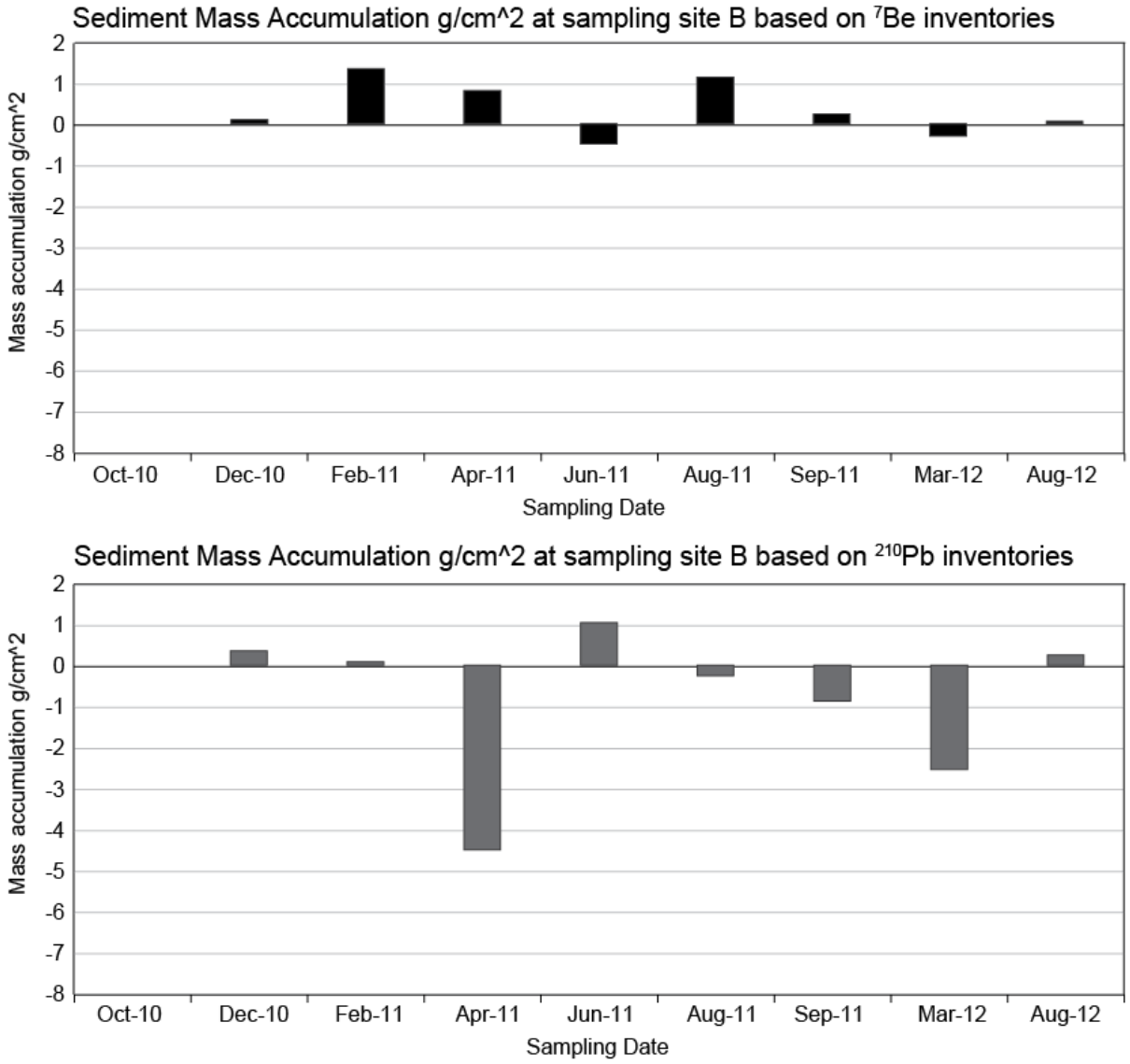

Figure 26. Mass accumulation in g/cm^2 at sampling site B based on ^{7}Be and ^{210}Pb inventories.

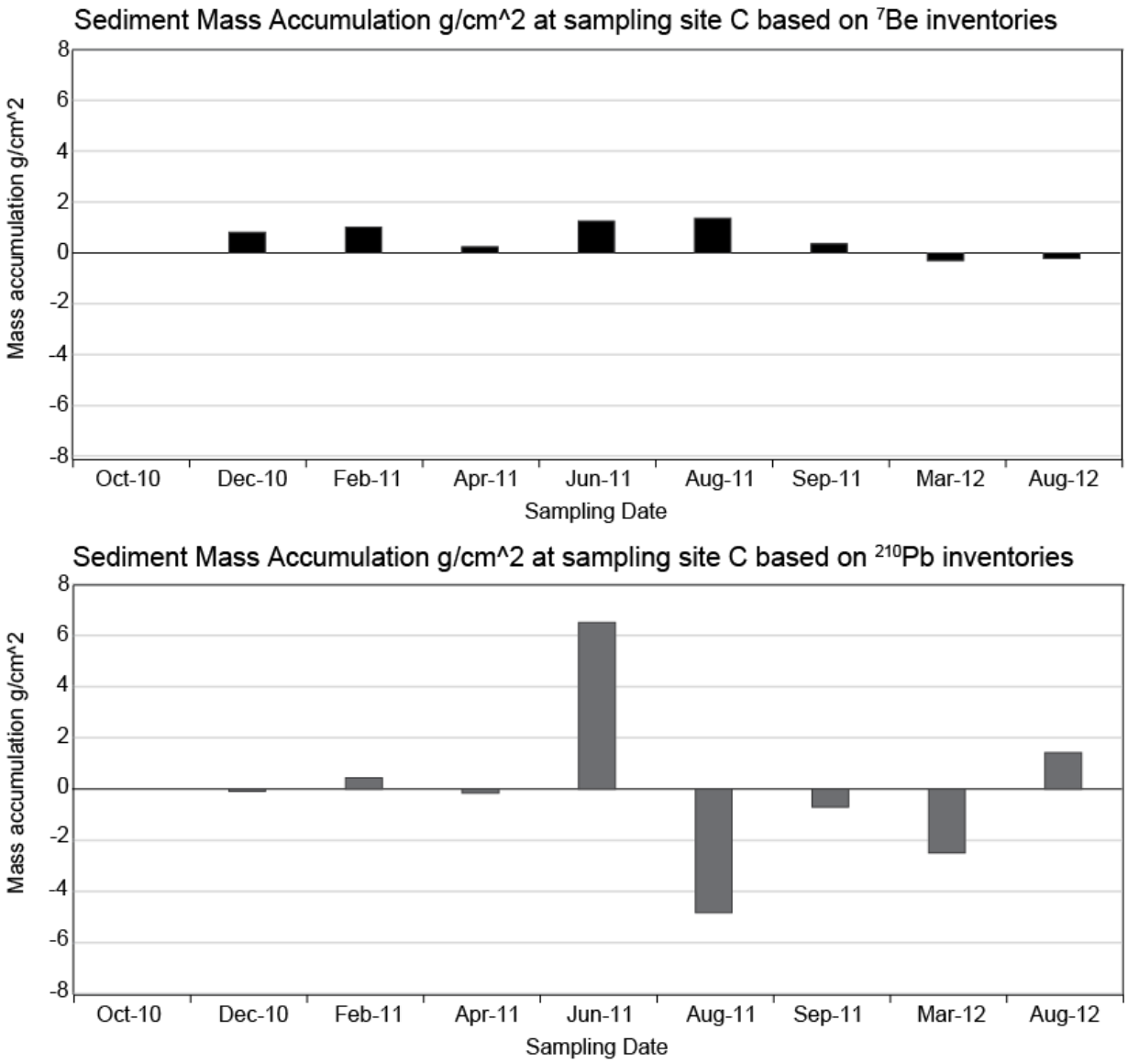

Figure 27. Mass accumulation in g/cm^2 at sampling site B based on ^{7}Be and ^{210}Pb inventories.

2.5.5 Feldspar.

The accretion of sediment on top of feldspar horizons varied widely among different sampling sites. Sediment deposition between the sampling periods ranged from complete removal to 7 cm accretion (Figure 28).

At site A initial deposition of two cm was completely removed during following sampling period. Sampling during last three field trips at this site showed increasing deposition of sediments totaling in 12 cm of material deposited on top of the feldspar.

At site B the highest deposition recorded was 1.5 cm, followed by a complete removal. The next deposition of 1.5 cm was slowly being removed from the feldspar until the end of the sampling period.

At site C the highest recorded deposition was 3.5 cm. During the last three sampling periods loss of the artificial horizon was observed. The feldspar was disintegrated and mixed in with sediments of the sampling transect.

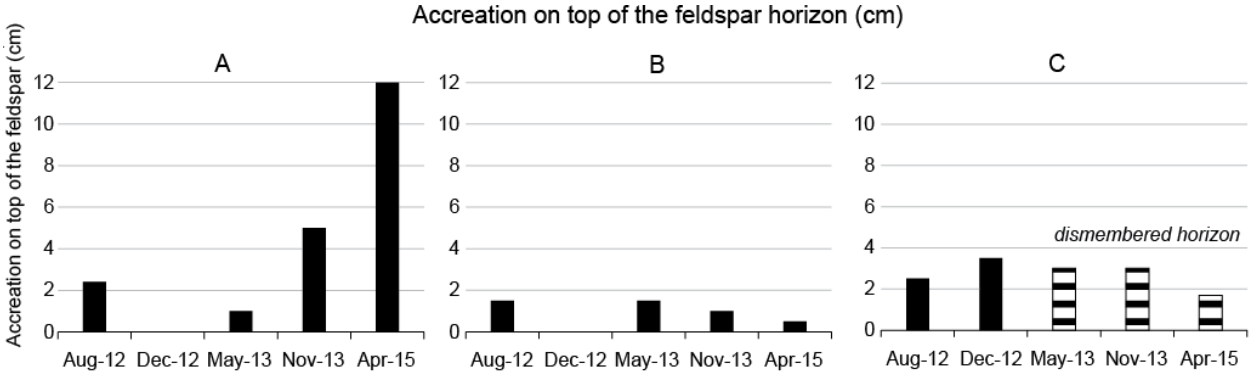

Figure 28. Accretion of sediments on top of the feldspar horizon at stations A, B and C.

2.5.6 Relationship between accretion and erosion events and length of inundations.

Correlations between inundations events and depositional and erosional events are presented in Table 3. Based on Bellucci et al. (2007) a positive correlation between the inundation frequency and deposition and inverse relationship with erosion was expected. Accordingly, in the erosional environment the negative correlation with deposition and positive with the erosion would be expected.

Correlations between number of inundations and their extent at site A are stronger with erosion than with deposition derived from ^{7}Be measurements, but both events show positive correlations with flooding events. The deposition/erosion events derived from ^{210}Pb activities show opposite relationship: strong positive correlation with deposition and weak inverse correlation with sediment removal.

The results from site B show that inundation frequency and extend have stronger relationship with erosion events derived from ^{7}Be, than with depositional events. The strongest correlation was between longer floods (3 days and more) and erosion, with an inverse relationship with deposition. Relationships with events derived from ^{210}Pb activities show, again opposite results, indicating a negative relationship with erosion.

At site C mass accumulation derived from ^{7}Be measurements shows stronger inverse relationship with number of inundations and their extent, at the same time erosional events also show a negative correlations. The evens derived from ^{210}Pb activities have week correlations, with a negative one with deposition events and positive one with erosion.

Table 3. Relationships between inundations and depositional and erosional events

Station		# of events	^{7}Be		^{210}Pb	
			Deposition	Erosion	Deposition	Erosion
A	# of inundations	278	0.4	**0.8**	**0.9**	-0.3
	# of days inundated	351	0.5	**0.9**	**1**	-0.2
	1-3 days	271	0.4	**0.8**	**0.9**	-0.3
	3 days and more	7	0.4	0.5	0.5	ND
B	# of inundations	466	0.1	0.5	0.2	**-0.7**
	# of days inundated	1435	-0.2	0.5	0.5	0.3
	1-3 days	383	0.2	0.5	-0.1	**-0.8**
	3 days and more	81	-0.2	**0.8**	0.5	0.3

C	# of inundations	815	**-0.6**	-0.5	-0.4	0.2
	# of days inundated	1072	**-0.6**	-0.4	-0.4	0.2
	1-3 days	784	**-0.6**	-0.5	**-0.6**	0.2
	3 days and more	31	-0.2	-0.2	-0.3	0.1

.

2.5.7 Relationship between accretion and erosion events and seasonality.

The accretion and erosion events were grouped by season and presented in figure 29. The results show seasonal dependency. In the winter (3 sampling trips) sediment cores at sites A and B recorded depositional and erosional events resulting in net erosion. Site C in the winter always recorded deposition.

In the spring (4 sampling trips) site A recorded either depositional or erosional events resulting in net sediment deposition at the site. Site B did not record erosion during the spring. Site C was exposed to both types of events and was net erosional.

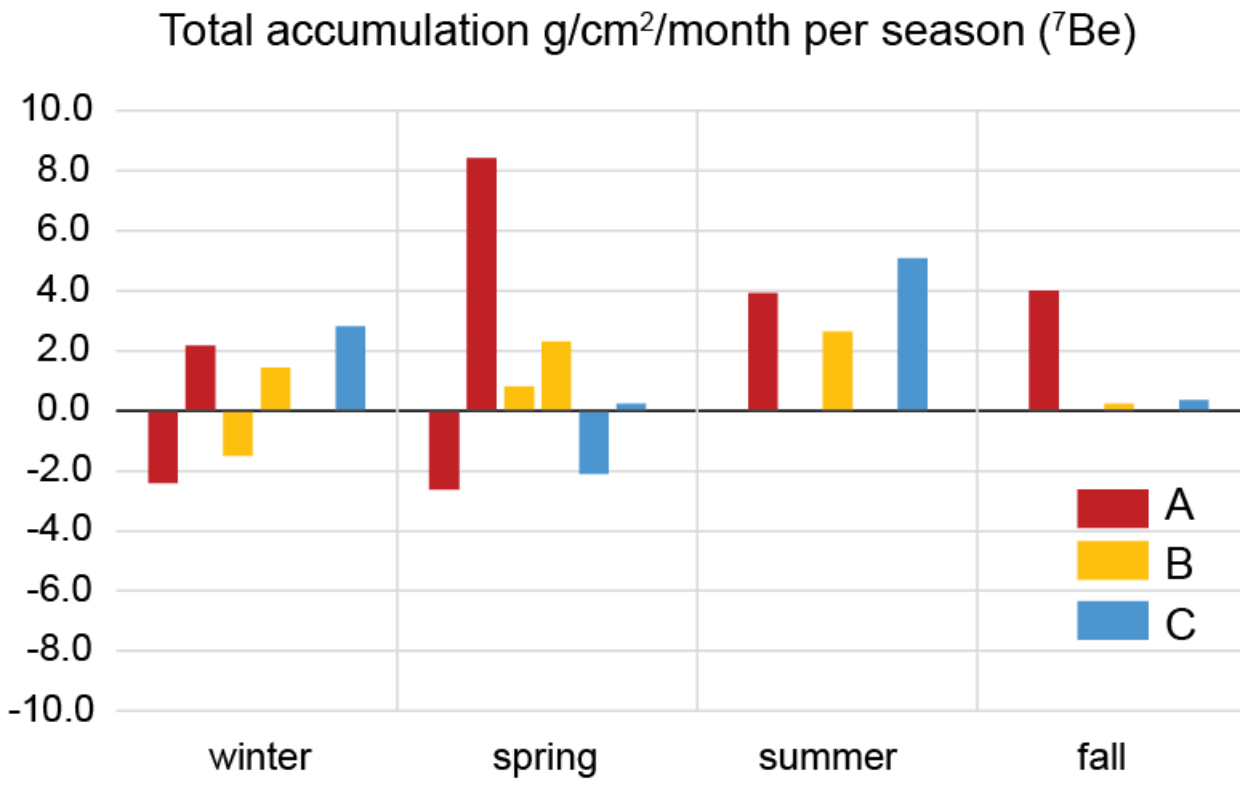

Figure 29. Total depositional and erosional evets at each site per season.

Summer and fall didn't record erosional events at any of the sites. Sites B and C recorded the highest deposition in the summer while fall deposition was almost negligible. Site C recorded significant depositional events through summer and fall. In the summer sediment was deposited at all sites and no erosion was recorded (Figure 29).

2.6 Discussion

2.6.1 Variations in sediment deposition and erosion.

Sediment deposition rates were highly variable between sampling periods and sites. Results derived from ^{7}Be fluxes vary greatly from results based on $^{210}Pb_{xs}$. Most of the inventories of excess $^{210}Pb_{xs}$ were lower than those expected from atmospheric deposition, indicating erosion. At the same time ^{7}Be inventories were suggesting deposition. The discrepancy may be a result of following factors: (1) freshly deposited materials come from and "old" source, not exposed to $^{210}Pb_{xs}$ fluxes, like from subsurface sediments from the alluvium, channel or banks (Jalowska, submitted). (2) $^{210}Pb_{xs}$ inventories integrate sedimentation history over longer time scale than ^{7}Be (3) $^{210}Pb_{xs}$ residual inventories could be eroded in between the sampling events and cause underestimation of new $^{210}Pb_{xs}$ flux. The seemingly contradictory results, may be revealing a hidden process of sediment replacement or local sediment removal and redistribution that were captured at the C site where flooding dismembered the feldspar horizon and caused redistribution of its pieces at depth with following inundations. Additionally the discrepancy between mass accumulation results and accumulation measured at the feldspar horizon can be explained by different sampling periods. Mass accumulations based on radionuclides were derived for October 2010 to August 2012 and feldspar results were collected between August 2012 and April 2015.

Net mass accumulation rates (Table 4) derived from ^{7}Be ($g/cm^2/yr$) indicate site A had the lowest accumulation rates (0.7 g/cm2/yr (~3.8 cm/yr)). This result is confirmed by the rates of sediment accretion measured from the feldspar horizon (4.5 cm/yr). Accretion on the horizon marker showed deposition event in August 2012, erosion event in December 2012 and then it indicated a steady increase in the amount of material being trapped at the site A. Steady mass accumulation rates at this site, can be explained by the highest concentrations of the sediment in the water column (Figure 22). Site A has highest elevation of the three sites, and is flooded least frequently (Figure 17). Site A was inundated for only 23% of the study time with short floods. Consequently sediment delivery or removal happens less often than at the other sites. Results of the suspended sediments show that Broad Creek is related to water fluctuations (Figure 17) hence when the inundation happens, the flooding waters carry more sediments. Sediment accretion rates at site C outpace the local rates of sea-level rise (0.3-0.4 cm/yr).

At site B, net mass accumulation rates (Table 4) derived from ^{7}Be ($g/cm^2/yr$) are 1.7 g/cm2/yr (3.8 cm/yr). Site B has the lowest elevation of all the sites, but at the same time is being protected by a vegetated levee. The accretion rate measured at the feldspar horizon is 0.2 cm/yr. Local topography results in high water-trapping efficiency. As a result, site B was inundated for 90 % of the study period, and dominated by floods longer than 3 days, with one inundation lasting over 50 days. Lacking frequent water and sediment exchange the site was trapping small amounts of sediment. Being below the mean sea-level elevation, with insufficient accretion rates, delta plain at site B cannot keep up with a sea level.

Table 4. Mean accumulation rates during the study period at each station.

Mean accumulation rates	A	B	C
^{7}Be ($g/cm^2/yr$)	0.6	1.6	2.7
$^{210}Pb_{xs}$ ($g/cm^2/yr$)	Erosional	Erosional	Erosional

Feldspar (cm/yr)	4.5	0.2	Erosional

Mass accumulation rates at site C were the highest and unrealistic during the study period 2.7 g/cm2/yr (9.5 cm/yr). Previous studies (Jalowska et al., 2015) reported that this site was net erosional with accumulation rates of 0.28 cm/yr. The study site was been inundated for 70% of the study period, and half of the floods were daily floods. The site measured the lowest of all three sites sediment concentrations in the water column (Figure 17). Frequent inundations with waters, depleted in sediments didn't facilitate sediment trapping and delta plain accretion. Additionally the feldspar horizon observations show clearly that water entering delta plain caries enough energy to dismember the feldspar horizon. There is a possibility that high mass accumulation rates were a result of local sediment redistribution during the frequent, high-energy inundations, as oppose to new depositional evets. The calculated rates of sediment accumulation indicated that site C is able to outpace the local rates of sea-level rise, however erosion of the whole feldspar horizon suggests that this site is erosional and cannot keep up with current sea-level rise.

2.6.2 Hydrologic and atmospheric drivers of depositional and erosional events.

Analyses of dependency of mass accumulation on inundation did not show unequivocal results. Previous studies, proved that hydrology is the main factor controlling floodplain sedimentation in alluvial floodplains (Allison et al., 1998; Hupp, 2000; Walling and He, 1998; Walling et al., 1998), and in deltaic-plain marsh environments (Bellucci et al., 2007; Christiansen et al., 2000; Stevenson et al., 1988; Temmerman et al., 2003). Marsh studies showed strong relationship between flooding frequency and deposition rates, however , similar to this study, Lagomasimo's (2013) study in Pamlico River did not find a clear relationship between the sediment deposition rates and inundation times.

In this study inundation patterns do not explain the depositional and erosional events suggesting that sediment delivery and removal is also dependent on sediment availability and local topography.

This study found positive relationship between erosion and sediments concentration. That in turn would suggest that most of the sediment in the water column come from erosion, a process concluded in Jalowska, (submitted). The study recorded suspended sediment concentrations only on the sampling dates and the obtained data provides only a time snapshot of these dependencies.

Another finding of this study is a relationship between elevation and net sediment accumulation. Variations in topography are known to affect accumulation rates within floodplain systems (Allison et al., 1998; Walling and He, 1998; Walling et al., 1998). In case of sites A, B and C there are other factors like sediment availability and elevation that control sediment accumulation.

Net mass accumulation per sampling site shows seasonal variability. With summer and fall being the non-erosional and summer being the time of largest deposition, at all there sites (Figure 29). Summer is also a time when all the sites experience the highest level of inundations during the year (Figure 20).

2.7 Conclusions

On decadal time scales the bayhead delta is erosional. On annual time scales the upper BHD is depositional in the anabranch channel, neutral at the Broad Creek junction with Roanoke River and erosional at site C in the lower bayhead delta plains. The study shows that delta plain floodplains are governed by different processes then alluvial floodplains and at much shorter time scales. The depositional and erosional processes happened much faster than sampling

frequency, and are difficult to diagnose. Lack of banks enables connectivity with the floodplains and anabranch channels facilitating both erosion and deposition. Sedimentation rates allow counteract the sea-level rise only at site A located in the upper bayhead delta, has highest elevation, highest concentration of suspended sediment. Combination of all three factors provide the optimal condition for sustainability. Sampling site in the middle and lower bayhead delta cannot keep up with sea-level, due to the lower elevation, lower TSM, higher inundation and frequency.

Another important finding of this study is a process of sediment replacement process that has been reported in Jalowska (submitted) and has implications for sediment and carbon budgets in the deltaic environments.

CHAPTER 3: TRACING SUSPENDED RIVER SEDIMENT INDICATES THAT RECYCLING OF THE DELTAIC SEDIMENTS IS AN IMPORTANT PROCESS DURING TRANSGRESSION [2]

3.1 Abstract

Floodplains are thought to be long-term depositional environments, but there remains limited understanding regarding timescales of depositional or erosional events, sediment delivery pathways and sediment storage. This study uses sediment concentration and flow information with sediment fingerprinting to examine the contribution of surface and subsurface sources to suspended sediment transiting the Lower Roanoke River, North Carolina, United States. The Lower Roanoke is disconnected from its upper reaches by a series of dams, which effectively restricts suspended sediment transport from the headwaters. Accordingly, sediments from the Lower Roanoke River basin are the primary source of suspended sediment downstream of the dams. Three potential end-member sources were sampled including surface sources: floodplains and topsoils f (n=60), subsurface sources: channel bed and banks (n=66), and deltaic sources: the delta front and prodelta (n=11). The fingerprinting method utilized fallout radionuclide tracers ($^{210}Pb_{xs}$ and ^{137}Cs) to examine the spatial variation of sediment source contributions to suspended sediment samples (n=79). The results show that with decreasing river slope and increasing influence of estuarine-driven flow dynamics, the contribution of surface sediments increases

[2] This chapter was submitted as an article to *Catena.* The original citation is as follow: Anna M. Jalowska, Brent A. McKee, J. Patrick Laceby, Antonio B. Rodriguez (2016), Tracing Suspended River Sediment Indicates that Recycling of the Deltaic Sediments is an Important Process During Transgression, **SUBMITTED**

from 20 (±2%) to 67% (±1%) and becomes the main source of sediments in the Roanoke bayhead delta. At the river mouth, the surface-sediment contribution decreases and, the delta front and prodelta sediments contribute 74% (±1%) to the suspended load. During delta transgression, erosion of the lower delta can become a source of sediment to the upper delta and deltaic plains, at the same time deltaic plains, regarded to be a sediment sink and long-term sediment storage, become erosional.

Recognition of this sediment pathway in the Roanoke River raises the question as to whether this is an important process in other eroding deltas. The lower river and distributary network of the delta plain, which was previously thought to be a unidirectional seaward dispersal system of eroded sediments, may have an important landward sediment dispersal component that provides nourishment and fortification to the upper bayhead delta, at the cost of the eroding lower delta.

3.2 Introduction

Rivers mediate the exchange of particulate and dissolved materials between land and ocean. The delivery of the sediments to the coastal zone may not be direct, and sediment transport pathways vary on different time scales (Fryirs et al., 2007; Harvey, 2002; Mattheus et al., 2009; Trimble, 1983; Walling, 1983). Suspended sediment transport biogeochemically important materials associated with particles, including particulate carbon, nutrients, trace elements and contaminants. Importantly, the suspended sediment load provides essential material for building and fortifying coastlines (Blum and Roberts, 2009; Gunnell et al., 2013; Mattheus et al., 2009; Nittrouer and Viparelli, 2014; Syvitski et al., 2009). Globally, over 20 Pg of particulate material is transported annually by rivers (Meade, 1996); however, approximately 80-90% of all sediment eroded annually from the landscape, is trapped in alluvial and colluvial systems before

being delivered to the ocean (Meade et al., 1990). Although the spatial and temporal scales for trapping and storing particulate materials is not well quantified (Hupp, 2000), previous studies indicate that most sediment storage occurs within reservoirs (Kondolf et al., 2014), and in floodplains, deltas and estuaries (McKee et al., 2004). Materials stored in floodplains, river banks and channels can be remobilized, along with their associated carbon, nutrients and pollutants (Hupp et al., 2015; Jalowska et al., 2015).

Previous studies demonstrate that a large fraction of riverine particulate material is transported during the rising limb of the hydrograph, and are stored during falling stages (Dunne et al., 1998; Meade et al., 1985). Consequently, during overall transport to marine and/or estuarine basins, particulate material may spend a large amount of time stored within the river system, specifically in its channels, floodplains, gullies and ditches. River channels often change dramatically in their lower reaches, they widen, inundate floodplains more frequently, bifurcate into distributary networks, and are exposed to lunar and/or wind-driven tides. Floodplains are thought to be long-term depositional environments (Fryirs et al., 2007; Wolman and Leopold, 1957), but there is still little understanding about timescales of depositional or erosional events, sediment delivery pathways and sediment storage within bayhead-delta plains (O'Connell et al., 2000). Extending knowledge about processes in these environments would improve estimates of material fluxes to the ocean, and improve understanding of the role that lower-river environments play in global carbon and nutrient cycles.

Modern sediment yields are controlled by five primary natural and anthropogenic factors, including: 1. land use (including vegetation cover); 2. climate (rainfall variability and runoff intensity); 3. geology (including soil type); 4. relief (elevation and basin slope); and, 5. Pleistocene history (Ludwig et al., 1998; Meade, 1996; Stallard, 1998). Over centennial

timescales, land use and climate change are the most relevant factors for sediment yield. A growing human population, and the associated need for resources and expansion of technology has resulted in substantial and pervasive alterations of Earth's environments (Vitousek et al., 1997). Human activities on land have caused an enhanced loss of terrestrial organic matter, mainly through deforestation, and consequently, has increased soil erosion, and transport to the coastal margins by rivers (Ver et al., 1999).

Sediment loads decrease following the placement of river impoundments. Over half of the world's largest river systems have been moderately to strongly affected by dams (Nilsson et al., 2005). Globally, dams have decreased particle transfers to the ocean by more than 50% (Meade et al., 1990; Vörösmarty et al., 2003). The magnitude and time scale of post-dam changes depend on the number and size of the impoundments within the watershed (Magilligan and Nislow, 2005; Williams and Wolman, 1984). River damming results in flow regulation, which often dramatically alters alluvial rivers through reduced water-release, and substantial reductions in sediment transported below dams (Brandt, 2000; Williams and Wolman, 1984) results in downstream sediment starvation, reducing further sediment delivery to the lowlands, deltas and estuaries (Kondolf, 1997). Flow regulations eliminate the lowest and highest peaks from the hydrographs, and limit overbank flows, which results in decreased connectivity between river channels and floodplains (Hupp, 2000). Another downstream impact of dams is channel incision and subsequent widening through bank erosion. Consequently, in a downstream direction, below the lowest dam, the dominant sediment source of the river's suspended load is changing as the influence of the dam on the graded stream profile, and the flow regime lessens. The physical and geomorphological foundations of these changes are known, however the pathways of sediment sourcing transformation along the river gradient, including the river delta,

as well as the scale of the transition zone, in terms of downstream distance, and magnitude are unknown. Here we investigate these questions by monitoring total suspended matter of the river load, conducting a cartographic analyses of the river basin, analyzing sediment grain-size, and imaging the riverbed. In addition, a sediment fingerprinting method was employed to distinguish between sources results were placed in context with changes in river hydrology.

3.3 Background

3.3.1 Study Area.

We chose the Roanoke River for this study because the history of natural and anthropogenic modifications to the system are well constrained (Hupp et al., 2009b; Jalowska et al., 2015; Schenk et al., 2010). The Roanoke River originates in the Valley and Ridge province of the Appalachian Mountains in Virginia and empties into the west end of the Albemarle Sound at an average annual rate of 252 m^3/s (Giese et al., 1979; Molina, 2002). The total drainage area of the River is 25,123 km^2. Albemarle Sound and the Roanoke bayhead delta are located in Northeastern North Carolina (Figure 30). The Sound is separated from the Atlantic Ocean by the Northern Outer Banks barrier-island chain. Direct water exchange with the ocean has been minimal since the closing of a tidal inlet in 1833, and present exchange with adjacent Pamlico Sound is possible only through narrow Croatan and Roanoke sounds (Jalowska et al., 2015). Consequently, the salinity of Albemarle Sound varies from the 5-15 ppt in the east to 0.5-5 ppt in the middle and < 0.5 ppt in its west end, at the mouth of the Roanoke River (NOAA SEA Division, 1998). Albemarle Sound is a wind-driven estuary, and astronomical tides are negligible near the Roanoke Bayhead Delta (Giese et al., 1979; Jalowska et al., 2015; Riggs and Ames, 2003). At the mouth of the Roanoke River, cyclical daily fluctuations in water levels, up to 0.6 m, have been associated with seiching (Luettich et al., 2002).

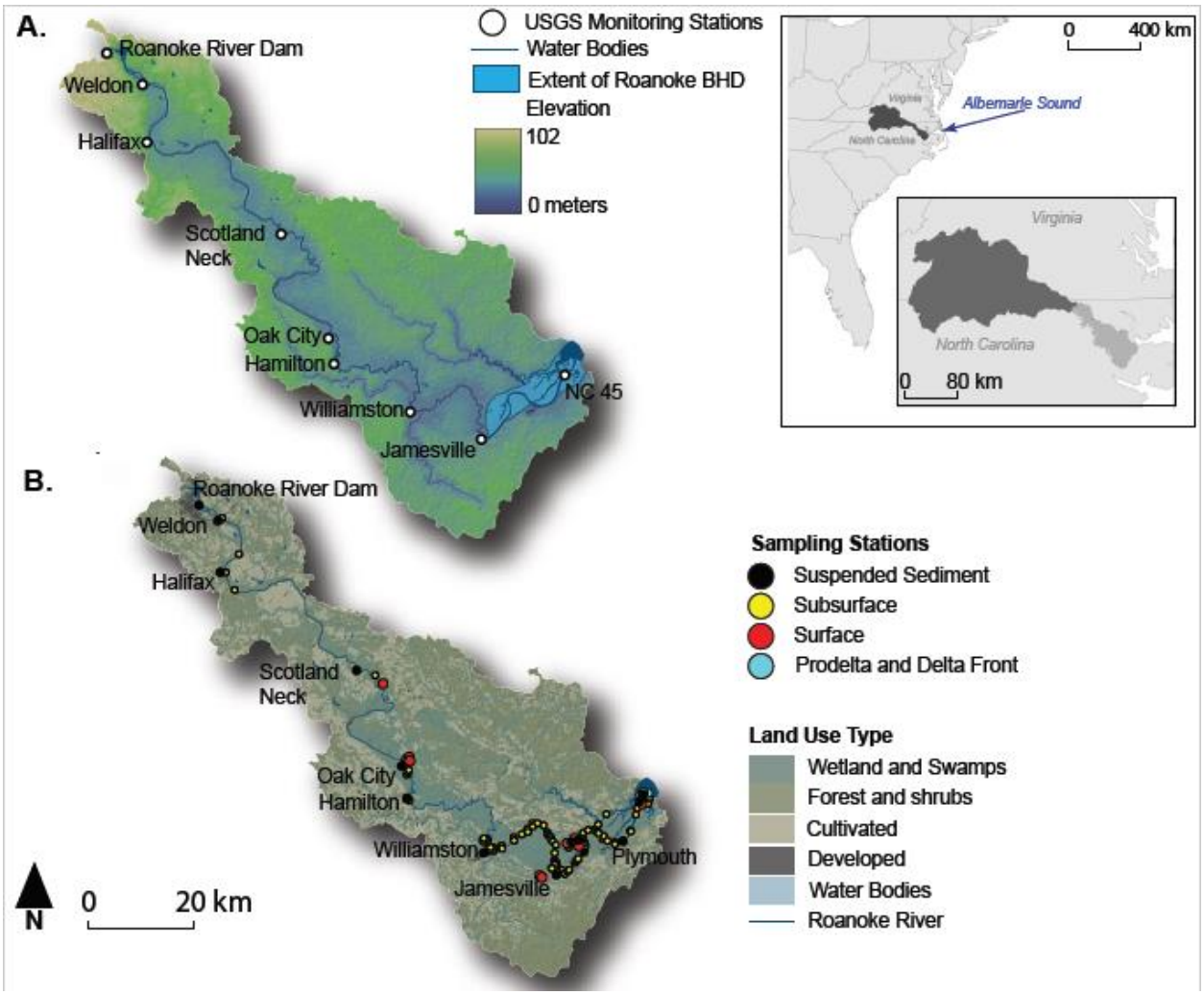

Figure 30. A. Lower Roanoke Basin elevation map with USGS monitoring stations B. Map of the land use in the Lower Roanoke basin with sampling locations. The insets show the location of the catchment within the United States.

The Lower Roanoke is 220 km long and drains an area of 3,392 km^2 (Figure 30). The Atlantic Seaboard fall line is considered the western boundary of the Lower Roanoke River, as it is almost completely disconnected from the upper reaches by a series of dams located above the fall line (Figure 30). The elevation gradient of the Roanoke is steepest (ca. 25%) 30 km below the fall line. Below that transition down to to the bayhead delta, the river gradually loses 8 m of elevation. The low gradient facilitated the formation of an extensive, up to 9-km wide, floodplain from 80 km below the fall line to the bayhead delta.

The Roanoke River watershed and Albemarle Sound have been impacted by European settlement in North America since the late 1600's AD. Between the 1600's and 1800's, intensive land clearing and primitive agriculture practices caused widespread erosion. Accordingly, sediment accumulated in the Lower Roanoke floodplains, banks and channel as a distinct, up to 10 meter deep layer of fine (<63 μm), orange-stained legacy sediments (Hupp et al., 2009b; Jacobson and Coleman, 1986; James, 2013; Wolman, 1967), and stabilized the Roanoke bayhead delta (Jalowska et al., 2015).

Before 1947, the water level and flow of the Lower Roanoke River was characterized by extreme variability in response to changes in precipitation over seasonal and event (storms) time scales (Richter et al., 1996). Between 1947 and 1963, three dams were constructed, with the most seaward dam at Roanoke Rapids completed in 1955. Dam-controlled water releases altered the hydrologic regime of the river by eliminating both the highest and lowest-magnitude flows (Jalowska et al., 2015; Richter et al., 1996). Removing high-magnitude flows caused a reduction in the hydrological capacity of the river and connectivity between the channel and floodplains. Additionally, the frequency of medium-magnitude flows increased over six times, which caused an increase in bank erosion (Hupp et al., 2009b).

After construction of the dams, sediment delivery to the Lower Roanoke and ultimately Albemarle Sound was reduced by 99% (Meade et al., 1990; Simmons, 1988) (Figure 31), leaving the Lower Roanoke banks, channels and floodplains, which are filled with legacy sediments, as the only source of sediments. Previous studies in US Piedmont watersheds (Devereux et al., 2010; Gellis et al., 2009; Mukundan et al., 2010) have grouped sediment sources into two categories: surface sources, which are mainly eroded soils delivered to the river with runoff, and subsurface sources, which are associated with bank/channel and gully erosion. Hupp et al. (2009)

and Schenk et al. (2010) measured bank erosion and floodplain deposition in the upper and middle reaches of the Lower Roanoke River, below the dam, using erosion pins and clay pads, respectively. The study showed that the rate of bank erosion, a subsurface sediment source, is between 0-52 cm/year, is highest along banks >2 m high in the middle reaches of the Lower Roanoke, and decreases downstream (Hupp et al., 2009; Schenk et al., 2010). Similar results were found in other watersheds in the region, such as in the Chesapeake Bay Watershed (Gellis et al., 2009) and North Fork Broad River, GA (Mukundan et al., 2010).

Although sediment delivery to the lower Roanoke River and Albemarle Sound decreased after construction of the dams, floodplain deposition increased downstream of the Roanoke Rapids Dam to a maximum of 0.9 cm/year recorded at the upper limits of the bayhead delta (Hupp et al., 2009; Schenk and Hupp, 2008). That rate of floodplain deposition is comparable to sedimentation rates reported for the bayhead delta by the Environmental Protection Agency (2008; 0.2-0.8 cm/yr) and by Jalowska et al. (2015; 0.28-0.88 cm/year). Jalowska et al. (2015) reported landward movement of the Roanoke bayhead delta shoreline, a shift from depositional to non-depositional or an erosional state of the prodelta and net erosion of floodplains proximal to Albemarle Sound. Those measurements suggested that delta retreat was associated with sea-level rise and a decrease in sediment supply resulting from improved agricultural practices and damming upstream. A variety of methods were utilized to investigate possible changes in river sediment source downstream from the Roanoke Rapids Dam and upstream from the eroding bayhead delta front.

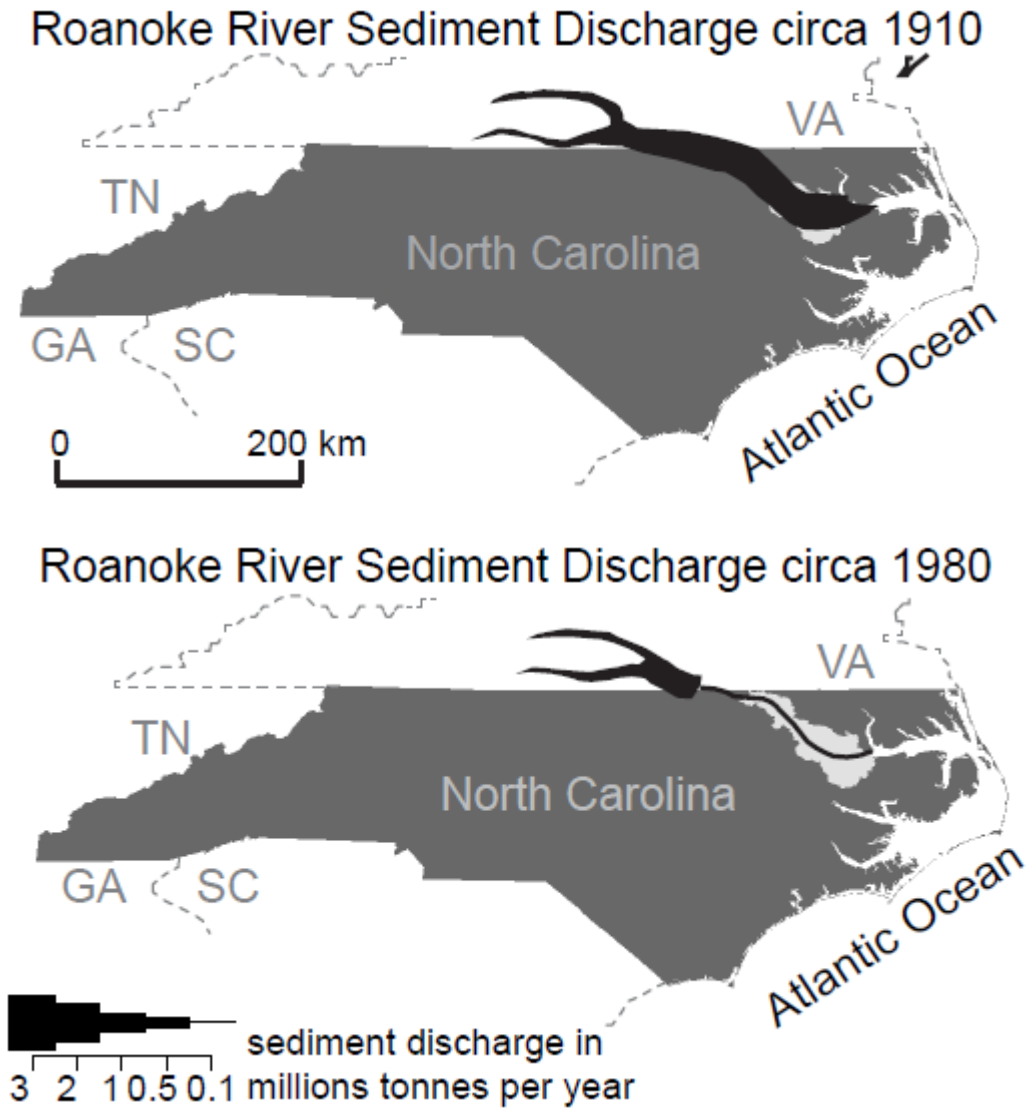

Figure 31. River suspended sediment discharge during two periods, circa 1910 and circa 1980 showing the decrease in sediment loads associated with dam placement (based on (Meade et al., 1990)).

3.3.2 Sediment fingerprinting approach.

To trace suspended sediment in river catchments, it is important to identify the various sediment sources and fates, and since the 1970's, geochemical and physical properties have been used as sediment fingerprinting properties (Collins et al., 1998; Davis et al., 2009; Oldfield et al., 1985). Sediment fingerprinting assumes that a set of biogeochemical and/or physical sediment properties provide a unique fingerprint allowing investigators to calculate the relative sediment

contribution from various sources (Davis et al., 2009). Importantly, the set of unique properties should not change during the erosion, transport and deposition processes, or should change in a predictable way (Laceby and Olley, 2015; Motha and Wallbrink, 2002) .

The use of fallout radionuclide tracers, especially ^{137}Cs and $^{210}Pb_{xs}$ (Olley et al., 2013, 1993; Wallbrink et al., 1999, 1998; Walling and Woodward, 1992; Walling et al., 1999) is common in sediment fingerprinting. ^{137}Cs ($t_{1/2}$=30y) is present in the environment as a result of fallout from the testing of thermonuclear weapons, primarily from 1954–1968. In natural areas, watershed surface soils are enriched in ^{137}Cs (Olley et al., 2013) because of direct exposure to the fallout. In agricultural areas, the surface soil values may be lower than undisturbed one, due to mixing associated with tillage. Consequently, absence of ^{137}Cs indicates that sediments were not exposed to fallout and they are derived from subsurface sources. ^{137}Cs is strongly associated with particles in fresh water environments, while in saline environments ^{137}Cs desorbs from particles (Hong et al., 2012). In this study, the most seaward sampling site- the delta front/prodelta - always recorded salinity of 0 ppt during the sampling period, thus the restraints associated with a potential ^{137}Cs desorption do not apply. Accordingly, this study region provides a unique environment to apply a sediment fingerprinting approach in a deltaic environment.

^{210}Pb ($t_{1/2}$=22y) is a naturally produced radionuclide as a decay product of ^{238}U present in the Earth's crust (Curie et al., 1898; Rutherford, 1904). It has two pathways of becoming associated with lithogenic particles. An in-situ contribution through the ^{238}U decay chain in the particle's matrix referred to as a background ^{210}Pb. Another path is through wet and dry fallout, associated with the escape of ^{222}Rn (part of ^{238}U decay chain) from soils to the atmosphere, and its decay to ^{210}Pb, referred to as the 'excess' ^{210}Pb ($^{210}Pb_{xs}$) after its subsequent fallout. Surface soils have high $^{210}Pb_{xs}$ values, due to a recent exposure to the fallout while low $^{210}Pb_{xs}$ activities

would correspond with sediments buried within last 150 years (five half-lives) and derived from erosional sites (Walling and Woodward, 1992).

3.4 Methodology and Sampling

3.4.1 GIS Analyses, Stream Data and Total Suspended Sediment.

The slope of the river and channel width were measured using a digital elevation model (DEM; 6 m grid-cell spacing) obtained from NC DOT-GIS Unit (North Carolina Department of Transportation, 2003) and processes in ArcMap software (ESRI (Environmental Systems Resource Institute), 2015).

The Lower Roanoke watershed was classified according to land use type using the Earth Satellite Corporation land cover dataset (Earth Satellite Corporation (EarthSat), 1997) and mapped using ArcMap software (ESRI (Environmental Systems Resource Institute), 2015) (Figure 30B, Table 5).

Table 5. Land use in the Lower Roanoke River.

Land use type and subtypes	**Area (km^2)**	**Percentage**
Forest and shrubs (Broadleaf Evergreen Forest, Deciduous Shrubland, Evergreen Shrubland Mixed Hardwoods/Conifers, Mixed Shrubland, Southern Yellow Pine, Other Needleleaf Evergreen Forests, Mixed Upland Hardwoods, Needle leaf Deciduous)	1327	39%
Wetlands (Unmanaged Herbaceous Wetland, Oak/Gum/Cypress, Bottomland Forest/Hardwood Swamps)	1052	31%
Cultivated (Unmanaged Herbaceous Upland, Unconsolidated Sediment, Managed Herbaceous Cover, Cultivated)	919	27%
Water	64	2%
Developed (Low Intensity Developed, High Intensity Developed)	30	1%
total	3392	100%

Discharge data for the Roanoke River USGS stations at Roanoke Rapids (station number 02080500), and gage height data Hamilton (station number 02081028), Williamston (station number 02081054), Jamesville (station number 02081094) and NC45 NR Westover, NC (station number 0208114150, located downstream from Plymouth) were obtained from the USGS Water Data website (United States Geological Survey, 2012) (Figure 30). These data were used to calculate minimum, maximum and average water levels at the stations. To understand the influence of the dam on the hydrology downstream, hydrographs for stations in Hamilton, Williamston, Jamesville and Plymouth were compared to the hydrograph from Roanoke Rapids, and the correlation coefficients were derived for the sampling period (Table 6).

Table 6. Discharges, water level data and correlation with dam releases during sampling period.

USGS gage station	**Distance below the dam (km)**	**Drainage area below the dam (km^2)**	**Discharge range**	**Mean discharge**	**Correlation coefficient (r) with discharges from Roanoke Rapids Dam**
Roanoke Rapids	0	0	45 to 810 m^3s^{-1}	187 m^3s^{-1}	
Hamilton	118	1311	0.05 to 0.50 m	0.21 m	0.91
Williamston	155	1777	0.68 to 3.52 m	2.04 m	0.88
Jamesville	182	2243	-0.20 to 1.68 m	0.51 m	0.69
Plymouth (NC45)	208	3305	-0.21 to 1.98 m	0.41 m	0.12

Total suspended matter (TSM) concentrations were measured between 2/20/2009 and 11/16/13 at 11 locations in the Lower Roanoke River (Figure 30B). To measure TSM, river water samples were collected in one litter, acid cleaned bottles at each station, and vacuum-filtered through pre-weighed 0.22 µ, nitrocellulose filters. After filtering, samples were flushed with 1L of deionized water. The filters were then dried in a 40^{o}C oven for 48h, and weighed again. TSM concentrations were recorded as mg/L.

Table 7. Sample location information including number of total suspended sediment concentration samples and channel width.

Station Location	Channel width (m)	Number of TSM observations in this study	Date Range of EPA observations	Number of EPA TSM observations
Roanoke Rapids, NC Km 0	~60	1	02/20/1997 - 11/28/2007	69
Weldon, NC Km 11	~130	3	NA	NA
Scotland Neck, NC Km 57	~90	NA	02/20/1997 - 11/28/2007	49
Oak City, NC Km 105	~90	8	NA	NA
Hamilton, NC Km 118	~90	11	NA	NA
Williamston, NC Km 155	~90	27	03/11/2008 - 09/04/2013	20
Jamesville, NC Km 182	~120	29	NA	NA
Welch Creek near Plymouth, NC Km 199	~330	NA	02/24/2008 - 07/17/2012	11
Plymouth, NC Km 202	~160	25	NA	NA
NC 45 at Sans Souci Km 208	~480	6	03/18/1997 - 11/14/2007	70
Eastmost River Km 212	~50	13	NA	NA
Albemarle Sound at Batchelor Bay Near Black Walnut	~370	NA	03/18/1997 - 04/18/2007	62
Prodelta Km 214	NA	8	NA	NA

Despite its local significance, there is no continuous record of suspended sediment concentrations from the Roanoke River. Previous studies provided single sets of measurements (Alexander et al., 1998; Meade et al., 1990), and used Secchi disk observations as a proxy for suspended matter (Hupp et al., 2009a; Schenk et al., 2010). Non-continuous, historical data of

suspended sediment concentration, were obtained from the EPA STORET website (United States Environmental Agency, 2007) to validate results from this study (stations and time periods listed in Table 7).

3.4.2 Sample Collection, Sampling Frequency and Processing.

Sediment samples (245) were collected mostly in calm weather conditions and no sampling occurred during event conditions like tropical storms. Materials from subsurface (86 samples) and surface (60 samples) sources were collected to from both erosional and depositional environments during the time period February 2009 to March 2012, including: floodplains (surface; n=58), agricultural topsoils (surface; n=2), river-channel bed (subsurface; n=17), banks (subsurface; n=33), and gullies (subsurface; n=16; Figure 32). The eroding delta front and prodelta were categorized as a separate suspended sediment source and sediment from these environments were collected at the river's mouth (n=11).

Samples from floodplains, agricultural fields and dry gullies were collected by integrating the top 3-cm layer of short 10-cm diameter cores. Subaqueous samples from the channel bed and submerged banks were collected with bottom grab samples or as short 10-cm diameter cores, in both cases, the top 3-cm layer was integrated into a sample. Samples from the banks were collected with a spatula, and similar to the other sources, the top 3 cm of sediment was integrated into a sample. Suspended sediment samples (n=78) were collected at 13 locations, 8 of which were at USGS water-level monitoring stations (Figure 30A). USGS stations in Jamesville, Williamston and Plymouth were sampled biweekly for bulk suspended sediment and sediment concentration. The remaining USGS stations were sampled bimonthly or annually because they are only accessible by boat or are located in the upper reaches of the river (Figure 30A and B).

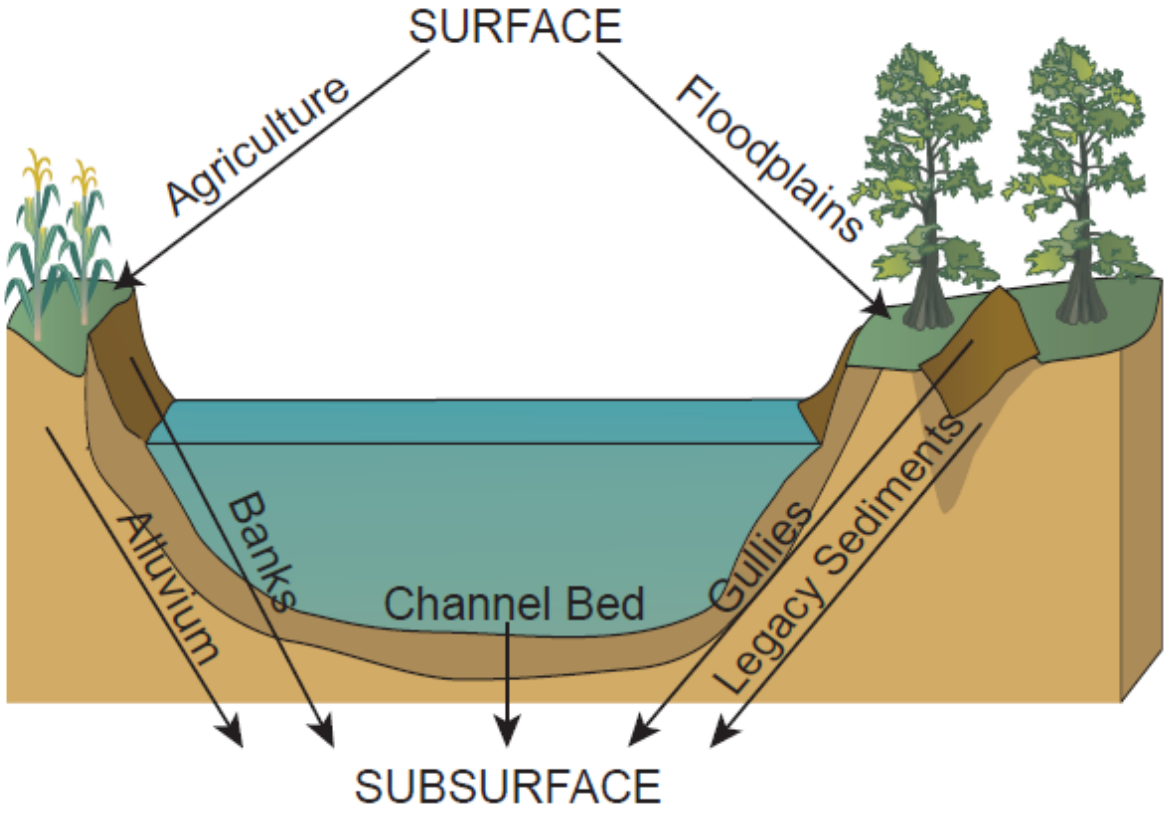

Figure 32. Sources of sediment to suspended load.

Water samples for suspended sediment were collected in 70 L acid-cleaned plastic carboys, and particles were harvested from the water through continuous flow centrifugation.

3.4.3 Grain-size Distribution and Side Scan Sonar Data.

56 channel sediment subsamples were analyzed for grain size using a CILAS 1180 to measure particle sizes from 0.04 to 2500 mm in 100 size classes by laser diffraction. Grain sizes were binned into coarse (>62μm), and fine (<62μm) classes.

To explore the subaqueous geomorphology of the Roanoke River channel, side-scan sonar data were collected using an Edgetech 4200 dual-frequency (120/410 kHz) system. Data were collected using 410 kHz, at a 50-m range and in a discontinuous grid pattern. Data were

processed by applying a time-varying gain and mosaicked using Chesapeake Technology Inc. SonarWiz software.

3.4.4 Radionuclide Analyses.

Bulk sediment samples were freeze-dried, subsampled for grain size analyses, packed into standardized vessels and petrie dishes, and sealed for three weeks to allow ^{222}Rn equilibration. Radionuclide tracer activities were measured by gamma spectrometry. Gamma counting was conducted on one of four low-background, high-efficiency, high-purity Germanium detectors (Coaxial-, BEGe-, and Well-types) coupled with a multi-channel analyzer. Detectors were calibrated using a natural matrix standard (IAEA-300) at each region of interest in the standard counting geometry for the associated detector. Activities were corrected for self-adsorption using a direct transmission method (Cutshall et al., 1983). Total ^{210}Pb and ^{137}Cs activity was directly determined by measuring the 46.5-KeV and 661.64-KeV gamma photo-peaks respectively. To calculate the $^{210}Pb_{xs}$ values, a background ^{210}Pb activity was subtracted from total ^{210}Pb activity. The background levels of ^{210}Pb (^{226}Ra activity) were determined by measuring the gamma activity of ^{226}Ra granddaughter ^{214}Bi (609 KeV).

3.4.5 Mixing Model.

Most studies modeling the relative contribution of endmembers to the observed suspended load use a multivariate mixing model (Haddadchi et al., 2013). In this study, we used the distribution model proposed by Laceby and Olley, (2015) that minimizes mixing model difference (MMD) (Equation 1):

$$MMD = \sum_{i=1}^{n} \left| \left(C_i - \left(\sum_{s=1}^{m} P_s S_{si} \right) \right) / C_i \right| \qquad (1)$$

where n is the number of tracers included in the model; C_i is the normal distribution of tracer parameters ($_i$) in the suspended sediment sample; m is the number of sediment sources used in

the model; P_s is the percentage contribution of the sediment source ($_s$); S_{si} is the normal distribution of the tracer parameter ($_i$) in the sediment source ($_s$). The proportional contribution from each source (P_s) was modelled as a normal distribution ($0 \leq x \leq 1$) with a mixture mean (μ_m) and standard deviation (σ_m) (Caitcheon et al., 2012; Laceby and Olley, 2015; Olley et al., 2013).

One study, testing the accuracy of mixing models reported, that this approach is one of the more accurate modelling approaches (Haddadchi et al., 2014). Further, the use of tracer-specific correction factors (Collins et al., 1996) or an individual source elemental concentration correction factor (Collins et al., 2012, 2010) were not found to improve model performance (Laceby and Olley, 2015). Thus, these correction factors were not included in the model.

Prior to modelling, $^{210}Pb_{xs}$ and ^{137}Cs were tested for non-conservativeness, to ensure sediment radionuclide concentrations plotted within the source concentration range (Collins et al., 1996). The mean and standard deviation of each source and in-stream sediment tracers was used to define their normal distributions. To incorporate the tracer distributions, the mixing model was optimized with the OptQuest algorithm that is a part of Oracle's Crystal Ball software (Oracle, 2015). The OptQuest algorithm is used to search for and find optimal solutions in Monte Carlo simulation models.

In the program, each source's contribution (P_s) distribution (both μ_m and σ_m) was repeatedly varied when simultaneously solving Equation (1) 5000 times with 5000 stratified samples drawn from each suspended sediment (Ci) and source (S_{si}) distribution. The median MMD was minimized in the model when solving Equation (1). A constraint for the optimization was that sum of proportional contributions of the sources (P_s) must total one. This process of deriving the optimal source contribution mixture distribution (P_s) for all 5000 randomly generated simulations was repeated 5000 times. The median P_s from these additional 5000

simulations is reported as the source contribution. Uncertainty of the contribution was calculated by summing modelled standard deviation of the mixture, plus the median absolute deviation (MAD) of the modelled standard deviation for an additional 5000 simulations, plus MAD of the individual sources median proportional contribution for 5000 simulations (Laceby et al., 2015).

3.5 Results

3.5.1 GIS analyses, Stream Data and Total Suspended.

Results show land cover for the Lower Roanoke River basin is 39% forest and shrubs, 33% wetlands and water bodies, and 27% cultivated and 1% urban areas (Figure 30, Table 5). Land proximate to the river channel is mostly a forested floodplain and connectivity with the cultivated and urban parts of the watershed is limited.

The river changes elevation from 66 to 0 meters above sea level (MASL) (NAD1983) over the 152 km distance below the Roanoke Rapids Dam (Figure 33). TSM concentration increases along the river's highest gradient to about km 105 (Figure 33). Below that marker, the concentration of TSM decreases along with the decreasing slope of the river. TSM concentrations slightly increase again in the area of eroding delta front/prodelta. Data collected during the study period are consistent with those data recorded by EPA (Figure 33).

Correlations between water level at the Roanoke Rapids Dam and stations along the river decrease in a downstream direction. Between Roanoke Rapids Dam and Hamilton, water level is controlled by the dam releases 91% of the time or more often (Figure 34). When the river reaches the elevation of 0 MASL dam releases begin to become less of a controlling factor for water level. The water level at Williamston (km 155, elevation 0 MASL) is controlled by the dam releases 88% of the time, and nearby at Jamesville (km 186), the river elevation drops to

between 0 and -1 MASL, and the water level is controlled by dam releases only 69% of the time. That transition (Jamesville) marks the upstream boundary of the bayhead delta.

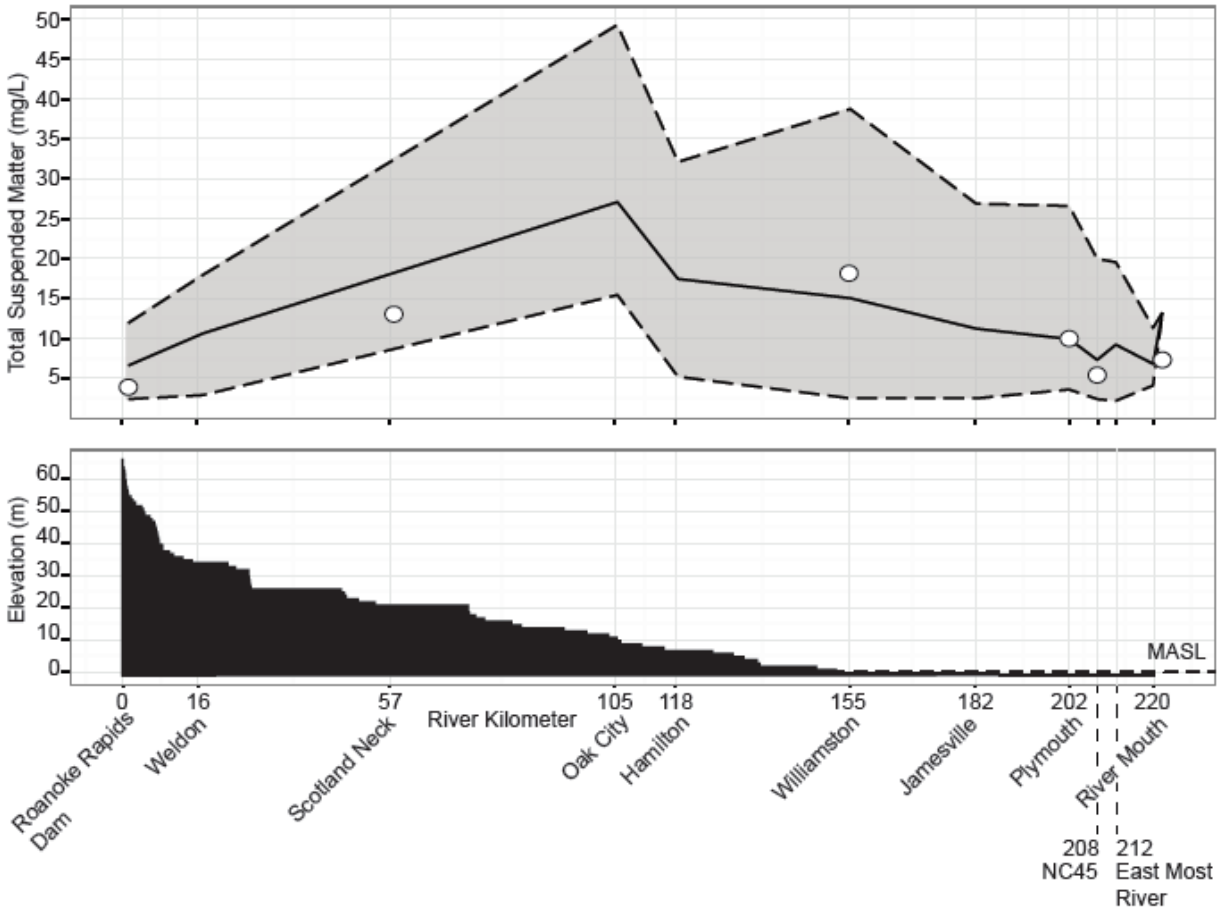

Figure 33. Upper panel: Suspended sediment concentrations presented as mean (solid line) and minimum and maximum values (dashed lines) at the station in the sampling period 2/20/2009 to 11/16/13.The open circles represent mean sediment concentrations from EPA STORET for period 02/20/1997 - 11/28/2007. Lower panel: Slope of the Lower Roanoke River.

The river widens seaward from Jamesville (Table 7) and the influence of water-level fluctuations in Albemarle Sound becomes more pronounced and a major forcing factor at Plymouth (km 208, elevation -1 MASL), where the correlation with discharges from the dam decreases to 12% of the time (Figures 33 and 34) (Table 6). Additionally, the hydrograph from Plymouth station shows a seasonal pattern and semi-diurnal fluctuations in water level,

confirming that water level in the bayhead delta is controlled by water movement in Albemarle Sound.

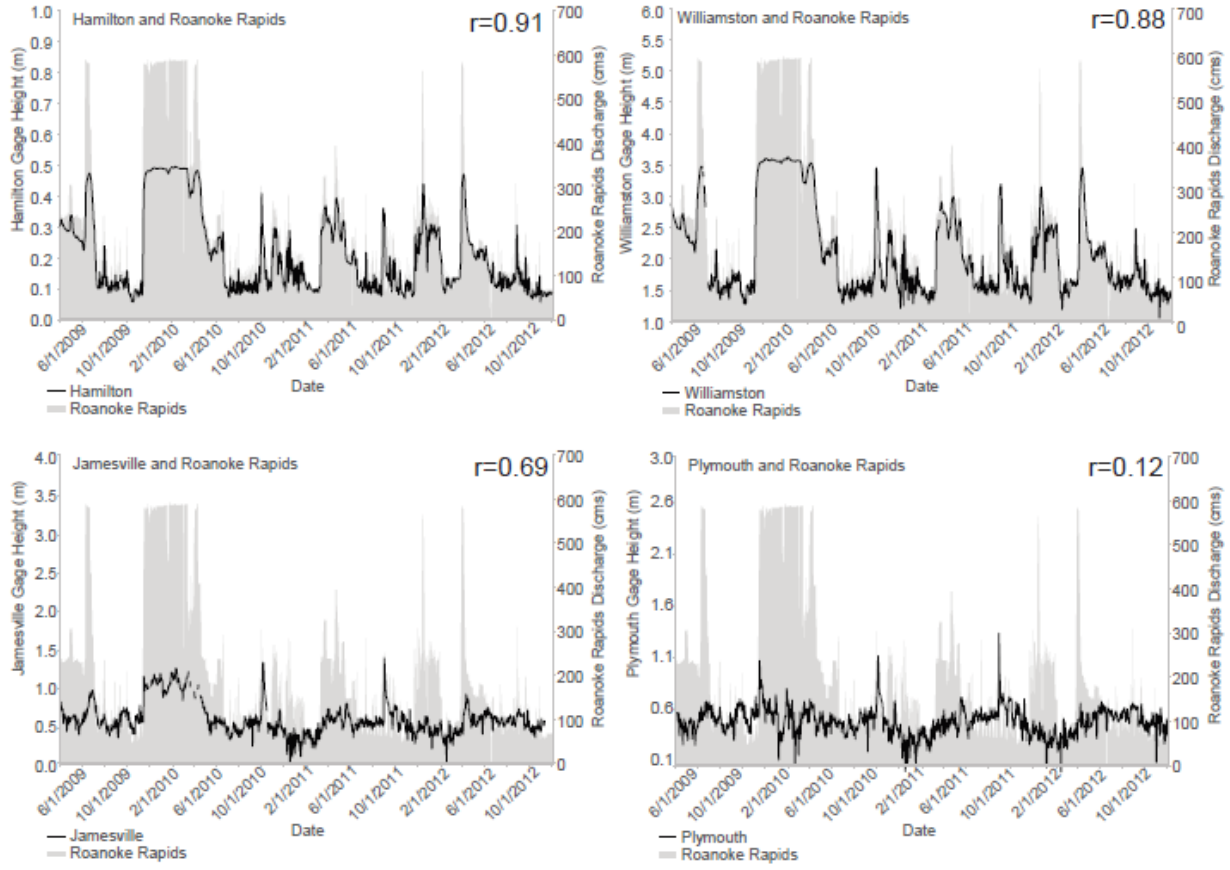

Figure 34. Hydrographs at four stations, compared with discharges from the Roanoke Rapids Dam. Correlation coefficients (r) are provided in a left upper corner of each panel.

3.5.2 Grain-size distribution and in-channel sedimentation.

Grain size analyses of the channel sediments show a clear transition between the Lower Roanoke River and bayhead delta (Figure 35). Channel bed sediments between river km 150 and 186 are composed of about 80% of coarse material (fine sands). Along this reach, riverbanks, walls and beds of the rills and floodplain channels are composed of more than 70% fine-grained material. At km 180, the grain size of the channel bed sediment starts decreasing, and the

channel bed below km 190 is composed of <20% sand. The shift in bottom-sediment type is also resolved with side-scan sonar data, showing the presence and absence of channel bed forms upstream and downstream, respectively. The location of the transition to a fine particle-dominated channel bed corresponds with the upstream boundary of the bayhead delta (Figure 35).

3.5.3 Sediment Fingerprinting.

For distribution modeling, surface sediments were represented by floodplains (n=58), and agricultural topsoils (n=2). To verify if the activities of two samples from agriculture (3-5 Bq/kg) were representative, their values were compared with values reported for the region. Surface Piedmont soils ^{137}Cs concentrations in the Chesapeake Bay watershed range between 1.8 and 9.5 Bq/kg (Clune et al., 2010; Gellis et al., 2009) (all data decay corrected to 2009).

Floodplain samples (n=58) recorded activities between 0 and 35 Bq/kg (mean 9 Bq/kg). These values were higher than agricultural sources. To validate the activity range, the results from floodplain samples were compared to those from depositional environments in coastal North Carolina, where there is a preserved original or focused layer of sediments exposed to the fallout. The maximum peaks for ^{137}Cs varied from 3-135.3 Bq/kg with a mean of 39.4 Bq/kg (Benninger and Wells, 1993; Corbett et al., 2007; Giffin and Corbett, 2003; Lagomasino et al., 2013; Mattheus et al., 2009; Pruitt et al., 2010; Ritchie, 1962) (data decay corrected to 2009). Values reported in this study for surface sediments fit in the range reported in literature.

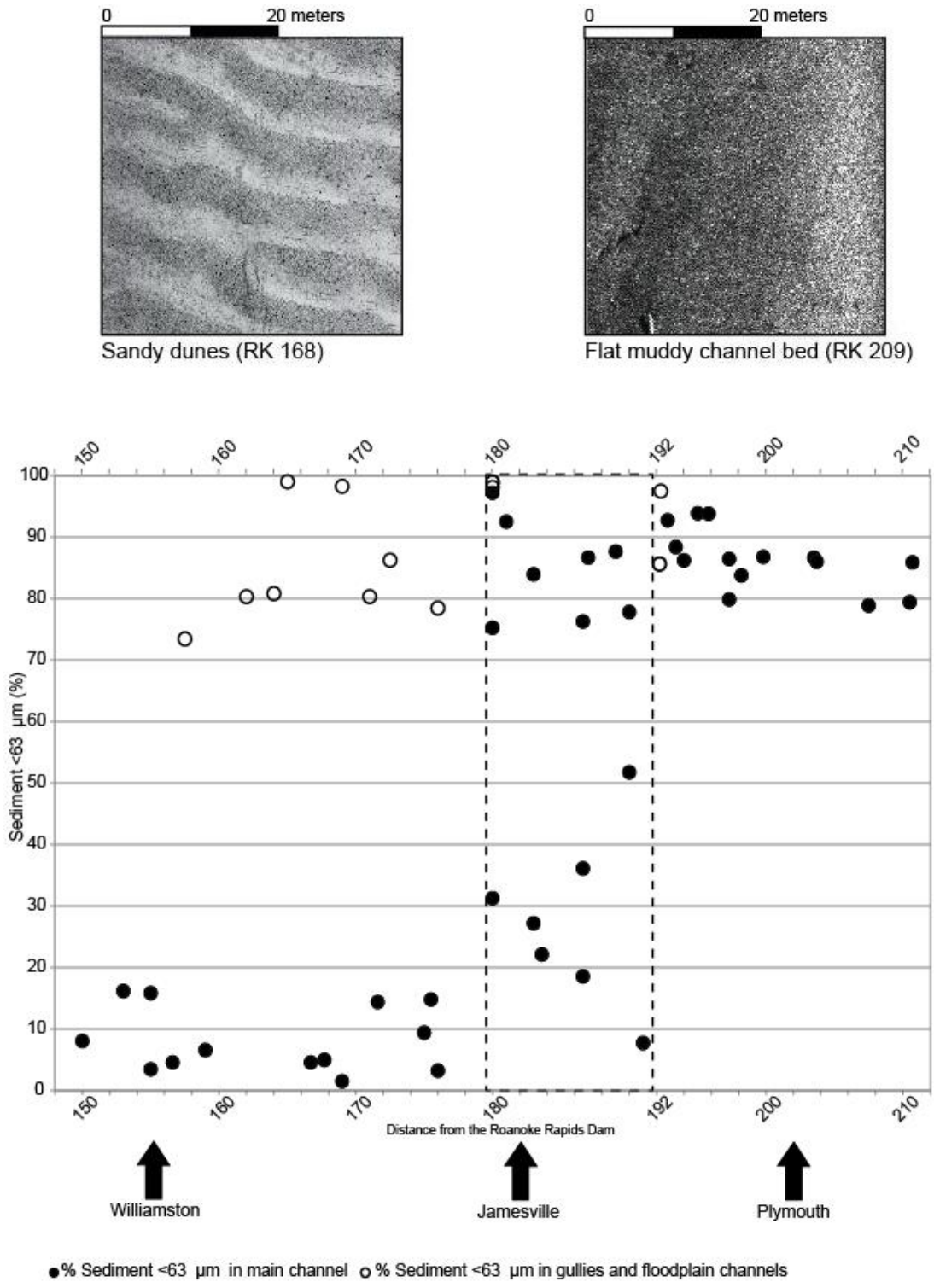

Figure 35. Grain size data (% silts and clays) of the channel bed and gullies by river km. Transition between Lower Roanoke River and bayhead delta is highlighted with a dashed line. Above the plot are examples of the bedforms characteristic for the Lower Roanoke River above the transition and for the fine-grained, flat channel bed in the bayhead delta.

Subsurface, surface and delta front/prodelta sediment sources (Figure 32) were best discriminated by $^{210}Pb_{xs}$ activity that is higher in surface soils. Mann-Whitney U-tests indicate statistically significant differences between all sources at $p < 0.001$. Activity of ^{137}Cs was also higher in surface soils, significantly discriminated between subsurface and surface, and subsurface and delta front/prodelta sources ($p < 0.001$), but not between surface and delta front/prodelta sources (Table 8 and Figure 36).

Table 8. Results of Mann-Whitney U-test.

	$^{210}Pb_{xs}$ (p-value)			^{137}Cs (p-value)		
	Subsurface	Surface	Prodelta	Subsurface	Surface	Prodelta
Subsurface						
Surface	< 0.001			< 0.001		
Prodelta	< 0.001	< 0.001		< 0.001	0.342	

Radionuclide activities of samples grouped by source are provided in Table 9. Surface sediment samples had a mean $^{210}Pb_{xs}$ activity value of 134.0 (σ 53.0) Bq/kg and mean ^{137}Cs of 9.0 (σ 4.0) Bq/kg. Subsurface sediments representing banks, channels and gullies sediments (Figure 32) had a mean $^{210}Pb_{xs}$ activity value of 10.0 (σ 16.0) Bq/kg and mean ^{137}Cs of 1.0 (σ 1.0) Bq/kg. The eroding delta front/prodelta sediment, considered as a source for the sediment at the mouth of the river, had a mean $^{210}Pb_{xs}$ activity value of 27.0 (σ 20.0) Bq/kg and mean ^{137}Cs of 6.0 (σ 2.0) Bq/kg.

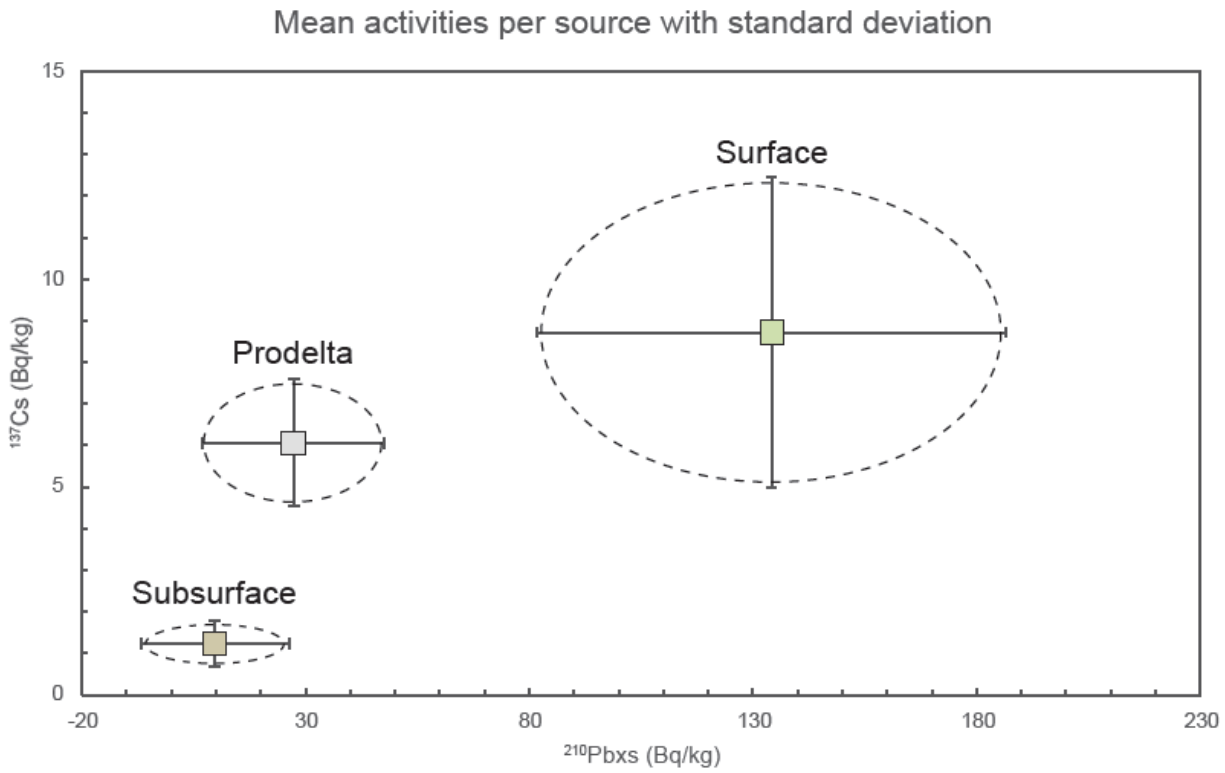

Figure 36. $^{210}Pb_{xs}$ and ^{137}Cs activities in source sediments with the error bars representing one standard deviation of the mean.

Table 9. Fingerprinting properties of sediment sources and suspended sediment per station.

Source and grain size		**Mean $^{210}Pb_{xs}$ activities (Bq/kg)**	**Mean ^{137}Cs activities (Bq/kg)**
Surface (n=60)		134 (σ 53)	9 (σ 4)
Subsurface (n=66)		10 (σ 16)	1 (σ 1)
Eroding Prodelta (n=11)		27 (σ 20)	6 (σ 2)
Suspended Sediment (Surface water 0-0.5 m depth))	Hamilton (n=6)	77 (σ 68)	3 (σ 2)
	Williamston (n=22)	91 (σ 66)	7 (σ 5)
	Jamesville (n=21)	130 (σ 81)	7 (σ 6)
	Plymouth (n=17)	155 (σ 88)	12 (σ 6)
	Prodelta (n=13)	75 (σ 60)	8 (σ 5)

The distribution model was applied to suspended sediment samples at five different stations along the river to predict source contribution with decreasing river gradient. Suspended sediments collected in Hamilton (km 118) were modeled as 80% (±2%) being sourced from

subsurface sediments. The subsurface contribution decreases downstream with decreasing river gradient, and in Williamston its contribution was modeled to be 63% (±1%). The suspended sediment at the next downstream sampling station in Jamesville, located just 4 km above the transition zone with the bayhead delta, was modeled as being composed of 53% (±1%) subsurface sediment. Within the bayhead delta at the sampling station in Plymouth, we see a dramatic shift in the source of suspended sediment, with a modeled subsurface input of only 33% (±1%) and a substantial increase in the contribution of surface sediments to 67% (±1%).

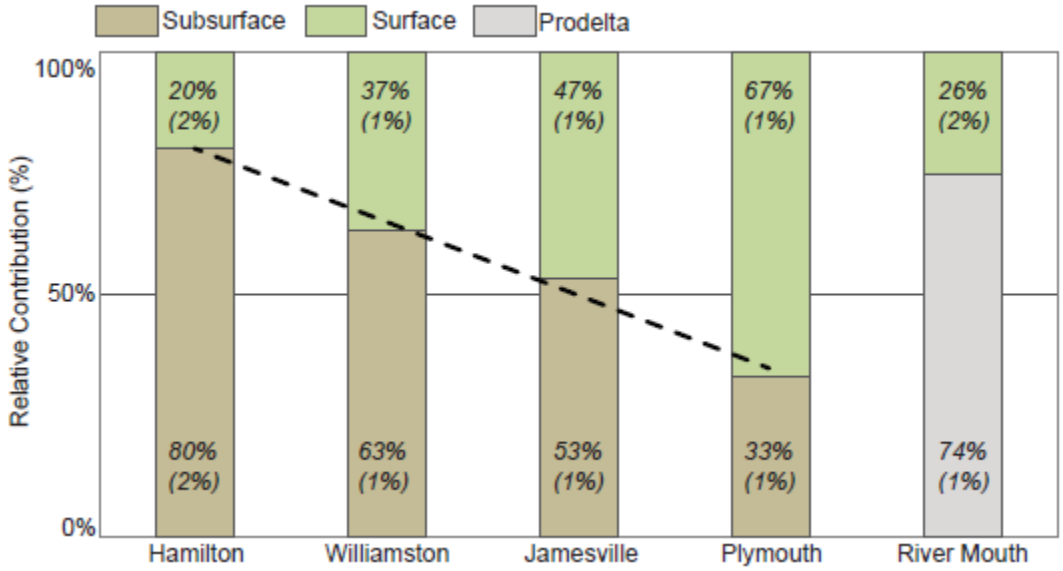

Figure 37. Results of the multivariate mixing model showing relative contributions of surface and subsurface sediments to the suspended load (uncertainty in parenthesis) and decreasing trend in subsurface sediment contribution.

Suspended sediment at the river mouth, modeled with surface and subsurface sources, resulted in an increase in the contribution of subsurface sediments (60%). Suspended sediment at previous stations showed a strong decreasing trend (R^2=0.99) in subsurface sediment contribution with increasing distance downstream (Figure 37), thus the increased input of subsurface source at the last station was unexpected. Because previous studies showed erosion of the delta front and prodelta, the suspended sediment at the river mouth was modeled with surface

and delta front/prodelta sources to determine if that distal deltaic sediment was part of the river's load. The river mouth station exhibited a much lower contribution from surface sediments and a dominant, 74% (± 1%), contribution of particles from the eroding delta front/prodelta (Figure 37).

3.6 Discussion

Based on elevation, flow, grain size and geomorphic features, the Lower Roanoke River can clearly be divided into two subsections: the Lower Roanoke River (LRR) and the bayhead delta (BHD) (Figure 38). The LRR has an elevation above 0 MASL and a river gradient higher than 0 degrees. The LRR has prominent banks and levees and the river in this subsection has characteristic bed-forms consisting of coarse sediments (>63µm) (Figure 35). The LRR has a unidirectional flow, and instead of tributaries, the river has a network of rills, gullies and floodplain channels that connect the river with the watershed. Flow in this part of the river is controlled by dam releases. The BHD subdivision is defined by a 0 or lower elevation (MASL). In the BHD, the river is characterized by no slope, lack of banks and levees, and the presence of distributary channels (Figures 30 and 33). The flow in the BHD becomes bidirectional due to wind-tide forcing (Jalowska et al., 2015; Luettich et al., 2002) (Figures 34 and 38). Channel-bed sediments are composed of fine-grained material and there are no pronounced bedforms (Figure 35). The transition between the LRR and the BHD subdivisions correspond with the change in sediment sourcing and distribution.

This study demonstrated a downstream trend of decreasing contribution of subsurface sediments and increasing surface sediment input to the suspended load of the river. Material from LRR channel is not transported to the BHD because controlled dam releases do not provide enough energy to the system to move the coarser sediments (Figure 35).

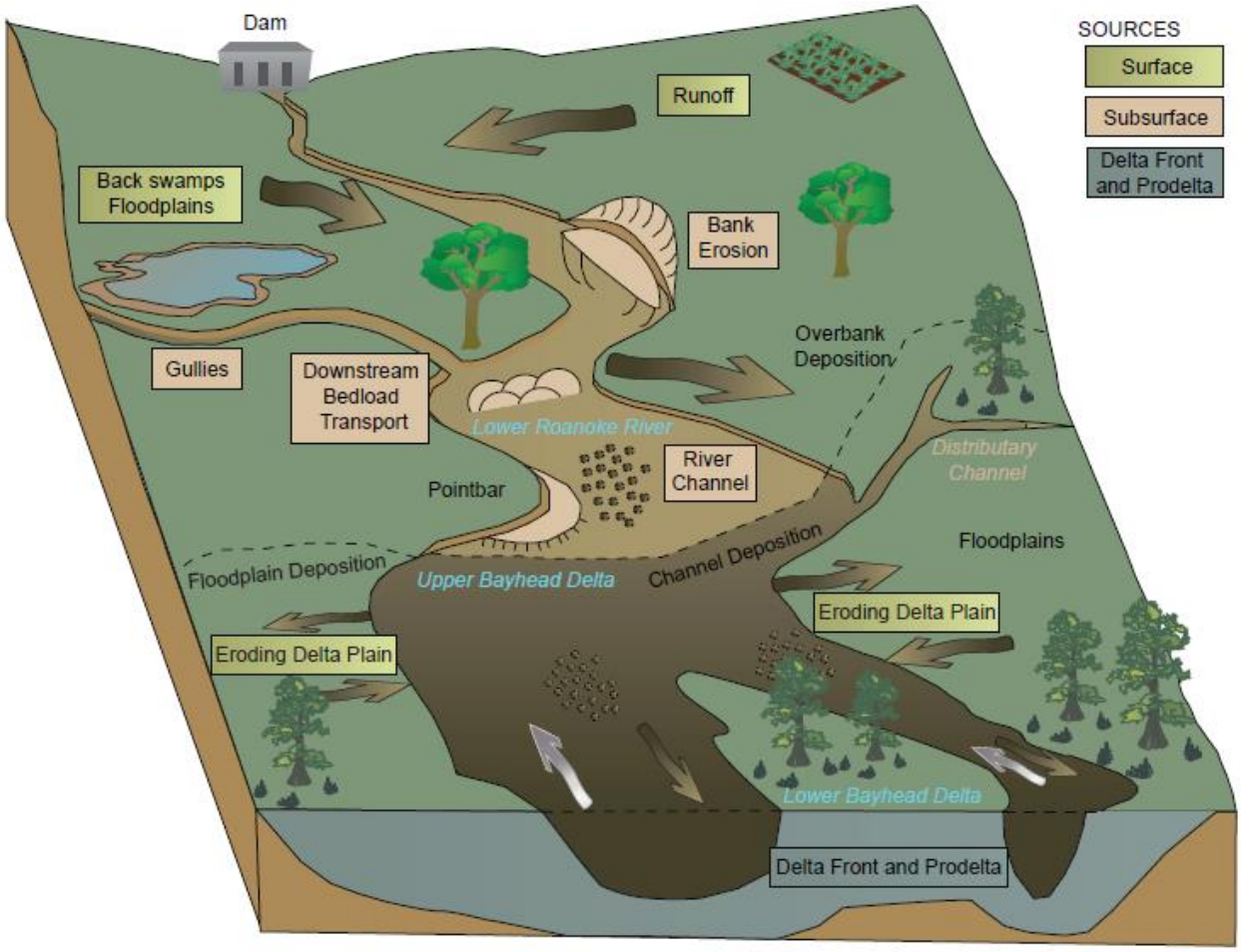

Figure 38. Conceptual diagram of the sediment sources and fate in the Lower Roanoke River and bayhead delta (Symbols for diagrams courtesy of the Integration and Application Network ian.umces.edu/symbols and Dunne et al., 1998).

The relative contribution of fine sediments from subsurface sources to the BHD decreases to 33%. This change is governed by increase in the surface sediment contribution. The rise in surface sediment contribution is, in turn associated with increased hydrologic connectivity between river channel and floodplains downstream along the LRR, while within the BHD, the increased connectivity is facilitated by the lack of gradient, low or non-existent banks, and flooding due to changing water-level in Albemarle Sound.

Previous studies reported the highest bank erosion between 95–137 river km below the dam (Hupp et al., 2009b). The bank erosion processes are strongly featured in the modeling

results from the Hamilton station located at river km 118, where 80% (± 2%), of the suspended sediment during the study period was contributed from subsurface sediments (Figure 37, Table 9). An additional factor controlling relative sediment contributions at the Hamilton site is the high banks (mean bank height 4.1 m (Hupp et al., 2009b)), that effectively limit hydrologic connectivity between floodplains and the channel. With decreasing bank height (mean bank height 1.7 m between km 138 and 175 (Hupp et al., 2009b)) and decreasing river gradient (Figure 33), there is a significant ~38% reduction in bank erosion from 63.3 mm/year to 24.2 mm/year (Hupp et al., 2009b). The modeling results, presented here, corroborate the findings of Hupp et al. (2009) by showing a reduction in the contribution of subsurface sediments; however, the decline is not as pronounced. Hupp et al. (2009), showed the difference between Hamilton (km118) and Williamston (km 155) being 25% (± 1%) lower, and between Hamilton (km118) and Jamesville (km182) being 34 % (±1%) lower (Figure 37). The discrepancy in the magnitude of the subsurface-sediment contribution to the suspended load between Hupp et al. (2009) and our study indicates that in addition to bank erosion, other subsurface sources, which have not been monitored, contribute to the suspended-sediment load, such as sediment from channel incision or gully erosion.

The increase in surface sediments downstream is more likely to be associated with forested floodplain erosion and runoff, than agriculture runoff, because the cultivated land in the Lower Roanoke River watershed represents less than 30% of the land cover (Figure 30B). The increase in floodplain connectivity downstream is reflected in the surface contribution at Williamston (km 155) being 17% (±1%) higher than at Hamilton, and at Jamesville (km 182) being 27% (±1%) higher than at Hamilton (Figure 37). Below Jamesville lies the transition between LRR and BHD that coincides with the recorded transition to finer grain sizes in the

riverbed (Figure 35). The contribution of subsurface sediments to the suspended load at Plymouth is low and 67 % (±1%) of the suspended load consists of surface sediments.

Concentrations of TSM decrease downstream, which can be associated with a loss of sediment to deposition or dilution from an increase in water volume due to widening of the river below Jamesville (from 120 m wide in Jamesville to 200 m wide at the transition, Table 7). The decrease in the subsurface contribution to the suspended load in Plymouth (km 202), coincides with increasing floodplain deposition below Jamesville (km 189) reported by Hupp et al. (2015). That study demonstrated that the highest floodplain sedimentation rates were in the backswamps between Williamston (km 155) and Jamesville (km 189), where a rate of 0.56 cm/year was recorded. The furthest downstream location in that study (at km 193), within the upper BHD recorded rates of 0.23 to 0.28 cm/year. That rate is close to the lower range of sedimentation reported for the delta plain by Jalowska et al. (2015), the EPA Remediation Study (2008) and also by Hupp et al. (2009) between km 151 and 193 (0.28 cm/yr, 0.2 cm/yr and 0.25 cm/yr, respectively).

Modeling results show that suspended sediment collected at the mouth of the Lower Roanoke is mostly composed of sediment derived from the eroding delta front/prodelta (74% ± 1%) and connectivity with the floodplain is low. These results suggest that sediments from the river are not all released into proximate waters of the Albemarle Sound, but a fraction is dispersed inland with river back-flow and are being redeposited within the upper portions of the BHD. The role of the lower delta floodplain and the delta front/prodelta shifts from being a sediment sink to a sediment source when delta-evolution shifts from being regressive to transgressive.

The discrepancy between reported floodplain deposition in the upper BHD (Hupp, 2000; Schenk and Hupp, 2008) while simultaneously observed higher contribution of floodplain sediments to the suspended load in the lower of the BHD (this paper), suggests an unaccounted floodplain connectivity and an internal sediment redistribution function of the BHD floodplains (Figure 38). Upper BHD floodplains accrete with sediment mainly sourced from the lower delta plain, and possibly the delta front/prodelta, as opposed to sediment from upstream (Figure 3). Eroded material from the lower parts of the BHD is transported upstream during periods of high water in Albemarle Sound and redeposited in the upper BHD floodplains. This sediment recycling in the BHD tempers transgression by nourishing the upper BHD with eroded delta front/prodelta and delta plain sediment, fortifying the upper bayhead delta against inundation. This BHD sediment recycling process sheds new light on sediment-transport pathways during BHD transgression and the source to sink paradigm in fluvial deltaic systems, which are heavily biased towards upstream sources and downstream sinks.

3.7 Conclusions

The Lower Roanoke River has been extensively dammed causing significant downstream geomorphological changes to the river and floodplains. The study shows a downstream trend of increasing surface-sediment input and decreasing subsurface-sediment input to the suspended load of the river. Consequently, contribution of material, from subsurface sources is significantly reduced and is being replaced by sediments from the eroding prodelta and delta front, and from the delta plain.

Major and minor dammed rivers around the world do not have enough sediment supplied from upstream to nourish and fortify deltas. Without a substantial upstream sediment source, the deltas cannot outpace sea-level rise and they retreat. The results of this study suggests that in the

process of retreat, sediment starved deltas recycle sediment from eroding parts of the lower delta to build the upper delta. Upstream sediment transport during the retreat process, results in the delta and its floodplains becoming a source and sink for sediments at the same time. This largely unaccounted for process would lead to overestimation of sediment and nutrient budgets for deltaic environments and downstream basins. Further study focused on mechanisms and time scales of the floodplain retreat, pathways and dynamics of sediment redistribution in the BHD are needed. Understanding the scale of these processes would have a significant impact on management practices, and would allow restoration and conservation efforts to focus on those upper parts of the delta wetland that are being naturally nourished by eroded sediments from the lower delta.

APPENDIX

Additionally, depending on the core depth, 10-40 cm of each core was analyzed for ^{210}Pb activities alpha spectrometry. This method assumes that ^{210}Po, granddaughter isotope of ^{210}Pb, are in secular equilibrium with each other (de Vleeschouwer et al., 2010; El-Daoushy et al., 1991; Flynn, 1968; Matthews et al., 2007). Every core interval was subsampled, and analyzed for $^{210}Pb_{xs}$ chronology via isotope-dilution alpha spectrometry. ^{210}Po (Curie et al., 1898) is a naturally occurring α-emitter with a half-life of 138.4 days (Be et al., 2008). ^{210}Po is a product of decay within the ^{238}U series as decay product of ^{210}Pb. ^{210}Pb activities were determined via isotope-dilution alpha spectrometry for the ^{210}Pb granddaughter isotope ^{210}Po, that are in secular equilibrium with each other (El-Daoushy et al., 1991; Flynn, 1968; Matthews et al., 2007). Fine fraction of the sediment (grain size <63 μm) was packed into Teflon vessels, 1.5-2.1g each. Each sample was treated with 1.0ml (~20dpm) ^{209}Po tracer diluted in 1M Certified ACS Plus, hydrochloric acid and 15 ml of Certified ACS Plus, 15M nitric acid (Matthews et al., 2007) The tracer activity has been obtained using certified natural reference standard IAEA-300. The vials were securely closed and undergone microwave digestion in a Microwave Accelerated Reaction System (MARS 5) (Sanchez-Cabeza et al., 1998) for 4 hours and 20 minutes in 3 cycles at temperatures up to 90°C. Cooled vessels were placed under a fume hood. Content of the vessels was transferred to appropriately labeled 50 ml centrifuge tubes. Teflon vessels were rinsed with deionized water to recover all content using minimal amount of DI water- to minimize the sample volume in next steps. Samples were centrifuge at 3500 rpm for 8 minutes in a centrifuge. The separated supernate was transferred into appropriately labeled Teflon beakers and placed on the hotplate. Sediment in each vial was treated with 5ml of 15M nitric acid, vortexed and once more centrifuged at 3500 rpm for 8 minutes. The supernate was combined with the rest of the

leached samples in the Teflon beakers on the hot plate. The remaining sediment was discarded. Temperature of the hot plate has been kept between 85-90°C not to exceed 95°C to avoid losses due to volatilisation of the ^{209}Po tracer (Martin and Blanchard, 1969). When the solution in the beakers has warmed up, 1-2ml of 10.3M hydrogen peroxide was titrated to each beaker and let effervesce. Addition of hydrogen peroxide allows to destroy the organic components not destroyed by heating with nitric acid. Nearly dried samples were then dissolved in 15ml deionized water. In the next step samples were titrated with ammonium hydroxide to raise the pH to 7 – 8.5. Change in pH allowed iron precipitation. Precipitated iron was collected via centrifugation 8 minutes at 3500 rpm and then rinsed twice with 30ml of deionized water. Iron precipitate was dissolved with 3.75ml 10M Certified ACS Plus hydrochloric acid and treated with ~50/60 mg of ascorbic acid to eliminate the interference of iron by reducing it to the ferrous state Fe3+ to Fe2+(Blanchard, 1966). Samples were transferred back to Teflon beakers with labeled stainless steel disks and stirrers. The stainless steel discs are coated with foil on one side. Previously stainless steel discs were used in electroplating (Ordoñez-Regil and Iturbe G., 1993). To assure maximum yields samples were allowed spontaneous deposition for 20-24h with stirrers at 200-300 rpm at room temperature. The next day the discs were removed from a solution, rinsed with a deionized water and left to air-dry for 24 hours. Planchettes were transferred to α-particle spectrometry utilizing Passivated Implanted Planar Silicon (PIPS®) detector for counting for 24 hours. Detector efficiencies were calculated using certified reference material and were between 0.21-0.28%. ^{209}Po and ^{210}Po activities was directly determined by measuring their photopeaks at 4.88MeV and 5.30MeV respectively, with allowed tailing. Thereafter the background values were subtracted and the ratio of net counts in both peaks was calculated. To calculate ^{210}Pb activity, the ratio of ^{210}Po and ^{210}Po was adjusted for sample mass

and activity of the tracer and chemical yields were calculated to check the tracer recovery. The recovery of the tracer was between 55-78%, median 65%. Equivalently to gamma procedure supported, in alpha spectrometry procedure levels of ^{210}Pb also have to be subtracted from total ^{210}Pb activities to calculate $^{210}Pb_{xs}$ activity (Appleby and Oldfield, 1992; Demaster et al., 1985; McKee et al., 1983; Nittrouer et al., 1979). Supported levels of ^{210}Pb (^{226}Ra activity) was determined by measuring the gamma activity of ^{226}Ra granddaughter- ^{214}Bi (609 KeV), and averaged over top 5 samples per core.

REFERENCES

Alexander, R.B., Slack, J.R., Ludtke, A.S., Fitzgerald, K.K., Schertz, T.L., 1998. Data from selected U.S. Geological Survey National Stream Water Quality Monitoring Networks. Water Resour. Res. 34, 2401. doi:10.1029/98WR01530

Aller, R.C., Blair, N.E., Brunskill, G.J., 2008. Early diagenetic cycling, incineration, and burial of sedimentary organic carbon in the central Gulf of Papua (Papua New Guinea). J. Geophys. Res. 113, 1–22. doi:10.1029/2006JF000689

Allison, M.A., Kuehl, S.A., Martin, T.C., Hassan, A., 1998. Importance of flood-plain sedimentation for river sediment budgets and terrigenous input to the oceans: Insights from the Brahmaputra-Jamuna River. Geology 26, 175–178. doi:10.1130/0091-7613(1998) 026<0175:IOFPSF>2.3.CO;2

Appleby, P.G., Oldfield, F., 1992. Application of Pb-210 to sedimentation studies, in: Ivanovich, M., Harmon, R.S. (Eds.), Uranium Series Disequilibrium: Applications to Earth, Marine and Environmental Sciences. Oxford Sciences Publications, New York, pp. 731–778.

Appleby, P.G., Oldfield, F., 1978. The Calculation of Lead-210 Dates Assuming a Constant Rate of Supply of Unsupported 210Pb to the Sediments. Catena 5, 1–8.

Baskaran, M., 2011. Po-210 and Pb-210 as atmospheric tracers and global atmospheric Pb-210 fallout : a Review. J. Environ. Radioact. 102, 500–513. doi:10.1016/j.jenvrad.2010.10.007

Battin, T.J., Kaplan, L.A., Findlay, S., Hopkinson, C.S., Marti, E., Packman, A.I., Newbold, J.D., Sabater, F., 2009. Biophysical controls on organic carbon fluxes in fluvial networks. Nat. Geosci. 2, 595–595. doi:10.1038/ngeo602

Be, M., Chiste, V., Dulieu, C., Browne, E., Chechev, V., Kuzmenko, N., Kondev, F., Luca, A., Galan, M., Pearce, A., Huang, X., 2008. Monographie BIPM-5 Table of Radionuclides vol.4. Sèvres BIPM 2008 Bureau International des Poids et Mesures, Pavillon de Breteuil, F-92310 S`evres, France.

Bé, M., Chisté, V., Dulieu, C., Chechev, V., Kuzmenko, N., Galán, M., 2008. Table of Radionuclides, Bureau International Des Poids Et Mesures.

Bellis, V.J., O'Connor, M.P., Riggs, S.R., 1975. Estuarine shoreline erosion in the Albemarle-Pamlico region of North Carolina. Sea Grant Program, North Carolina State University, Raleigh.

Bellucci, L.G., Frignani, M., Cochran, J.K., Albertazzi, S., Zaggia, L., Cecconi, G., Hopkins, H., 2007. 210Pb and 137Cs as chronometers for salt marsh accretion in the Venice Lagoon - links to flooding frequency and climate change. J. Environ. Radioact. 97, 85–102. doi:10.1016/j.jenvrad.2007.03.005

Benninger, L.K., Wells, J.T., 1993. Sources of sediment to the Neuse River estuary, North Carolina. Mar. Chem. 43, 137–156. doi:10.1016/0304-4203(93)90221-9

Bhandari, N., Lal, D., others, 1970. Vertical structure of the troposphere as revealed by radioactive tracer studies. J. Geophys. Res. 75, 2974–2980. doi:10.1029/JC075i015p02974

Bianchi, T.S., Mead, A.A., 2009. Large-river delta-front estuaries as natural "'recorders'" of global environmental change. PNAS 106, 8085–8092.

Blanchard, R., 1966. Rapid determination of lead-210 and polonium-210 in environmental samples by deposition on nickel. Anal. Chem. 38, 189–192.

Blum, M.D., Roberts, H.H., 2009. Drowning of the Mississippi Delta due to insufficient sediment supply and global sea-level rise. Nat. Geosci. 2, 488–491. doi:10.1038/ngeo553

Braje, T.J., Erlandson, J.M., 2014. Looking forward, looking back: Humans, anthropogenic change, and the Anthropocene. Anthropocene 4, 116–121. doi:10.1016/j.ancene.2014.05.002

Brandt, S.A., 2000. Classification of geomorphological effects downstream of dams. Catena 40, 375–401. doi:10.1016/S0341-8162(00)00093-X

Brazier, R.H.B., MacRae, J., Tanner, H.S., Dawson, F.B., Knight, J., 1833. A new map of the state of North Carolina. John MacRae, Fayetteville, N.C.

Brill, A.L., 1996. The Suffolk Scarp, a Pleistocene barrier island in Beaufort and Pamlico Counties, NC. Duke University.

Brown, P.M., Miller, J.A., Swain, F.M., 1972. Structural and Stratigraphic Framework, and Spatial Distribution of Permeability of the Atlantic Coastal Plain, North Carolina to New York. U.S. Geol. Surv. Prof. Pap. 796, 79.

Cahoon, D.R., Turner, E.R., 1989. Accretion and Canal Impacts in a Rapidly Subsiding Wetland II. Feldspar Marker Horizon Technique. Estuaries 12, 260–268.

Caitcheon, G.G., Olley, J.M., Pantus, F., Hancock, G., Leslie, C., 2012. The dominant erosion processes supplying fine sediment to three major rivers in tropical Australia, the Daly (NT), Mitchell (Qld) and Flinders (Qld) Rivers. Geomorphology 151-152, 188–195. doi:10.1016/j.geomorph.2012.02.001

Canuel, E., Martens, C., Benninger, L., 1990. Seasonal variations in 7Be activity in the sediments of Cape Lookout Bight, North Carolina. Geochim. Cosmochim. Acta 54, 237–245. doi:10.1016/0016-7037(90)90211-3

Chmura, G.L., 2013. What do we need to assess the sustainability of the tidal salt marsh carbon sink? Ocean Coast. Manag. 83, 25–31. doi:10.1016/j.ocecoaman.2011.09.006

Christiansen, T., Wiberg, P.L., Milligan, T.G., 2000. Flow and Sediment Transport on a Tidal Salt Marsh Surface. Estuar. Coast. Shelf Sci. 50, 315–331. doi:10.1006/ecss.2000.0548

Clune, J.W., Gellis, A.C., McKee, L.G., 2010. Agricultural soil erosion rates for the Linganore creek watershed in the piedmont physiographic province of the Chesapeake Bay watershed, in: 2nd Joint Federal Interagency Conference, Las Vegas, NV, June 27 - July 1, 2010. Las

Vegas, pp. 1–8.

Collins, A.L., Walling, D.E., Leeks, G.J.L., 1998. Use of composite fingerprints to determine the provenance of the contemporary suspended sediment load transported by rivers. Earth Surf. Process. 23, 31–52. doi:10.1002/(SICI)1096-9837(199801)23:1<31::AID-ESP816>3.0.CO;2-Z

Collins, A.L., Walling, D.E., Leeks, G.J.L., 1996. Composite fingerprinting of the spatial source of fluvial suspended sediment : a case study of the Exe and Severn river basins, United Kingdom. Géomorphologie Reli. Process. Environ. 2, 41–53. doi:10.3406/morfo.1996.877

Collins, A.L., Walling, D.E., Webb, L., King, P., 2010. Apportioning catchment scale sediment sources using a modified composite fingerprinting technique incorporating property weightings and prior information. Geoderma 155, 249–261. doi:10.1016/j.geoderma.2009.12.008

Collins, A.L., Zhang, Y., McChesney, D., Walling, D.E., Haley, S.M., Smith, P., 2012. Sediment source tracing in a lowland agricultural catchment in southern England using a modified procedure combining statistical analysis and numerical modelling. Sci. Total Environ. 414, 301–317. doi:10.1016/j.scitotenv.2011.10.062

Corbett, D., Vance, D., Letrick, E., Mallinson, D., Culver, S., 2007. Decadal-scale sediment dynamics and environmental change in the Albemarle Estuarine System, North Carolina. Estuar. Coast. Shelf Sci. 71, 717–729. doi:doi:10.1016/j.ecss.2006.09.024

Costanza, R., de Groot, R., Sutton, P., van der Ploeg, S., Anderson, S.J., Kubiszewski, I., Farber, S., Turner, R.K., 2014. Changes in the global value of ecosystem services. Glob. Environ. Chang. Glob. Environ. Chang. 26, 152–158.

Crozaz, G., Picciotto, E., 1964. Antarctic Snow Chronology with Pb TM 69.

Culver, S.J., Farrell, K.M., Mallinson, D.J., Horton, B.P., Willard, D.A., Thieler, E.R., Riggs, S.R., Snyder, S.W., Wehmiller, J.F., Bernhardt, C.E., Hillier, C., 2008. Micropaleontologic record of late Pliocene and Quaternary paleoenvironments in the northern Albemarle Embayment, North Carolina, U.S.A. Palaeogeogr. Palaeoclimatol. Palaeoecol. 264, 54–77.

Curie, P., Curie, M., Bémont, G., 1898. Sur une substance nouvelle radio-active, contenue dans la pechblende. Comptes Rendus 127, 175–178.

Cutshall, N.H., Larsen, I.L., Olsen, C.R., 1983. Direct analysis of 210Pb in sediment samples: Self-absorption corrections. Nucl. Instruments Methods Phys. Res. 206, 309–312. doi:10.1016/0167-5087(83)91273-5

Dagg, M., 2004. Transformation of dissolved and particulate materials on continental shelves influenced by large rivers: plume processes. Cont. Shelf Res. 24, 833–858. doi:10.1016/j.csr.2004.02.003

Dalrymple, R.W., Zaitlin, B.A., Boyd, R., 1992. Estuarine facies models: conceptual basis and stratigraphic implications. J. Sediment. Petrol. 1992, 1130–1146.

Davis, C.M., Asce, M., Fox, J.F., 2009. Sediment Fingerprinting: Review of the Method and Future Improvements for Allocating Nonpoint Source Pollution. J. Environ. Eng. 135, 490–505. doi:10.1061/(ASCE)0733-9372(2009)135:7(490), 490-504.

Day, J.W., Pont, D., Hensel, P.F., Ibanez, C., 1995. Impacts of Sea-Level Rise on Deltas in the The Gulf of Mexico and the Mediterranean: Importance of Pulsing Events to Sustainability. Estuaries 18, 636–647.

de Vleeschouwer, F., Sikorski, J., Fagel, N., 2010. Development of Lead-210 Measurement in Peat Using Polonium Extraction. A Procedural Comparison. Geochronometria 36, 1–8.

DeGravelles, W.W., 2010. Two-year growth and mortality of sub-canopy baldcypress (Taxodium distichum [L.] Rich.) released in artificial canopy gaps in a North Carolina swamp. Clemson University.

DeLaune, R.D., Baumann, R.H., Gosselink, J.G., 1983. Relationships among Vertical Accretion, Coastal Submergence, and Erosion in a Louisiana Gulf Coast Marsh. J. Sediment. Petrol. 53, 147–157.

Demaster, D.J., Mckee, B.A., Nittrouer, C.A., Jiangchu, Q., Guodong, C., 1985. Rates of sediment accumulation and particle reworking based on radiochemical measurements from continental shelf deposits in the East China Sea. Cont. Shelf Res. 4, 143–158. doi:10.1016/0278-4343(85)90026-3

Devereux, O.H., Prestegaard, K.L., Needelman, B.A., Gellis, A.C., 2010. Suspended-sediment sources in an urban watershed, Northeast Branch Anacostia River, Maryland. Hydrol. Process. 24, 1391–1403. doi:10.1002/hyp.7604

Dibb, J.E., 1989. Atmospheric Deposition of Beryllium 7 in the Chesapeake Bay Region. J. Geophys. Res. 94, 2261–2265. doi:10.1029/JD094iD02p02261

Dunbar, G.S., 1958. Historical geography of the North Carolina Outer Banks. Louisiana State University Press, Baton Rouge.

Dunne, T., Meade, R.H., Richey, J.E., Forsberg, B.R., 1998. Exchanges of sediment between the flood plain and channel of the Amazon River in Brazil. GSA Bull. 110, 450–467. doi:10.1130/0016-7606(1998)110<0450:EOSBTF>2.3.CO;2

Earth Satellite Corporation (EarthSat), 1997. Land Cover - 1996, Raster.

El-Daoushy, F., Ollson, K., Garcia-Tenorio, R., 1991. Accuracies in Po-210 determination for lead-210 dating. Hydrobiologia 214, 43–52.

EPA, 2010. First Five-Year Review Report for Weyerhaeuser Company Superfund Site. Plymouth, Martin County, NC.

EPA, USFWS, USEPA, USGS, NCDENR, 2008. Remedial Project on the Domtar Papermill Site, Martin County, NC.

Erlich, R.N., 1980. Early Holocene to recent development and sedimentation of the Roanoke

River area, North Carolina. University of North Carolina Chapel Hill.

ESRI (Environmental Systems Resource Institute), 2015. ArcMap 10.1 ESRI.

Fielding, L., Kneass, W., 1822. North Carolina. B. T. Welch & Co., Baltimore.

Fisher, J.J., 1962. Geomorphic expression of former inlets along the outer banks of North Carolina. University of North Carolina Chapel Hill.

Flynn, W.W., 1968. The Determination of Low Levels of Polonium-210 in Environmental Materials. Anal. Chim. Acta 43, 221–227.

Fryirs, K.A., Brierley, G.J., Preston, N.J., Kasai, M., 2007. Buffers, barriers and blankets: The (dis)connectivity of catchment-scale sediment cascades. Catena 70, 49–67. doi:10.1016/j.catena.2006.07.007

Gellis, A.C., Hupp, C.R., Pavich, M.J., Landwehr, J.M., Banks, W.S.L., Hubbard, B.E., Langland, M.J., Ritchie, J.C., Reuter, J.M., 2009. Sources, Transport, and Storage of Sediment at Selected Sites in the Chesapeake Bay Watershed, U.S. Geological Survey Scientific Investigations Report 2008–5186. U.S. Geological Survey.

Giese, G., Wilder, H.B., Parker, G.G., North Carolina Department of Natural Resources and Community Development., 1979. Hydrology of major estuaries and sounds of North Carolina. U.S. Geological Survey, Water Resources Division, Raleigh, N.C.

Giffin, D., Corbett, D.R., 2003. Evaluation of sediment dynamics in coastal systems via short-lived radioisotopes. J. Mar. Syst. 42, 83–96. doi:10.1016/S0924-7963(03)00068-X

Giosan, L., 2014. Protect the world's deltas. Nature 516, 5–7.

Giosan, L., Goodbred, S.L.J., 2007. Fluvial environments; deltaic environments, in: Elias, S.A. (Ed.), Encyclopedia of Quaternary Science; Volume 1. Elsevier, Amsterdam, Netherlands; Boston [Mass.], pp. 693–703.

Goldberg, E.D., 1963. Geochronology with 210Pb, in: Radioactive Dating. Proceedings of a Symposium, International Atomic Energy Agency, Vienna. pp. 21–131.

Golosov, V., Walling, D.E., 2015. Using fallout radionuclides to investigate recent overbank sedimentation rates on river floodplains: an overview. Proc. Int. Assoc. Hydrol. Sci. 367, 228–234. doi:10.5194/piahs-367-228-2015

Gomez, B., Eden, D.N., Hicks, D.M., Trustrum, N.A., Peacock, D.H., Wilmshurst, J., 1999. Contribution of floodplain sequestration to the sediment budget of the Waipaoa River, New Zealand. Floodplains Interdiscip. Approaches 163, 69–88\r330. doi:10.1144/GSL.SP.1999.163.01.06

Gomez, B., Eden, D.N., Peacock, D.H., Pinkkey, E.J., 1998. Floodplain construction by recent, rapid vertical accretion: Waipaoa River, New Zealand. Earth Surf. Process. Landforms 23, 405–413. doi:10.1002/(SICI)1096-9837(199805)23:5<405::AID-ESP854>3.0.CO;2-X

Gunnell, J.R., Rodriguez, A.B., Mckee, B.A., 2013. How a marsh is built from the bottom up.

Geology 41, 859–862. doi:10.1130/G34582.1

Haddadchi, A., Olley, J., Laceby, P., 2014. Accuracy of mixing models in predicting sediment source contributions. Sci. Total Environ. 497-498, 139–152. doi:10.1016/j.scitotenv.2014.07.105

Haddadchi, A., Ryder, D.S., Evrard, O., Olley, J., 2013. Sediment fingerprinting in fluvial systems: Review of tracers, sediment sources and mixing models. Int. J. Sediment Res. 28, 560–578. doi:10.1016/S1001-6279(14)60013-5

Hanson, P.J., Evans, D.W., Colby, D.R., 1993. Assessment of elemental contamination in estuarine and coastal environments based on geochemical and statistical modeling of sediments. Mar. Environ. Res. 36, 237.

Harvey, A.M., 2002. Effective timescales of coupling within fluvial systems. Geomorphology 44, 175 – 201. doi:10.1016/S0169-555X(01)00174-X

Hong, G., Hamilton, T.F., Baskaran, M., Kenna, T.C., 2012. Applications of Anthropogenic Radionuclides as Tracers to Investigate Marine Environmental Processes, in: Baskaran, M. (Ed.), Handbook of Environmental Isotope Geochemistry. Springer Berlin Heidelberg, pp. 367–394. doi:10.1007/978-3-642-10637-8

Horton, B.P., Peltier, W.R., Culver, S.J., Drummond, R., Engelhart, S.E., Kemp, A.C., Mallinson, D., Thieler, E.R., Riggs, S.R., Ames, D.V., Thomson, K.H., 2009. Holocene sea-level changes along the North Carolina Coastline and their implications for glacial isostatic adjustment models. Quat. Sci. Rev. 28, 1725–1736.

Hupp, C.R., 2000. Hydrology , geomorphology and vegetation of Coastal Plain rivers in the south-eastern USA. Hydrol. Process. 14, 2991–3010.

Hupp, C.R., Pierce, A.R., Noe, G.B., 2009a. Floodplain Geomorphic Processes and Environmental Impacts of Human Alteration Along Coastal Plain Rivers, USA. Wetlands 29, 413–429. doi:10.1672/08-169.1

Hupp, C.R., Pierce, A.R., Townsend, P.A., 2008. Floodplain Geomorphic Processes, Sedimentation, and Ecological Impacts of Hydrologic Alteration along Coastal Plain Rivers. Integr. Sci. Into Restor. Manag. Floodplain Ecosyst. Southeast.

Hupp, C.R., Schenk, E.R., Kroes, D.E., Willard, D.A., Townsend, P.A., Peet, R.K., 2015. Patterns of floodplain sediment deposition along the regulated lower Roanoke River, North Carolina: Annual, decadal, centennial scales. Geomorphology 228, 666–680. doi:10.1016/j.geomorph.2014.10.023

Hupp, C.R., Schenk, E.R., Richter, J.M., Peet, R.K., Townsend, P.A., 2009b. Bank erosion along the dam-regulated lower Roanoke River, North Carolina. Geol. Soc. Am. 451, 97–108. doi:10.1130/2009.2451(06).

IPCC, 2014. Climate Change 2013: The Physical Science Basis. Contribution of Working Group I to the Fifth Assessment Report of the Intergovernmental Panel on Climate Change. Cambridge University Press, Cambridge, United Kingdom and New York, NY, USA.

doi:doi:10.1017/CBO978110741532

Jacobson, R.B., Coleman, D.J., 1986. Stratigraphy and Recent evolution of Maryland Piedmont flood plains. Am. J. Sci. 286, 617–637.

Jaffe, B.E., Smith, R.E., Foxgrover, A.C., 2007. Anthropogenic influence on sedimentation and intertidal mudflat change in San Pablo Bay, California: 1856-1983. Estuar. Coast. Shelf Sci. 73, 175–187.

Jalowska, A., McKee, B., Rodriguez, A., 2012. Use of Naturally Occurring Radionuclides in Assessment of Longitudinal and Lateral Connectivity of The River Channel with Frequently Inundated Floodplains. Geol. Soc. Am. Abstr. with Programs, 44, 182.

Jalowska, A.M., McKee, B.A., Laceby, J.P., Rodriguez, A.B., n.d. Tracing Suspended River Sediment Indicates that Recycling of the Deltaic Sediments is an Important Process During Transgression. Submited.

Jalowska, A.M., Rodriguez, A.B., McKee, B.A., 2015. Responses of the Roanoke Bayhead Delta to variations in sea level rise and sediment supply during the Holocene and Anthropocene. Anthropocene 9, 41–55. doi:10.1016/j.ancene.2015.05.002

James, L.A., 2013. Legacy sediment: Definitions and processes of episodically produced anthropogenic sediment. Anthropocene 2, 16–26. doi:doi:10.1016/j.ancene.2013.04.001

Karwan, D.L., Siegert, C.M., Levia, D.F., Pizzuto, J.E., Aufdenkampe, A.K., 2014. Beryllium-7 (7Be) wet deposition variation with storm synoptic classification and canopy state in the mid-Atlantic USA. Geochim. Cosmochimca Acta In review. doi:10.1002/hyp.10571

Kaste, J.M., Norton, S. a., Hess, C.T., 2003. Environmental Chemistry of Beryllium-7. Rev. Mineral. Geochemistry 50, 271–289. doi:10.2138/rmg.2002.50.6

Kemp, A.C., Horton, B.P., Donnelly, J.P., Mann, M.E., Vermeer, M., Rahmstorf, S., 2011. Climate related sea-level variations over the past two millennia. Proc. Natl. Acad. Sci. U. S. A. 108, 11017–22. doi:10.1073/pnas.1015619108

Kim, G., Hussain, N., Scudlark, J.R., Church, T.M., 2000. Factors Influencing the Atmospheric Depositional Fluxes of Stable Pb , 210 Pb , and 7 Be into Chesapeake Bay. J. Atmos. Chem. 36, 65–79.

Kondolf, G.M., 1997. Hungry water: Effects of dams and gravel mining on river channels. Environ. Manage. 21, 533–551. doi:10.1007/s002679900048

Kondolf, G.M., Rubin, Z.K., Minear, J.T., 2014. Dams on theMekong: Cumulative sediment starvation. Water Resour. Res. 50, 5158–5169. doi:10.1002/2012WR013085

Kopp, R.E., Kemp, A.C., Bittermann, K., Horton, B.P., Donnelly, J.P., Gehrels, W.R., Hay, C.C., Mitrovica, J.X., Morrow, E.D., Rahmstorf, S., 2016. Temperature-driven global sea-level variability in the Common Era 1–8. doi:10.1073/pnas.1517056113

Kremer, H.H., Tissier, M.D.A. Le, Burbridge, P.R., Talaue-McManus, L., Rabalais, N.N.,

Parslow, J., Crossland, C.J., Young, B., 2005. LOICZ Land – Ocean Interactions in the Coastal Zone Science Plan and Implementation Strategy.

Krishnaswamy, S., Lal, D., Martin, J., Meybeck, M., 1971. Geochronology of lake sediments. Earth Planet. Sci. Lett. 11, 407–414.

Laceby, J.P., McMahon, J., Evrard, O., Olley, J.M., 2015. Comparison of geological and statistical approaches to element selection for sediment fingerprinting. J. Soils Sediments 8212, 2117–2131. doi:10.1007/s11368-015-1111-9

Laceby, J.P., Olley, J., 2015. A new modelling approach to tracing sediment sources that incorporates distributions and their elemental correlations. Hydrolo 29, 1669–1685. doi:10.1002/hyp.10287

Lagomasino, D., Corbett, D.R., Walsh, J.P., 2013. Influence of Wind-Driven Inundation and Coastal Geomorphology on Sedimentation in Two Microtidal Marshes, Pamlico River Estuary, NC. Estuaries and Coasts 36, 1165–1180. doi:10.1007/s12237-013-9625-0

Lal, D., Rama, Zutshi, P.K., 1960. Radioisotopes P32,Be7 and S35 in the Atmosphere. J. Geophys. Res. 65, 669–674.

Lankford, R.R., Rogers, J.J.W., 1969. Holocene Geology of the Galveston Bay Area. Houston Geological Society, Houston.

Lecce, S.A., Pease, P.P., Gares, P.A., Wang, J., 2006. Seasonal controls on sediment delivery in a small coastal plain watershed, North Carolina, USA. Geomorphology 73, 246–260. doi:10.1016/j.geomorph.2005.05.017

Lewis, S., Carey, M., 1818. North Carolina From the Latest Surveys. Mathew Carey, Philadelphia.

Ludwig, W., Probst, J., Budgets, G., 1998. River sediment discharge to the oceans; present-day controls and global budgets. Am. J. Sci. 298, 265–295. doi:10.2475/ajs.298.4.265

Luettich, R.A., Carr, S.D., Reynolds-Fleming, J. V., Fulcher, C.W., McNinch, J.E., 2002. Semi-diurnal seiching in a shallow, micro-tidal lagoonal estuary. Cont. Shelf Res. 22, 1669–1681. doi:doi:10.1016/S0278-4343(02)00031-6

Magilligan, F.J., Nislow, K.H., 2005. Changes in hydrologic regime by dams. Geomorphology 71, 61–78. doi:10.1016/j.geomorph.2004.08.017

Mallinson, D., Burdette, K., Mahan, S., Brook, G., 2008. Optically stimulated luminescence age controls on late Pleistocene and Holocene coastal lithosomes, North Carolina, USA. Quat. Res. 69, 97–109.

Mallinson, D., Riggs, S., Thieler, E.R., Culver, S., Farrell, K., Foster, D.S., Corbett, D.R., Horton, B., Wehmiller, J.F., 2005. Late Neogene and Quaternary evolution of the northern Albemarle Embayment (mid-Atlantic continental margin, USA). Mar. Geol. 217, 97–117.

Martin, A., Blanchard, R.L., 1969. The thermal volatilisation of Caesium-137, Polonium-210 and

Lead-210 from in vivo labelled samples. Analyst 94, 441–446. doi:10.1039/an9699400441

Mattheus, C.R., Rodriguez, A.B., 2011. Controls on late Quaternary incised-valley dimension along passive margins evaluated using empirical data. Sedimentology 58, 1113–1137.

Mattheus, C.R., Rodriguez, A.B., McKee, B.A., 2009. Direct connectivity between upstream and downstream promotes rapid response of lower coastal-plain rivers to land-use change. Geophys. Res. Lett. 36, 1–6. doi:10.1029/2009GL039995

Matthews, K.M., Kim, C.K., Martin, P., 2007. Determination of 210Po in environmental materials: A review of analytical methodology. Appl. Radiat. Isot. 65, 267–279. doi:10.1016/j.apradiso.2006.09.005

McEwen, M.C., 1969. Sedimentary Facies of the Modern Trinity Delta, in: Lankford, R.R., Rogers, J.J.W. (Eds.), Holocene Geology of the Galveston Bay Area. Houston Geological Society, Houston, pp. 53–77.

Mckee, B.A., 2003. RiOMar The Transport, Transformation and Fate of Carbon in River-dominated Ocean Margins, in: Report of the RiOMar Workshop, 1-3 November 2001. Tulane University, New Orleans, LA.

McKee, B.A., 1998. The Role of RiOMar Systems in Global Change, in: RiOMar. pp. 5–10.

McKee, B.A., Aller, R.C., Allison, M.A., Bianchi, T.S., Kineke, G.C., 2004. Transport and transformation of dissolved and particulate materials on continental margins influenced by major rivers: benthic boundary layer and seabed processes. Cont. Shelf Res. 24, 899–926. doi:10.1016/j.csr.2004.02.009

McKee, B.A., Nittrouer, C.A., DeMaster, D.J., 1983. Concepts of sediment deposition and accumulation applied to the continental shelf near the mouth of the Yangtze River. Geology 2, 631–633.

Meade, R.H., 1996. River-sediment Inputs to Major Deltas, in: Milliman, J.D., Haq, B.U. (Eds.), Sea Level Rise and Coastal Subsidence. Kulwer Academic Publishers, Netherlands, pp. 63–85.

Meade, R.H., 1982. Sources, sinks, and storage of river sediment in the Atlantic drainage of the United States. J. Geol. 90, 235–252. doi:10.1086/628677

Meade, R.H., Dunne, T., Richey, J.E., De Santos, U.M., Salati, E., 1985. Storage and remobilization of suspended sediment in the lower Amazon river of Brazil. Science 228, 488–90. doi:10.1126/science.228.4698.488

Meade, R.H., Yuzyk, T.R., Day, T.J., 1990. Movement and storage of sediment in rivers of the United States and Canada, in: Wolman, G.M., Riggs, S.R. (Eds.), The Geology of North Amerca Vol. O-1 Surface Water Hydrology. GSA, Boulder, CO, pp. 255–280.

Molina, J.R., 2002. Estuarine Exchange Model of the Pamlico and Albemarle Sounds. North Carolina State University.

Motha, J., Wallbrink, P., 2002. Tracer properties of eroded sediment and source material. Hydrol. Process. 16, 1983–2000. doi:10.1002/hyp.397

Mouzon, H., 1775. An Accurate Map of North and South Carolina With Their Indian Frontiers, Shewing in a distinct manner all the Mountains, Rivers, Swamps, Marshes, Bays, Creeks, Harbours, Sandbanks and Soundings on the Coasts, with The Roads and Indian Paths;..., The American atlas. 1775. John Bennett and Robert Sayer, London.

Mukundan, R., Radcliffe, D.E., Ritchie, J.C., Risse, L.M., McKinley, R.A., 2010. Sediment fingerprinting to determine the source of suspended sediment in a southern Piedmont stream. J. Environ. Qual. 39, 1328–1337. doi:10.2134/jeq2009.0405

Nichols, F.H., Cloern, J.E., Luoma, S.N., Peterson, D.H., 1986. The modification of an estuary. Science (80-.). 231.

Nilsson, C., Reidy, C.A., Dynesius, M., Revenga, C., 2005. Fragmentation and flow regulation of the world's large river systems. Science 308, 405–8. doi:10.1126/science.1107887

Nittrouer, C.A., Sternberg, R.W., Carpenter, R., Bennett, J.T., 1979. The Use of Pb-210 Geochronology as a Sedimentological Tool: Application to the Washington Continental Shelf. Mar. Geol. 31, 297–316.

Nittrouer, J.A., Viparelli, E., 2014. Sand as a stable and sustainable resource for nourishing the Mississippi River delta. Nat. Geosci. 7, 350–354. doi:10.1038/ngeo2142

NOAA SEA Division, 1998. North Carolina Estuaries: Biologically Based Salinity. South Atlantic Fishery Management Council.

Noe, G.B., Hupp, C.R., 2009. Retention of Riverine Sediment and Nutrient Loads by Coastal Plain Floodplains. Ecosystems 12, 728–746. doi:10.1007/s10021-009-9253-5

North Carolina Department of Transportation, 2003. Connect NCDOT [WWW Document]. URL https://connect.ncdot.gov/resources/gis/pages/cont-elev_v2.aspx

O'Connell, M., Baldwin, D.S., Robertson, A.I., Rees, G., 2000. Release and bioavailability of dissolved organic matter from floodplain litter: influence of origin and oxygen levels. Freshw. Biol. 45, 333–342. doi:10.1046/j.1365-2427.2000.00627.x

Oaks, R.Q., DuBar, J.R., 1974. Post-Miocene stratigraphy, central and southern Atlantic coastal plain. Utah State University Press, Logan.

Oldfield, F., Maher, B., Donghue, J., Pierce, J., 1985. Particle-size related, mineral magnetic source sediment linkages in the Rhode River catchment, Maryland, USA 142, 1035–1046. doi:10.1144/gsjgs.142.6.1035

Olley, J., Burton, J., Smolders, K., Pantus, F., Pietsch, T., 2013. The application of fallout radionuclides to determine the dominant erosion process in water supply catchments of subtropical South-east Queensland, Australia. Hydrol. Process. 27, 885–895. doi:10.1002/hyp.9422

Olley, J.M., Murray, A.S., Wallbrink, P.J., 1993. Identifying sediment sources in a partially logged catchment using natural and anthropogenic radioactivity. Water Resour. Res. 29, 1037–1043.

Olsen, C.R., Larsen, I.L., Lowry, P.D., Cutshall, N.H., Todd, J.F., Wong, G.T.F., Casey, W.H., 1985. Atmospheric Fluxes and Marsh-Soil Inventories of 7Be and 210Pb. J. Geogr. Sci. 90, 10487–1095.

Oracle, 2015. Oracle Crystal Ball.

Ordoñez-Regil, E., Iturbe G., J.L., 1993. Isolation and electroplating of 210Po. J. Radioanal. Nucl. Chem. 175, 47–53.

Parham, P.R., Riggs, S.R., Culver, S.J., Mallinson, D.J., Wehmiller, J.F., 2007. Quaternary depositional patterns and sea-level fluctuations, northeastern North Carolina. Quat. Res. 67, 83–99.

Pels, R.J., 1967. Sediments of Albemarle Sound, North Carolina. University of North Carolina atChapel Hill.

Phillips, J., 1992. Delivery of upper-basin sediment to the lower neuse river, North Carolina, USA. Earth Surf. Process. Landforms 17, 699–709. doi:10.1002/esp.3290170706

Phillips, J.D., Slattery, M.C., 2007. Downstream trends in discharge, slope, and stream power in a lower coastal plain river. J. Hydrol. 334, 290–303. doi:10.1016/j.jhydrol.2006.10.018

Price, J., Strother, J., 1808. To David Stone and Peter Brown Esqrs. This First Actual Survey of the State of North Carolina Taken by the Subscribers is respectfully dedicated By their humble Servants Jona. Price. John Strother. Charles P. Harrison, Philadelphia.

Pringle, C.M., Freeman, M.C., Freeman, B.J., 2000. Regional Effects of Hydrologic Alterations on Riverine Macrobiota in the New World: Tropical-Temperate Comparisons. Bioscience 50, 807–823.

Pruitt, R.J., Culver, S.J., Buzas, M.A., Corbett, D.R., Horton, B.P., Mallinson, D.J., 2010. Modern Foraminiferal Distribution and Recent Environmental Change in Core Sound, North Carolina, Usa. J. Foraminifer. Res. 40, 344–365. doi:10.2113/gsjfr.40.4.344

Pulich, W.M., White, W.A., 1991. Decline of Submerged Vegetation in the Galveston Bay System Chronology and Relationships to Physical Processes. J. Coast. Res. 7, 1125–1138.

Reimer, P.J., Bard, E., Bayliss, A., Beck, W.J., Blackwell, P.G., Bronk Ramsey, C., Buck, C.E., Cheng, H., Edwards, L.R., Friedrich, M., Grootes, P.M., Guilderson, T.P., Haflidason, H., Hajdas, I., Hatté, C., Heaton, T.J., Hoffmann, D.L., Hogg, A.G., Hughen, K.A., Kaiser, K.F., Kromer, B., Manning, S.W., Niu, M., Reimer, R.W., Richards, D.A., Scott, M.E., Southon, J.R., Staff, R.A., Turney, C.S.M., van der Plicht, J., Bp, Y.C.A.L., Beck, J.W., Bronk, C., Caitlin, R., Hai, E.B., Edwards, R.L., 2013. IntCal13 and Marine13 Radiocarbon Age Calibration Curves 050,000 Years cal BP. Radiocarbon 55, 1869–1887.

Richter, B., Baumgartner, J., Powell, J., Braun, D., 1996. A Method for Assesing Hydrologic

Alteration within Ecosystems. Conserv. Biol. 10, 1163–1174. doi:10.1046/j.1523-1739.1996.10041163.x

Riggs, S.R., 2011. The battle for North Carolina's coast evolutionary history, present crisis, and vision for the future. University of North Carolina Press, Chapel Hill.

Riggs, S.R., Ames, D. V., 2003. Drowning the North Carolina coast: Sea-Level Rise and Estuarine Dynamics, North Carolina Sea Grant.

Riggs, S.R., Culver, S.J., Ames, D. V., Mallison, D.J., Corbett, D.R., Walsh, J.P., 2008. North Carolina's Coasts In Crisis: a Vision for The Future.

Riggs, S.R., O'Connor, M.P., Bellis, V.J., UNC Sea Grant College Program., North Carolina., D. of A., 1978. Estuarine shoreline erosion in North Carolina : cause and effect. N.C. Coastal Resources Commission, [Raleigh, N.C.?].

Ritchie, J.C., 1962. Distribution of Fallout Cesium-137 in Litter , Humus , and Surface Soil Layers Under Natural Vegetation in the Great Smoky Mountains. University of Tennessee.

Rodriguez, A.B., Greene, D.L., Anderson, J.B., Simms, A.R., 2008. Response of Mobile Bay and eastern Mississippi Sound, Alabama, to changes in sediment accommodation and accumulation. Geol. Soc. Am. Spec. Pap. 443 , 13–29. doi:10.1130/2008.2443(02)

Rodriguez, A.B., Simms, A.R., Anderson, J.B., 2010. Bay-head deltas across the northern Gulf of Mexico back step in response to the 8.2ka cooling event. Quat. Sci. Rev. 29, 3983–3993.

Rutherford, E., 1904. Slow transformation products of radium. Philos. Mag. 8, 636–650. doi:10.1080/14786440509463376

Sanchez-Cabeza, J. a., Masque, P., Ani-Ragolta, I., 1998. 210Pb and 210Po analysis in sediments and soils by microwave acid digestion. J. Radioanal. Nucl. Chem. 227, 19–22. doi:10.1007/BF02386425

Sanchez-Cabeza, J.A., Ruiz-Fernández, A.C., 2012. 210Pb sediment radiochronology: An integrated formulation and classification of dating models. Geochim. Cosmochim. Acta 82, 183–200. doi:10.1016/j.gca.2010.12.024

Schenk, E.R., Hupp, C.R., 2010. Floodplain Sediment Trapping, Hydraulic Connectivity, and Vegetation Along Restored Reaches of The Kissimmee River, Florida, in: 2nd Joint Federal Interagency Conference, Las Vegas, NV, June 27 - July 1, 2010.

Schenk, E.R., Hupp, C.R., 2008. A Sediment Budget for the Regulated Lower Roanoke River, NC, in: Geological Society of America Abstracts with Programs. GSA, p. 92.

Schenk, E.R., Hupp, C.R., Richter, J.M., Kroes, D.E., 2010. Bank erosion , mass wasting , water clarity , bathymetry and a sediment budget along the dam-regulated lower Roanoke River, North Carolina, U.S. Geological Survey Open-File Report 2009-1260. U.S. Geological Survey Open-File Report 2009-1260, 112 p.

Shen, Z., Törnqvist, T.E., Mauz, B., Chamberlain, E.L., Nijhuis, A.G., Sandoval, L., 2015.

Episodic overbank deposition as a dominant mechanism of floodplain and delta-plain aggradation. Geology 43, 875–878. doi:10.1130/G36847.1

Simmons, C.E., 1988. Sediment characteristics of North Carolina streams, 1970-79, U.S. Geological Survey Open-File Report 87-701. U.S. Geological Survey Open-File Report 87-701, 130 p.

Simms, A.R., Rodriguez, A.B., 2014. Where do coastlines stabilize following rapid retreat? GRL Geophys. Res. Lett. 41, 1698–1703.

Snedden, G.A., Cable, J.E., Swarzenski, C., Swenson, E., 2007. Sediment discharge into a subsiding Louisiana deltaic estuary through a Mississippi River diversion. Estuar. Coast. Shelf Sci. 71, 181–193. doi:10.1016/j.ecss.2006.06.035

Stallard, R.F., 1998. Terrestrial sedimentation and the carbon cycle: Coupling weathering and erosion to carbon burial. Global Biogeochem. Cycles 12, 231–257.

Stanley, D.J., Hait, A.K., Jean Stanley, D., 2000. Deltas, radiocarbon dating , and measurements of sediment storage and subsidence. Geology 28, 295–298. doi:10.1130/0091-7613(2000)028<0295:DRDAMO>2.3.CO;2

Stevenson, J.C., Ward, L.G., Kearney, M.S., 1988. Sediment transport and trapping in marsh systems: Implications of tidal flux studies. Mar. Geol. 80, 37–59. doi:10.1016/0025-3227(88)90071-0

Syvitski, J.P.M., 2008. Deltas at risk. Sustain. Sci. 3, 23–32. doi:10.1007/s11625-008-0043-3

Syvitski, J.P.M., Kettner, A.J., Overeem, I., Hutton, E.W.H., Hannon, M.T., Brakenridge, G.R., Day, J., Vörösmarty, C., Saito, Y., Giosan, L., Nicholls, R.J., 2009. Sinking deltas due to human activities. Nat. Geosci. 2, 681–686. doi:10.1038/ngeo629

Temmerman, S., Govers, G., Wartel, S., Meire, P., 2003. Spatial and temporal factors controlling short-term sedimentation in a salt and freshwater tidal marsh, scheldt estuary, Belgium, SW Netherlands. Earth Surf. Process. Landforms 28, 739–755. doi:10.1002/esp.495

Todd, J.F., Wong, G.T.F., Larsen, L., 1989. Atmospheric Depositional Characteristics of Beryllium 7 and Lead 210 Along the Southeastern Virginia Coast. J. Geophys. Res. 94, 106–116.

Trimble, S.W., 1983. A Sediment Budget for Coon Creek Basin in the driftless Area, Wisconsin, 1853-1977. Am. J. Sci. 283, 454–474. doi:10.2475/ajs.283.5.454

Trimble, S.W., 1974. Man-induced soil erosion on the southern Piedmont, 1700-1970. Soil Conservation Society of America, Ankeny, Iowa.

U.S. Department of Agriculture (USDA), 2012. NAIP JPEG2000 ENTITY ID: M_3507603_NW_18_1_20120603_20120813, Aerial Imagery, National Agriculture Imagery Program. USGS Earth Resources Observations and Science Center (EROS), Sioux Falls, South Dakota.

U.S. Geological Survey (USGS), 1954. Aerial Single Frame Photo ID: 1VCR000020013, Aerial Photography, Single Frame Aerial Photography. USGS Earth Resources Observations and Science Center (EROS) Center., Sioux Falls, South Dakota.

United States Coast Survey, 1860. Albemarle Sound, N. Carolina: western part, from the Pasquotank River to the Roanoke and Chowan rivers. United States Coast Survey, Washington, D.C.

United States Coast Survey, Halter, R.E., Bradford, J.S., Lee, S.P., Bache, A.D., 1864. Mouths of Roanoke River, North Carolina. U.S. Coast Survey, Washington, D.C.

United States Environmental Agency, 2007. Monitoring and Assesing Water Quality [WWW Document]. STORET. URL http://www.epa.gov/storet/index.html

United States Geological Survey, 2012. National Water Information System [WWW Document]. URL http://waterdata.usgs.gov/nwis/

Ver, L.M.B., Mackenzie, F.T., Lerman, A., 1999. Biogeochemical Responses of the Carbon Cycle to Natural and Human Perturbations: Past, Present, and Future. Am. J. Sci. 299, 762–801. doi:doi:10.2475/ajs.299.7-9.762

Vitousek, P.M., Mooney, H.A., Lubchenco, J., Melillo, J.M., 1997. Human Domination of Earth's Ecosystems. Science (80-.). 277, 494–499. doi:10.1126/science.277.5325.494

Vörösmarty, C.J., Meybeck, M., Fekete, B., Sharma, K., Green, P., Syvitski, J.P.M., 2003. Anthropogenic sediment retention: major global impact from registered river impoundments. Glob. Planet. Change 39, 169–190. doi:10.1016/S0921-8181(03)00023-7

Wallbrink, P.J., Murray, A.S., 1994. Fallout of 7Be in South Eastern Australia. J. Environ. Radioact. 25, 213–228. doi:10.1016/0265-931X(94)90074-4

Wallbrink, P.J., Murray, A.S., Olley, J.M., 1998. Determining sources and transit times of suspended sediment in the Murrumbidgee River, New South Wales, Australia, using fallout 137Cs and 210Pb. Water Resour. Res. 34, 879–887. doi:10.1029/97WR03471

Wallbrink, P.J., Olley, J.M., Murray, A.S., 1999. Relating Suspended Sediment to its Original Soil Depth Using Fallout Radionuclides. Soil Sci. Soc. Am. J. 63, 369. doi:10.2136/sssaj1999.03615995006300020015x

Walling, D.., He, Q., 1998. The spatial variability of overbank sedimentation on river floodplains. Geomorphology 24, 209–223. doi:10.1016/S0169-555X(98)00017-8

Walling, D.E., 2013. Beryllium-7: The Cinderella of fallout radionuclide sediment tracers? Hydrol. Process. 27, 830–844. doi:10.1002/hyp.9546

Walling, D.E., 1983. The sediment delivery problem. J. Hydrol. 65, 209–237. doi:10.1016/0022-1694(83)90217-2

Walling, D.E., Owens, P.N., Leeks, G.J.L., 1999. Fingerprinting suspended sediment sources in the catchment of the River Ouse, Yorkshire, UK. Hydrol. Process. 13, 955–975.

doi:10.1002/(SICI)1099-1085(199905)13:7<955::AID-HYP784>3.0.CO;2-G

Walling, D.E., Owens, P.N., Leeks, G.J.L., 1998. The role of channel and floodplain storage in the suspended sediment budget of the River Ouse, Yorkshire, UK. Geomorphology 22, 225–242. doi:10.1016/S0169-555X(97)00086-X

Walling, D.E., Woodward, J.C., 1992. Use of radiometric fingerprints to derive information on suspended sediment sources., in: Bogen, J., Walling, D.E., Day, T. (Eds.), Erosion and Sediment Transport Monitoring Programmes in River Basins. Centre for Ecology and Hydrology IAHS Press, Wallingford, Oxfordshire, UK, pp. 153–164.

Walsh, J.P., Nittrouer, C.A., 2004. Mangrove-bank sedimentation in a mesotidal environment with large sediment supply, Gulf of Papua. Mar. Geol. 208, 225–248. doi:10.1016/j.margeo.2004.04.010

White, W.A., Morton, R.A., Holmes, C.W., 2002. A comparison of factors controlling sedimentation rates and wetland loss in f luvial – deltaic systems , Texas Gulf coast. Geomorphology 44, 47–66.

Williams, G.P., Wolman, M.G., 1984. Downstream effects of dams on alluvial rivers. U.S. Geol. Surv. Prof. Pap. 1286, 1–83. doi:10.1002/rrr.3450010210

Wimble, J., 1738. ...Chart of his Majesties Province of North Carolina... William Mount and Thomas Page, London.

Wolman, M.G., 1967. A cycle of sedimentation and erosion in urban river channels. Geogr. Ann. 49, 385–395. doi:10.1177/0309133311414527

Wolman, M.G., Leopold, L.B., 1957. River Flood Plains : Some Observations On Their Formation, Physiographic and Hydraulic Studies of Rivers, US Geological Survey Professional Paper. United States Government Printing Office, Washington, D.C.

Yokoyama, Y., Lambeck, K., De Deckker, P., Johnston, P., Fifield, L.K., 2000. Timing of the Last Glacial Maximum from observed sea-level minima. Nature 406, 713–716.

Zehetner, F., Lair, G.J., Gerzabek, M.H., 2009. Rapid carbon accretion and organic matter pool stabilization in riverine floodplain soils. Global Biogeochem. Cycles 23, 1–7. doi:10.1029/2009GB003481